24036

National Library of Canada | Bibliothèque nationale du Canada | CANADIAN THESES ON MICROFICHE | THÈSES CANADIENNES SUR MICROFICHE

NAME OF AUTHOR/*NOM DE L'AUTEUR* RAM NANIKRAM GIDWANI

TITLE OF THESIS/*TITRE DE LA THÈSE* SOLID DISPERSIONS OF DRUGS: A DETERMINATION OF PHYSICAL CHARACTERISTICS AND CERTAIN PHARMACOKINETICS PARAMETERS OF SELECTED SYSTEMS

UNIVERSITY/*UNIVERSITÉ* UNIVERSITY OF ALBERTA

DEGREE FOR WHICH THESIS WAS PRESENTED/*GRADE POUR LEQUEL CETTE THÈSE FUT PRÉSENTÉE* PH. D

YEAR THIS DEGREE CONFERRED/*ANNÉE D'OBTENTION DE CE GRADE* 1975

NAME OF SUPERVISOR/*NOM DU DIRECTEUR DE THÈSE* DR. A. J. ANDERSON

Permission is hereby granted to the NATIONAL LIBRARY OF CANADA to microfilm this thesis and to lend or sell copies of the film.

The author reserves other publication rights, and neither the thesis nor extensive extracts from it may be printed or otherwise reproduced without the author's written permission.

L'autorisation est par la présente, accordée à la BIBLIOTHÈQUE NATIONALE DU CANADA de microfilmer cette thèse et de prêter ou de vendre des exemplaires du film.

L'auteur se réserve les autres droits de publication; ni la thèse ni de longs extraits de celle-ci ne doivent être imprimés ou autrement reproduits sans l'autorisation écrite de l'auteur.

DATED/*DATÉ* 5/23/75 SIGNED/*SIGNÉ* R. Gidwani

PERMANENT ADDRESS/*RÉSIDENCE FIXE* 43-44 Kissena Blvd
Apt # 6L, Flushing, New York
N.Y. 11355

NL-91 (3-74)

THE UNIVERSITY OF ALBERTA

SOLID DISPERSIONS OF DRUGS: A DETERMINATION OF PHYSICAL CHARACTERISTICS AND CERTAIN PHARMACOKINETIC PARAMETERS OF SELECTED SYSTEMS

by

© RAM NANIKRAM GIDWANI

A THESIS

SUBMITTED TO THE FACULTY OF GRADUATE STUDIES AND RESEARCH

IN PARTIAL FULFILMENT OF THE REQUIREMENTS FOR THE DEGREE

OF DOCTOR OF PHILOSOPHY

IN

BIOPHARMACEUTICS

FACULTY OF PHARMACY AND PHARMACEUTICAL SCIENCES

EDMONTON, ALBERTA

SPRING, 1975

THE UNIVERSITY OF ALBERTA

FACULTY OF GRADUATE STUDIES AND RESEARCH

The undersigned certify that they have read, and recommend to the Faculty of Graduate Studies and Research, for acceptance, a thesis entitled "Solid Dispersions of Drugs: A Determination of Physical Characteristics and Certain Pharmacokinetic Parameters of Selected Systems", submitted by Ram Nanikram Gidwani in partial fulfilment of the requirements for the degree of Doctor of Philosophy in Biopharmaceutics.

Arthur J. Hendrickson
Supervisor

L. G. Chatten

J. A. Rogers

D. K. Madan

Abe Fuson

Dennis G. Watts
External Examiner

Date April 21, 1975

ABSTRACT

Sulfisoxazole, sulfamethoxazole, and methisazone were selected as sparingly water soluble drugs. Solid dispersions of these drugs in urea and polyvinylpyrrolidone were prepared. To characterize the solid dispersions formed, phase diagrams were constructed from thermal analysis data obtained on evaporated mixtures. It was found that urea forms incongruent or peritectic complexes with sulfisoxazole and methisazone. To confirm complex formation, equilibrium solubility studies were conducted. Based on the solubility data, the association equilibrium constants, free energy changes, heats of formation, and entropy changes were determined. Stoichiometric ratios were calculated for the complexes. Dissolution rate studies of the pure drugs, physical mixtures, and solid dispersions were conducted by the rotating-basket and rotating-disc methods. Significant differences were found in the dissolution rates of the test preparations. The studies revealed that the dissolution rate of methisazone is a diffusion-controlled process and is dependent on the effective surface area.

A simple and rapid colorimetric method was developed for the quantitative analysis of methisazone in biological fluids. Bioavailability profiles following single-dose oral administration of pure drugs, physical mixtures, and

solid dispersions were compared by estimating the rate and extent of absorption in rats based on the evaluation of blood levels and urinary excretion data. Significant differences were found in the bioavailabilities of the test preparations. Some pharmacokinetic parameters of sulfisoxazole and sulfamethoxazole were determined. It was found that these drugs exhibited dose-independent kinetics.

ACKNOWLEDGEMENTS

I wish to express my gratitude to Dr. A. J. Anderson for his unremitting guidance and invaluable advice throughout the present study. Without his help and assistance, this investigation would not have been made possible. I am grateful to him for his kindness, congeniality, and above all for his genuine concern about the general state of my affairs.

My sincere thanks are due to members of the supervisory committee for their helpful comments and constructive criticism.

I am greatly indebted to my colleagues and both academic and non-academic members of the Faculty of Pharmacy for their support and friendship.

TABLE OF CONTENTS

LIST OF TABLES

LIST OF FIGURES

INTRODUCTION

A. HISTORICAL BACKGROUND

Pharmaceutical drugs usually can be presented in more than one dosage form, depending to a great extent upon the routes of administration by which these drugs can be given conveniently with maximum therapeutic efficacy. Some of the critical factors that can influence biological availability of sparingly water-soluble drugs are: particle size and physical state of the drug, dissolution rate of the drug from the solid dosage form, and interaction between the drug and pharmacologically inert adjuvants. Levy (1) has emphasized the fact that in instances where drug absorption is rate-limited by the dissolution process, the increase in specific surface area of drug exposed to a dissolution environment can result in more rapid and more complete drug absorption. The delivery rate and the amount of drug delivered from a solid dosage form can be regulated by controlling the particle size of the drug. The effect of particle size on dissolution and bioavailability of drugs has been reviewed by Fincher (2). Miller and Fincher (3) have shown that particle size of a phenobarbital suspension, following an intramuscular injection in dogs, has a marked effect on the bioavailability.

Numerous attempts have been made in the past to develop new techniques to achieve particle size reduction as a means of enhancing bioavailability. Sekiguchi *et al.* (4)

introduced a novel technique for achieving particle size reduction of the antifungal agent griseofulvin by a solvation and desolvation method using chloroform. It was demonstrated by Sekiguchi and co-workers (5,6) that particle size reduction of both sulfathiazole and chloramphenicol to the colloidal range through solid dispersion techniques resulted in faster in vitro dissolution rates and consequently in rapid and complete in vivo absorption. The solid dispersion approach has been successfully applied by others to the formulation of fast-release dosage forms containing water-insoluble drugs (7-24). The scope of solid dispersion systems has been thoroughly reviewed by Chiou and Riegelman (16). According to Noyes and Whitney's equation (25) dissolution rate can be enhanced either by reducing the particle size or by increasing the saturation solubility of the drug. The solubility, a physicochemical property, can be related to the physical form of the drug. For example, a drug may occur either in a crystalline form or in an amorphous form. The amorphous form of the drug is usually more soluble than the crystalline form. Mullins and Macek (26), using amorphous and crystalline forms of novobiocin, demonstrated that the amorphous form was readily soluble and therapeutically active whereas the crystalline form was not. Some drugs have a tendency to form hydrates or solvates when crystallized from aqueous or organic solvents. Ampicillin, for example, is available in two distinct forms, anhydrous and trihydrate.

Poole et al. (27,28) have demonstrated in animals as well as humans that both the aqueous solubility and the biological availability of anhydrous ampicillin are significantly greater than those of the hydrated form. On the other hand, if the physical form of a drug is crystalline, it is possible for the crystalline drug to exist in more than one crystal form. The different crystal forms (called polymorphs) of a drug differ in their solubility characteristics. The metastable crystal form of a drug generally shows higher solubility than the thermodynamically stable crystal form of the same drug. Higuchi et al. (29) have shown that the metastable polymorph of methylprednisolone is approximately 80% more soluble than the stable polymorph at room temperature. While investigating the effect of the polymorphic state on the absorption of chloramphenicol from chloramphenicol palmitate, Aguiar et al. (30) were able to show that the absorption of the metastable polymorph of chloramphenicol palmitate was greater than the absorption of the stable polymorph.

It has been reported (31-37) that complex formation in pharmaceutical preparations may lead to either a decrease or an increase in the solubility of the drugs. The formation of a water-insoluble complex with a low dissociation constant would slow down the dissolution rate and delay absorption. Conversely, the formation of a water-soluble complex with a low association constant would enhance dissolution and

absorption rates. In the case of solid dispersion dosage forms, the enhancement of dissolution rate could be attributed to either particle size reduction or solubilization of drugs. Therefore, in the evaluation of solid dispersion systems the importance of both mechanisms should be recognized. In particular, the possibility of solubilization of water-insoluble drugs by water-soluble carriers should not be overlooked.

Sulfisoxazole, N^1-(3,4-dimethyl-5-isoxazolyl) sulfanilamide, melts at about 196°C with decomposition, and exists in two polymorphic forms (38). Sulfamethoxazole, N^1-(5-methyl-3-isoxazolyl) sulfanilamide, melts at about 170°C, and exists in three polymorphic forms (38). Methisazone, N-methyl-isatin β-thiosemicarbazone, melts at about 250°C with decomposition, and occurs as an orange-yellow powder (39). The pharmacokinetic profiles of sulfisoxazole (40) and sulfamethoxazole (41) have been reported. Reports on the pharmacokinetic studies of methisazone are lacking. Although studies on the effects of particle size (42) and surface-active agents (43) on gastrointestinal and rectal absorption of sulfisoxazole have been reported in the literature, there is none pertaining to the assessment of solid dispersion systems containing sulfisoxazole, sulfamethoxazole, or methisazone.

B. AIMS AND OBJECTIVES OF THE STUDY

The objectives of the present study included the preparation and characterization of solid dispersions of sparingly water-soluble drugs. The study was also designed to determine the usefulness of solid dispersion systems in the enhancement of both the dissolution rate and biological availability of such drugs.

Three relatively water-insoluble drugs were selected for this investigation. Sulfisoxazole, sulfamethoxazole, and methisazone were selected on the basis of their limited aqueous solubility, their hydrophobicity, and their relatively high melting points. Selection of these drugs was further influenced by the fact that no reference to biopharmaceutical evaluation of solid dispersions containing these drugs could be found in the literature. Polyvinylpyrrolidone and urea were chosen as water-soluble carriers on the basis of their general acceptance as safe and nontoxic materials.

A suitable analytical procedure for the determination of sulfisoxazole and sulfamethoxazole in biological fluids was readily available in the Bratton-Marshall method. On the other hand, a suitable assay procedure for methisazone could not be located in the literature. For that reason, it became necessary to develop a method for the determination of methisazone levels in biological fluids.

LITERATURE REVIEW

A. POLYMORPHISM

Polymorphism is the ability of a crystalline drug to exist in more than one crystal form. The polymorphs can differ in physicochemical properties such as solubility, melting point, density, X-ray diffraction pattern, infrared spectra, and differential thermal analysis thermograms. Two polymorphs will have different crystal lattices, and will exhibit different optical crystallographic properties due to a marked difference in space-lattice arrangements of their crystal structures. Different polymorphs of a drug may be classified as isotropic or anisotropic depending on whether the velocity of the light transmitted through the crystal is the same in all directions or different in different directions. The subject of optical crystallography and its application to the identification of polymorphs has been reviewed by Biles (44). When the conversion of polymorphic forms is reversible, it is referred to as enantiotropic; when the polymorphic change is irreversible, it is referred to as monotropic. When the conversion takes place from metastable to thermodynamically stable form, the stable polymorph always has the lowest free energy and the highest melting point.

If the rate of absorption of a sparingly soluble drug from a solid dosage form is dissolution-rate dependent, the

polymorphic state of the drug can influence the overall bioavailability, and, hence, the therapeutic efficacy of the formulation. The existence of polymorphism among therapeutic agents and the impact of polymorphism on solubility, dissolution, and absorption has been reviewed (29-30, 45). It is well known that some drugs offer improved therapeutic performance when presented in a metastable polymorphic form. In view of the physical instability of the metastable state, it sometimes becomes rather difficult to obtain solubility data, particularly for rapidly reverting polymorphic states. With this in mind, Milosovich (46) developed a rapid method for the determination of the solubility of metastable forms of drugs in order to measure thermodynamic properties such as heat of solution, enthalpy, and entropy. Haleblian and McCrone (47) have reviewed the literature pertaining to the pharmaceutical applications of polymorphism in greater depth. Callow and Kennard (48) have reported the presence of polymorphism in cortisone acetate, and have warned that incorporation of the wrong polymorph in the dosage form may cause formulation and stability problems due to phase transition of the metastable to the stable form.

B. SOLID DISPERSIONS

When a drug is dispersed in a physiologically inert carrier matrix in solid state by either fusion or evaporation techniques, a solid dispersion of the drug is said to result. The solid dispersions obtained by evaporation are

often referred to as co-precipitates, examples of which are sulfathiazole-polyvinylpyrrolidone (12) and reserpine-polyvinylpyrrolidone (21). Solid dispersions being such a broad term, encompassing various physicochemical phenomena, it is convenient to classify them into four major categories: (a) simple eutectic system, (b) eutectic system with complex formation, (c) solid solution, and (d) glass solution. By design this study will conform to the dictates of this classification.

Simple Eutectic System

Thermodynamically speaking, a eutectic mixture made from a sparingly water-soluble drug and a pharmacologically inert, readily water-soluble carrier may be regarded as an intimately blended physical mixture of its two interacting components. These components crystallize simultaneously in a fixed ratio, characteristic of the eutectic composition. The eutectic structure of such a binary mixture is that of fine-grained crystals of the individual components (49,51).

DTA thermograms of binary mixtures normally exhibit two endotherms, the first corresponding to the eutectic melt and the second to the subsequent melt of the component in excess of the eutectic composition. The peak of the first endotherm occurs at eutectic isotherm, and the peak of the second endotherm occurs at the liquidus line. On the other hand, a binary mixture of the eutectic composition will exhibit a single, major endotherm. In the case of a simple eutectic system, thaw points of binary mixtures of varying concentrations will invariably be equal to the eutectic temperature of the system.

Eutectic System with Complex Formation

In this binary system, two components interact to form a complex, in addition to a simple eutectic mixture. In other words, such a binary system will exhibit two isotherms, instead of one. When the complex formed is stable and melts to yield a liquid of the same composition as the solid it is said to possess a congruent melting point. However, if the complex formed is unstable in that it undergoes transition with formation of a new solid phase, it is said to have an incongruent or peritectic melting point. In the case of congruent reactions, the phase diagrams will show the presence of two discrete eutectic isotherms. However, in the case of peritectic reactions, the phase diagrams will depict the overlapping of the eutectic isotherm by the peritectic isotherm as a result of the formation of a new solid phase.

Solid Solution

When both components of a eutectic binary mixture show some degree of mutual solubility in each other in the solid state, a conglomerate of the two solid solutions is formed at the eutectic point (50,52). In practice, solid solution solubility of less than 2% is considered insignificant and solid solution formation negligible. It has been documented in the literature (53) that in binary systems where solid solution formation is evident, the phase diagrams are characterized by the appearance of thaw points at temperatures higher than the eutectic temperature.

Glass Solution

Chiou and Riegelman (13) were the first to report the application of the principle of glass solution formation (54) to enhance drug dissolution and absorption. A glass solution is a homogenous system in which a glassy or vitreous form of the carrier molecules solubilizes drug molecules in the matrix. Polyvinylpyrrolidone, dissolved in [redacted]c solvents, undergoes a transition to a glassy state on evaporation of the solvent. It was shown (13) that the dissolution rate of griseofulvin dispersed in a glass solution form was faster than that of the same drug dispersed in a solid solution form.

C. THEORY OF DISSOLUTION IN A NON-REACTIVE MEDIUM

The process of dissolution is regarded as a surface phenomenon, which occurs as a result of mass transfer of solute molecules from the surface of the dissolving solid to the bulk solution. Two transport models that can best describe the dissolution process are: (a) Interfacial Barrier Model, and (b) Diffusion Model. In the case of the former, the rate of dissolution is influenced by a high-energy barrier at the interface; in the case of the latter, a thin layer of saturated solution is formed at the surface of the dissolving solid so that the dissolution rate is determined by the rate at which the dissolved molecules diffuse through this layer into the bulk solution. Based on the concept that the solute molecules will have to be

activated in order to cross the energy barrier before diffusing into the bulk solution, the dissolution process can simply be described by consecutive transport processes involving energy changes at the interface followed by diffusion away from the interface. From a dissolution kinetics standpoint, either of the consecutive reactions can be a rate-determining step, depending on which one is slower. However, if both are of the same order of magnitude, the over-all dissolution rate will be a function of both processes.

1. Review of Dissolution Kinetics

Constant Surface Area Concept

According to the classic Noyes and Whitney law (25), the rate of dissolution of solids, $\frac{dC}{dt}$, is directly proportional to the difference between the concentration of the saturated solution of the solid, C_s, at the experimental temperature and the concentration of the solid in the dissolution medium, C_t, at any given time t:

$$\frac{dC}{dt} = k[C_s - C_t] \qquad \text{(Eq. 1)}$$

where k is the apparent dissolution rate constant with dimension 1/time. The derivation of the Noyes and Whitney differential equation is based on the assumptions that (a) the dissolution of the solid is a diffusion-controlled process and (b) the surface area of the exposed solid changes negligibly with time during dissolution process. The apparent rate constant, k, is dependent upon the surface area

of the exposed solid, the intensity of agitation, the temperature and the structure of the surface. Assuming that the dissolution rate under well-defined conditions of temperature and agitation is proportional to the surface area, S, equation 1, according to Noyes and Whitney (25) and Bruner and Tolloczko (55), could well be written as:

$$\frac{dC}{dt} = K'S\,[C_s - C_t] \qquad \text{(Eq. 1.1)}$$

where K' is the intrinsic dissolution rate constant. Using Fick's law of diffusion, Brunner (56) showed that equation 1.1 can more explicitly be expressed as:

$$\frac{dC}{dt} = \frac{DS}{hV}\,[C_s - C_t] \qquad \text{(Eq. 1.2)}$$

where D is the diffusion coefficient, S is the area of the exposed surface, h is the thickness of diffusion layer, and V is the volume of dissolution medium. From equations 1, 1.1, 1.2, it is evident that:

$$k = K'S = \frac{DS}{hV} \qquad \text{(Eq. 2)}$$

Therefore, when $K = \frac{D}{h}$, we have the following relationship:

$$K = \frac{kV}{S} \qquad \text{(Eq. 3)}$$

where K = cm.^{3}/time. cm.^{2} and therefore, has dimensions of length/time. Nogami et al. (57) have shown that the rate constant, k, is dependent upon both the surface area, S, and the volume of dissolution medium, whereas the intrinsic rate constant, K, is independent of these factors.

Variable Surface Area Concept

Considering those situations where the surface area of the dissolving solid could be constantly changing, Hixson and Crowell (58) derived their "cube root law" based on the assumptions that: (a) dissolution takes place normal to the surface of the dissolving solid, (b) there is no stagnation of the liquid, (c) the agitation effect is the same on all areas of the exposed surface, and (d) the dissolving solid remains intact during dissolution. The integrated form of their equation is:

$$K^* \cdot t = W_o^{1/3} - W_t^{1/3} \qquad \text{(Eq. 4)}$$

where W_o is the initial weight of the solid, W_t is the weight of the solid at time t, the constant, K^*, is the product of intrinsic rate constant, solubility, density, and other shape factors, and t is the time.

2. Some Factors Influencing Dissolution Rates

Inasmuch as there are several physico-chemical factors regulating the dissolution rate of solids in non-reactive media, only those that are considered relevant to the present study will be briefly discussed here.

Solubility

Under sink conditions where the concentration gradient $(C_s - C_t)$ is almost constant and the concentration build-up in the dissolution medium is negligible, the dissolution rate of the solid is directly proportional to the saturation solubility of the solid in the dissolution medium. An increase in saturation solubility, C_s, would

result in an increase in dissolution rate. Hamlin *et al.* (59) reported data for compounds representing various chemical species to show that the relationship between dissolution rate and solubility is linear.

Viscosity

The dissolution rate is inversely proportional to the viscosity of the dissolution medium if diffusion mechanism is operative. The dissolution rate controlled by interfacial reaction is not affected by the viscosity factor. In a diffusion-controlled reaction, an increase in viscosity will result in a slowing of the dissolution rate. This relationship was clearly demonstrated by Braun and Parrot (60) who showed that the dissolution rate of benzoic acid in aqueous sucrose solution and in methyl cellulose solution was inversely proportional to the viscosity of the dissolution medium.

Surface Tension

The apparent dissolution rate of sparingly soluble solids can be appreciably increased by lowering the interfacial tension between the hydrophobic surface of the solid and the dissolution medium. In a study concerned with wetting effects of surfactants below critical micelle concentration, Finholt and Solvang (61) found that the inclusion of polysorbate 80 in concentrations less that 0.01% w/v in the dissolution medium accelerated the

dissolution rate of phenacetin without affecting the solubility of phenacetin significantly. They attributed the effect of polysorbate 80 to the wetting of the hydrophobic surface of phenacetin.

Particle Size

An increase in the specific surface area as a result of reduction in particle size will enhance the rate of dissolution of sparingly water soluble solids. However, there are several instances where particle size reduction has little effect on the dissolution rate. This anomalous behavior could be ascribed to the acquisition of electrostatic charges during micronization. The effects of particle size on the dissolution and absorption rates have been well reviewed by Levy (1) and Fincher (2).

Temperature

In those instances where the solubility of the solid is a function of the temperature, an increase in temperature of the dissolution medium will enhance the rate of dissolution by increasing diffusion of the solute molecules through the diffusion layer into the bulk solution.

Agitation

For a diffusion-controlled reaction, it is apparent that the thickness of the diffusion layer is inversely proportional to the intensity of agitation. As the intensity of agitation is increased, the diffusion layer becomes thinner, and the dissolution rate is increased. The relationship be-

tween the dissolution rate and the intensity of agitation on an empirical basis may be expressed as:

$$R = a N^b \qquad \text{(Eq. 5)}$$

where R is the dissolution rate, N is the agitation in terms of revolutions per minute, and a and b are constants. It is evident from the above equation that the value of the constant, b, in the case of a diffusion-controlled reaction will approach unity, whereas in the case of an interfacial reaction where the dissolution rate is independent of agitation, the value of b will approach zero. Further, in order for a dissolution study to be more meaningful in detecting statistically significant differences in dissolution rates of diffusion-controlled reactions, a low agitation intensity will be desirable.

3. Methods for the determination of Dissolution Rates

Numerous techniques for the evaluation of in vitro dissolution profiles of solid dosage forms are available. These may be collectively grouped under two main headings - Methods for Intrinsic Dissolution Rates and Methods for Apparent Dissolution Rates. Two of the most commonly used methods are briefly reviewed here.

Rotating-Disc Method

The rotating-disc method was first introduced by Nelson (62) and later modified by Levy and Sahli (63). This method is useful in determining intrinsic dissolution rates

of sparingly soluble solids under sink and constant surface area conditions where the concentration build-up of solid in solution is negligible and where the surface area of the exposed solid is fixed by using a non-disintegrating, flat-faced disc mounted in a holder such that only one face of the disc is exposed. In this method, the disc holder is attached to the drive shaft of a constant speed motor so that the disc face can be rotated at a specific intensity of agitation expressed in terms of r.p.m. In order to demonstrate the dependence of the intrinsic rate constant, K, on the intensity of agitation, Cooper and Kingery (64) conducted a series of experiments at two different temperatures by rotating sodium chloride discs of constant surface area in glycerin at various speeds. They found that the plots of logarithm of K versus logarithm of r.p.m. were linear with slopes equal to 0.5, indicating that the intrinsic rate constant, K, is proportional to the square root of the agitation intensity. Their findings were based on the assumptions that the flow of a high viscosity liquid is laminar and that the rate of dissolution is diffusion-controlled.

Rotating-Basket Method

Searl and Pernarowski (65) pioneered the development of the rotating-basket method which now has been adapted as an official method in the N.F. XIII (66) and U.S.P. XVIII (67). Because of its simplicity, reliability and versatility, this method is widely used in the determination of apparent

dissolution rate constants. Using the rotating-basket method in the dissolution studies of constant-surface pellets of salicylic acid, Tingstad et al. (68) found a linear relationship between the dissolution rate and the intensity of agitation in the range of 50 to 150 r.p.m. Therefore, a low agitation intensity of not less than 50 r.p.m. should be selected in the comparative evaluation of dissolution rates of fast release preparations.

4. Interpretation of Dissolution Data

Constant Surface Area Concept

Under sink conditions where concentration change, $(C_s - C_t)$, is negligible, the term, C_t, drops out and Equation 1 reduces to:

$$\frac{dC}{dt} = k\, C_s \qquad \text{(Eq. 6)}$$

Equation 6 implies that, since the dissolution rate is constant, it must follow zero-order kinetics and remain independent of the concentration of the dissolving solid. Therefore, the initial concentration of the solid, C_o, could be substituted for the saturation solubility of the solid, C_s, in the above equation. Integration of the rate equation 6 between time t and zero time, followed by substitution of C_o for C_s will yield:

$$C_t = k\, C_o\, t \qquad \text{(Eq. 7)}$$

which is the same as:

$$C_t = \frac{K\,S}{V} C_o\, t \qquad \text{(Eq. 8)}$$

Rearrangement of Eq. 8 gives:

$$\frac{C_t}{C_o} = \frac{K\,S}{V}\, t \qquad \text{(Eq. 9)}$$

Since the concentration of the solid dissolved at time t over the initial concentration of the solid is equal to the fraction of the solid dissolved, Eq. 9 simplifies to:

$$F_t = \frac{K\,S}{V}\, t \qquad \text{(Eq. 10)}$$

where F_t is the fraction of the solid dissolved at time t. Therefore, a plot of the fraction dissolved versus time will yield a straight line with slope equal to KS/V. It should be noted that the slope is also equal to the apparent dissolution rate constant, k. The intrinsic dissolution rate constant, K, may simply be computed by first dividing the slope with the surface area, S, and then multiplying the quotient with the volume of dissolution medium, V.

Based on the Higuchi theoretical treatment (69) for diffusion-controlled drug release from insoluble, inert matrices under sink and constant surface area conditions, Desai *et al.* (70) were able to predict that a plot of the amount of drug released, Q, against the square root of time t would be linear if the diffusion-controlled mechanism

is operative, according to the following equation:

$$Q = K S t^{1/2} \qquad \text{(Eq. 11)}$$

While studying the behavior of drug release from wax matrices compressed in the form of tablets, Schwartz et al. (71) found that drug release conformed with the Higuchi diffusion-controlled release model as well as with the first-order release model which they depicted by the following relationship:

$$\log A = \log A_o - \frac{kt}{2.303} \qquad \text{(Eq. 12)}$$

where A is the amount of drug remaining in the tablet at time t, and A_o is the initial amount of drug in the tablet. In order to differentiate between the two mechanisms, they made use of the logarithmic form of Eq. 11 and demonstrated that a plot of log. Q versus log. t was linear with slope equal to 0.5, indicating that the drug release data fitted Higuchi's diffusion-controlled release model according to the following relationship:

$$\log Q = (\log K + \log S) + 1/2 \log t \qquad \text{(Eq. 13)}$$

Variable Surface Area Concept

Assuming that the percent surface area available for dissolution is proportional to the percent solid undissolved, Gibaldi and Feldman (72) showed that the dissolution process under sink conditions could be described by a first-order kinetic model. Introducing the concept that the surface a

available for dissolution under such conditions decreases exponentially with time, Wagner (73) derived a first-order rate expression for dissolution of solids whose surface area is constantly changing as follows:

$$A = A_o e^{-kt} \qquad \text{(Eq. 14)}$$

Thus, a plot of the logarithm of the percent undissolved versus time will be linear under sink conditions.

However, in many instances, the first-order dissolution data yield curved plots which are non-linear in the early part of dissolution. It is feasible that such first-order dissolution plots are merely artifacts. Under these conditions, Wagner (73) introduced a new concept of distribution functions as an alternative method of analyzing first-order dissolution data to estimate those dissolution parameters that adequately describe the data. His concept is based on the assumption that the percent dissolved is equal to the percent surface area made available for dissolution. Wagner suggested that the percent dissolved-time data which yield very poor first-order plots may be best approximated by logarithmic-normal distribution functions. When dissolution follows a log-normal distribution function, the percent dissolved-time data may be plotted on a logarithmic-probability graph paper to obtain a straight-line relationship so that parameters such as dissolution half-time could be estimated. The percent dissolved data is usually plotted on the probability scale and the corresponding time data on the logarithmic scale.

D. BIOPHARMACEUTICAL CONSIDERATIONS

In the development of solid dosage forms, the concepts of bioavailability have become very important. The assessment of bioavailability requires an understanding of the fate of drugs in terms of absorption, distribution, and elimination kinetics.

1. Drug Absorption

The absorption of drugs from the gastrointestinal tract may be defined as the transport of drugs from the extravascular depot into the blood. According to the pH-partition theory, the lipid-soluble drugs in unionized form are transported across the mucosal membrane by simple diffusion. However, the lipid-insoluble drugs are transported by an active transport mechanism. The rate of absorption of drugs from the small intestine is influenced by gastric emptying time. The presence of food in the stomach can delay gastric emptying which, in turn, can slow down the rate of absorption. Macdonald *et al.* (74) demonstrated that concomitant administration of food following a single oral dose of sulfisoxazole reduced significantly the rate but not the total amount of absorption of sulfisoxazole. The type of food can also influence the rate of drug absorption. For example, when a lipid-soluble drug is consumed with a high-fat meal, the drug absorption is enhanced. Kraml *et al.* (75) demonstrated in rats that plasma levels of micronized griseofulvin suspended in corn oil were significantly higher than those of the same material suspended in water.

The effects of prolonged starvation on the absorption of drugs in rats have been observed by Doluisio et al. (76). They found that the rates of drug absorption in rats decreased significantly when the animals were fasted for more than 20 hours. Intestinal transit time is another factor which influences drug absorption. For a given drug, the longer the intestinal transit time the greater will be its degree of absorption. An excellent review on the physiological factors influencing drug absorption has been written by Mayersohn (77).

2. Drug Distribution

Soon after a drug is absorbed into the general circulation, the drug is transported by blood to the various sites of action where it equilibrates rapidly between the plasma and the tissues. The distribution of drugs to the end organs will depend on the apparent volume of distribution, the interaction of drugs with plasma proteins, and the physicochemical properties of the drugs.

Apparent Volume of Distribution

The concept of apparent volume of distribution becomes useful in estimating the total amount of drug in the body. It is a hypothetical figure which reflects the distribution of drug between the blood and the rest of the body. It does not represent the true volume of the body, and has no physiological significance. For instance, the blood levels of two different drugs following administration of

equal doses in an individual may not be the same, yet the total amount of each drug in the body may be the same, assuming that the drugs are completely absorbed and are not eliminated from the body by either metabolism or excretion. These differences in the blood levels can be accounted for by the differences in the distribution of the two drugs. The apparent volume of distribution is also related to body weight and hence its value becomes a characteristic property of drugs. In general, the apparent volume of distribution for an obese individual will be less than that for a lean individual. Therefore, in order to minimize dosage errors due to such inter-subject variation, the blood level data should always be corrected for body weight. For these reasons, calculation of doses based on mg/kg is preferred to other methods.

Drug-Protein Binding

The binding of drugs by plasma or tissue proteins plays a key role in drug distribution in the body. The unbound drug is capable of diffusing through biological membranes and is responsible for eliciting drug action. Since protein binding follows simple saturation kinetics, the distribution of drugs will largely depend on the amount of free unbound drug in the blood. It is the plasma level of free unbound diffusible drug and not the total drug which is related to drug toxicity. A drug competing with some other drug for the same protein binding sites can enhance its

toxicity by displacing it from its binding sites. The diffusion of drugs into the erythrocytes can be affected by protein binding. The ratio of whole blood concentration to plasma concentration can be regarded as an index of free unbound diffusible drug. The uneven distribution of diphenylhydantoin between plasma and erythrocytes in humans was reported by Borondy et al. (78). They argued that the ratio of the order of 0.7 was due to a high degree of protein binding resulting in poor diffusion of diphenylhydantoin into the erythrocytes.

Physicochemical Properties

The distribution of weak electrolytes will depend on their pKa values and on differences between intracellular and extracellular pH values. The lipid-water partition coefficient of the unionized form of the drug is the rate-limiting factor in the distribution of drugs. Two drugs with the same pKa but different lipid solubility will exhibit different distribution characteristics.

3. Drug Elimination

The elimination of drugs from the body usually takes place by two competing pathways. Drugs, therefore, can be eliminated simultaneously by metabolism of drugs and excretion of both changed and unchanged drugs. The overall elimination rate constant is the sum of the first-order excretion and metabolism rate constants. Like the apparent volume of distribution, the elimination half-life becomes a characteristic property of drugs. The concept of biological

half-life becomes vital in calculating appropriate dosage regimens. The biological half-life may vary from individual to individual due to genetic differences. Further, plasma protein binding of drugs can decrease the overall elimination rate and thereby increase biological half-lives of drugs. In his overview of drug-protein binding, Gillette (79) stressed the importance of such binding on drug elimination. Similar concern was expressed earlier by Gibaldi and Weintraub (80) who pointed out that, unless the biological half-life of a drug was determined from the far end of the linear segment of the semilogarithmic plots of blood level and urinary excretion data, the true half-life would be underestimated.

E. SIGNIFICANCE OF OTHER IMPORTANT CONCEPTS

Total Body Clearance

In pharmacokinetics the total body clearance, ml/min, is defined as the ratio of the urinary excretion rate, mg/min, to the blood concentration, mg/ml. The total body clearance can also be expressed as the product of the overall elimination rate constant and the apparent volume of distribution. Rowland (81) has demonstrated on the basis of area analysis that the total body clearance can be determined by dividing an intravenous dose by the corresponding area under the blood concentration-time curve. The total body clearance is the sum of the renal and hepatic clearances. The higher the value of the total

body clearance the lower will be the bioavailability. Further, it should be emphasized here that the physiochemical properties of the drug, such as pKa and the lipid-water partition coefficient will determine whether the clearance of an organic weak acid or base will be influenced by the urinary pH changes.

Dose Dependence

Most biopharmaceutical evaluations are based on the assumption that pharmacokinetic events follow first-order kinetics. According to the classical chemical kinetics, dose-independent kinetics is just another name for first-order kinetics. In pharmacokinetics, the criterion for dose-independent kinetics is that the area under the blood concentration-time curve should be directly proportional to the dose administered. This implies that the fraction of the dose absorbed or eliminated will always be the same regardless of the dose level used. For a drug exhibiting dose-independent kinetics, the biological half-life and the clearance will be independent of the dose administered. If the pharmacokinetics of the drug exhibit dose-dependency, then the area under the curve and the biological half-life and the clearance will vary from dose to dose. The causes of departure from linearity could be many, but only a few are of importance. Among these are: the protein binding and the saturation of either absorption sites or metabolizing enzyme systems. It

is obvious then that the drugs exhibiting dose-dependent (non-linear) kinetics will follow Michaelis-Menton kinetics (saturation kinetics).

F. BIOAVAILABILITY

Dittert and DiSanto (82) have described bioavailability as the rate and extent of absorption of a drug into the systemic circulation. The relative bioavailability can be measured by comparing the area under the blood-concentration-time curve following administration of the test dosage form with the area under the curve following administration of a readily available dosage form. The reference standard dosage form is arbitrarily assigned an availability value of 100 percent. The drug is considered to be fully available when the area ratio is equal to unity. And if the ratio is less than unity, the drug is not completely available. Recently, Lalka and Feldman (83) presented a mathematical treatment showing that absolute bioavailability of drugs whose renal clearance is influenced by the urinary pH changes can be approximated without reference to a parenteral dose. After a drug is absorbed from the gastrointestinal tract it reaches the liver first before entering the systemic circulation. In the liver a certain fraction of the oral dose will be cleared by the hepatic metabolism. Gibaldi and Feldman (84) referred to this effect of metabolism a drug has to undergo before reaching systemic circulation as the first-

pass effect. The first-pass effect can be demonstrated by comparing the areas under blood concentration-time curves for a drug following peripheral vein and portal vein infusions. If the area under the curve following portal vein infusion is significantly less than the area under the curve following peripheral infusion, then it can be concluded that the first-pass phenomenon for the drug is viable.

In pharmacokinetics, the absorption rate constants are usually determined from the blood concentration-time plots by the method of feathering. Wagner and Nelson (85) introduced a method for the determination of absorption rate constants from the blood level data according to a one-compartment open model. They showed that the concentration of drug absorbed per unit volume of distribution at any time, t, can be determined from the blood level data following oral administration of the drug without having to determine the values of the fraction absorbed and the volume of distribution. They derived the following relationship:

$$(FD/V)_t = B_t + K_E \int_0^t B \cdot dt \qquad \text{(Eq. 15)}$$

where:

$\frac{FD}{V}$ = concentration of drug absorbed per unit volume of distribution

F = fraction of drug absorbed

V = volume of distribution

D = dose administered

B_t = blood concentration at time, t

K_E = elimination rate constant

Terms on the right-hand side of the equation can be determined experimentally from the blood level data. When the values of the right-hand side of the equation are plotted as a function of time, the curve will rise progressively until it reaches a plateau. Now, if the values of the right-hand side of the equation are expressed as percentages of the asymptotic value and plotted as a function of time, the resulting curve will be a straight line, the slope of which will give the absorption rate constant. The absorption rate constant will be expressed in terms of the percentage of the maximum drug which is absorbed per unit time. Similarly, Loo and Riegelman (86) derived the following equation according to a two-compartment open model:

$$(FD/V)_t = B_t + K_E \int_0^t B \cdot dt + T_t \qquad \text{(Eq. 16)}$$

where T_t is the tissue concentration at time, t. According to Eq. 15, the concentration of drug absorbed in terms of FD/V at time infinity could be determined from the following equation:

$$(FD/V)_\infty = 0 + K_E \int_0^\infty B \cdot dt \qquad \text{(Eq. 17)}$$

Using Equation 17, Wagner and Nelson (87) derived the following relationship for the estimation of relative bioavailability.

$$\frac{F_1 D}{V} \div \frac{F_2 D}{V} = \frac{\left[K_E \int_0^{\infty} B \cdot dt\right]_1}{\left[K_E \int_0^{\infty} B \cdot dt\right]_2} \qquad \text{(Eq. 18)}$$

where F_1 and F_2 are the fractions of dose absorbed from formulations 1 and 2. If the drug exhibits dose-independent kinetics, then the elimination rate constant, K_E, will be the same for both the formulations, and will, therefore, cancel out. Similarly, the dose, D, and the volume of distribution, V, will drop out too. The Equation 18, now, can be written as:

$$\frac{F_1}{F_2} = \frac{\left(\int_0^{\infty} B \cdot dt\right)_1}{\left(\int_0^{\infty} B \cdot dt\right)_2} = \frac{(AUC)_1}{(AUC)_2} \qquad \text{(Eq. 19)}$$

where AUC is the area under the blood concentration-time curve. Therefore, according to Equation 19, if a drug exhibits dose-independent kinetics, then the areas under the blood concentration-time curve following oral administration of two dosage forms containing the same dose of a given drug can be compared to estimate the relative bioavailability.

In the case of drugs that are poorly available, a fraction of the dose could undergo chemical degradation, hydrolysis, or biotransformation at the absorption site. The parallel loss of drug at the absorption site could lead to erroneous interpretations. Notari et al. (88) have demonstrated that, when two or more simultaneous first-order pathways compete for the same drug at the absorption site, the Wagner and Nelson method will overestimate the true absorption rate constant. The overestimation results in an apparent first-order rate constant which is the sum of the true absorption rate constant and the rate constant for parallel loss of drug to the extravascular compartment. They indicated that, in order to obtain the true absorption rate constant, the apparent rate constant should be multiplied by the fraction of the dose absorbed. However, Perrier and Gibaldi (89) determined experimentally that in instances where drugs are poorly absorbed, the true absorption rate constants can not be calculated by any method whether it be the Wagner and Nelson method or the feathering technique. In contrast to the findings of Perrier and Gibaldi, Leeson and Weintraub (90) have proposed an alternative technique of treating the data obtained prior to the onset of the lag time, which can determine the true absorption rate constant for some models.

EXPERIMENTAL

A. MATERIALS

Benzoic acid[1] (certified A.C.S. grade), methylcellulose[2] USP (1500 cps.), naphthalene[3] (scintillation grade), polyvinylpyrrolidone[4] (Povidone NF), sulfathiazole[5] BPC, and 1,4-dioxane[6] were used as received, without further purification. Calorimetric standards such as indium, lead, tin, and zinc were obtained from the Fisher Scientific Co. Methisazone[7], sulfisoxazole[8] USP, and sulfamethoxazole[9] NF were supplied by the manufacturers. The purity of these compounds as indicated by the certificates of analysis was 99.4%, 99.68%, and 99.80% respectively. Methisazone was used as supplied. Sulfisoxazole, sulfamethoxazole, and urea[10] (certified A.C.S. grade) were recrystallized from reagent grade methanol. All other chemicals and solvents employed in this study were reagent grade and they were used without further purification.

[1,2,6,10] Fisher Scientific Co., Fairlawn, N.J., U.S.A.

[3] BDH Chemicals Ltd., Poole, England

[4] Plasdone-C (K-30), supplied by the GAF corporation, New York, U.S.A.

[5] BDH Pharmaceuticals, Toronto, Canada

[7] Burroughs Wellcome & Co., Kent, England

[8,9] Hoffmann-LaRoche Ltd., Quebec, Canada

1. Preparation of Solid Dispersions

Solid dispersions were prepared by the solvent evaporation method. Methanol was employed as a solvent for both sulfisoxazole and sulfamethoxazole. The solvent system for methisazone consisted of a mixture of acetone and methanol in equal parts. The solid components of the solid dispersions were accurately weighed and then dissolved in a minimum amount of the proper solvent system. The solution was then carefully evaporated to dryness on a water bath. After complete evaporation of the solvent, the solidified mass was finely ground, sieved, and stored in a vacuum dessicator over anhydrous calcium sulphate.

2. Preparation of Physical Mixtures

Powdered drugs were first passed through sieves, and the fraction between 270 and 325 mesh was collected for use in this study. The physical mixtures of carrier and drug were then prepared by simply mixing.

3. Analysis of Test Preparations

The concentration of drugs in the solid dispersions and the physical mixtures was confirmed spectrophotometrically, using a Unicam[1] SP 1800 double-beam spectrophotometer. Both sulfisoxazole and sulfamethoxazole in distilled water obeyed Beer's law at a wavelength of 258 nm. Methisazone in 0.2 N

---

[1]Pye Unicam Ltd., York Street, Cambridge, England

NaOH also obeyed Beer's law at a wavelength of 380 nm. Neither urea nor polyvinylpyrrolidone interfered with the assay procedures at these wavelengths.

B. THERMAL ANALYSIS STUDIES

There are two methods of thermal analysis, the visual and the differential. The visual method employs the cooling curve and the thaw-melt techniques. Of these, the thaw-melt method utilizing the capillary melting point technique is more simple to use. However, it has a low sensitivity due to the fact that the measurements are based on subjective observations. This imposes a limitation on its use in detecting heat effects visually. On the other hand, the differential thermal analysis (DTA) method, by virtue of its inherent ability to detect very small energy changes, makes it possible to circumvent the limitation of the thaw-melt method in detecting heat effects. Since the capillary melting point method is effective in detecting melting points, DTA is often used as a complementary technique to aid in the detection of other phase changes. In the present study, both methods of analysis were employed in characterizing solid dispersions prepared.

1. Capillary Melting Point Method

A Thomas-Hoover capillary melting point apparatus[1] was employed for the determination of thaw and melting points of

---

[1]Arthur H. Thomas Co., Phila., Pa., U.S.A.

certain binary mixtures. The heating rate for the more heat stable samples was established at 8°C min^{-1}. However, for the more thermolabile samples a heating rate of 24°C min^{-1} was found to be necessary. A calibration curve for the melting-point apparatus was then constructed using organic standards obtained for this purpose.[1]

2. Differential Thermal Analysis Method

One advantage of DTA over conventional thermal methods of analysis is that it can provide useful quantitative information on the heats of fusion and transition of specimens under investigation. DTA is a simple, and sensitive analytical tool designed to detect and quantitate small changes in physical or chemical reactions associated with either heat loss or heat gain as a function of linear temperature rise. It can only record changes in energy content of reactions as exothermic or endothermic. It cannot identify the type of reaction involved. Prior knowledge of the type of reaction is a prerequisite for the interpretation of DTA peaks. A DTA thermogram is obtained when temperature differential between sample and reference is plotted against reference temperature. It has been shown by Borchardt and Daniels (91) that the total heat of reaction, ΔH, is proportional to the area under the DTA peak as described by the following relationship:

$$\Delta H = K \int_{t_1}^{t_2} \Delta T \cdot dt = K \cdot A \qquad \text{(Eq. 20)}$$

[1] Arthur H. Thomas Co., Phila., Pa., U.S.A.

where K is the proportionality constant, ΔT is the temperature differential, A is the area under the DTA peak, and t is the time.

Calibration of the DTA Instrument

A Fisher model 300 Quantitative Differential Thermal Analyzer[1], equipped with an automatically programmable furnace, was used for differential thermal analysis. When the instrument is calibrated against known weights of calorimetric standards whose heats of fusion or transition are known, DTA can lend itself to quantitative measurement of thermal effects. The calibration coefficient, J, is characteristic of the instrument used, and should always be empirically determined for the fusion or transition temperature of each compound whose heat of reaction is to be determined. The method of calibration basically consists of plotting the calibration coefficients against the corresponding peak temperatures of fusion or transition. The units of J can either be expressed in calories per square inch or in calories per degree per minute.

Using the method described by Guillory (92), the instrument was calibrated over a temperature range from 80 to 420°C. For this purpose 15.0±0.1 mg each of Naphthalene, Indium, Lead, Tin, and Zinc as standards versus the empty sample pan as reference were used. The areas under the endothermic

[1]Fisher Scientific Co., Instrument Division, Pittsburgh, Pa., U.S.A.

peaks were measured by means of a planimeter[1]. The values of the calibration coefficient, J, were computed from the following equation, using theoretical heats of fusion for the above calorimetric standards as reported in the literature (93) and a chart speed of 1 inch per minute.

$$J = \left[\frac{\Delta H \cdot M \cdot P}{A \cdot \Delta T_s \cdot T_s}\right]_{\text{standard}} = \left[\frac{\Delta H \cdot M \cdot P}{A \cdot \Delta T_s \cdot T_s}\right]_{\text{specimen}} \quad \text{(Eq. 21)}$$

where:

J = calibration coefficient, mcal deg^{-1} min^{-1}

ΔH = heat of fusion, mcal mg^{-1}

M = mass of sample, mg

P = program rate, deg min^{-1}

A = peak area, sq. in.

ΔT_s = differential temperature sensitivity, deg in^{-1}

T_s = reference temperature sensitivity, deg in^{-1}

Quantitative Determination of Heat of Reaction

The unknown samples were accurately weighed to ±0.1 mg and quantitatively placed into aluminum sample pans and encapsulated. The test samples were then heated at a specified linear programming rate, using an empty sample pan as reference. Three thermograms were obtained for each sample under identical operating conditions. The areas under the DTA

[1]Gelman Instrument Co., Ann Arbor, Michigan, U.S.A.

peaks were normalized to a chart speed of 1 inch per minute and the value of J corresponding to the temperature of the peak under consideration was obtained from the calibration curve for the instrument. The heat of reaction for the specimen was then computed by substituting the values of J, M, P, A, ΔT_s, and T_s in Equation 21 and then solving the equation for ΔH.

C. EQUILIBRIUM SOLUBILITY STUDIES

A series of solutions of increasing concentrations of carrier in equal increments of 0.5% w/v in distilled water was prepared. An excess amount of drug (about 200 mg) was placed in 15-ml glass vials fitted with rubber closures. Ten-ml samples of the aqueous solutions of the carrier in varying concentrations were quantitatively transferred to these vials containing drug, and the vials were then securely stoppered. The contents of the vials were continuously agitated in a Dubnoff[1] metabolic shaking incubator at 25 and 37°C constant temperatures for over 72 hours until equilibrium was attained under saturation conditions. When the vials were immersed in the constant-temperature water bath, care was exercised to ensure that the water level of the bath was well above the level of solution in the vials. Aliquot samples of the clear, supernatant, saturated solutions were withdrawn, using disposable syringes. The aliquots were immediately filtered through 0.45 micron pore size Millipore

[1]Precision Scientific Co., Chicago, Illinois, U.S.A.

filters[1], using 13 mm Swinney adaptors[1]. After suitable dilution with water, absorbance of each filtered sample was measured in a 1-cm cell against an appropriate blank at a predetermined wavelength. The amount of drug in solution was determined by dividing the absorbance by the slope of a previously constructed calibration curve for the drug.

D. DISSOLUTION RATE STUDIES

According to the laws of hydrodynamics, the dissolution from static solids, in the absence of any external applied agitation, will possibly occur under the influence of free convection of the dissolution medium as a result of the density gradient and the action of gravity. Therefore, under free convection, dissolution will not be controlled by diffusion alone, and the diffusion-controlled reaction will not be a rate-limiting step. In view of this, the dissolution rate measurements in this study were made in distilled water at 37°C under forced convection by the rotating-disc and by the rotating-basket methods.

In comparative dissolution studies, variable factors such as wetting ability, particle size distribution and hence specific surface area of the dissolving solid particles, if not controlled, can influence the dissolution rates. To minimize these untoward effects, non-disintegrating,

[1]Millipore Corp., Bedford, Mass., U.S.A.

flat-faced pellets were used throughout the study. It was assumed that the geometry of these pellets remained constant during the dissolution process. While imposing this restriction on the surface area, it was further assumed that any change in surface area due to the dissolution of the solid would be negligible relative to the total surface area of the exposed solid. The pellets were either mounted in a rotating disc holder or placed in a rotating basket assembly, and rotated at a constant speed of 54 r.p.m. such that the applied agitation was just sufficient to generate a forced convection flow of the dissolution medium around the dissolving solid.

1. Preparation of Pellets

A 400 mg quantity of each test material was compressed into a flat-faced pellet in a 5/8 inch die at a suitable pressure for 1 minute, using a Carver[1] laboratory press.[2] The exposed surface was flushed with gentle air puffs (with the aid of a rubber bulb) to remove any loose powder.

2. Rotating-Basket Method

This method employs a USP-NF rotating basket technique, the details of which are essentially the same as described under U.S.P. XVIII (67) and N.F. XIII (66). In this method, the pellets after compression were removed from the die and stored in a dessicator containing anhydrous calcium

---

[1] Fred S. Carver Inc., Summit, N.J., U.S.A.
[2] See Table XI for details of actual pressures employed.

sulfate until ready for use. The finished pellets were placed inside the rotating basket and the whole assembly was connected to the drive motor.

3. Rotating-Disc Method

This procedure was based on a method as reported by Levy and Sahli (63). The compression of the pellets in the die was carried out first by placing a metal plug over the test material and then by compressing the two together under desired pressure such that the plug remained secured in the die following the removal of the punch. The open end of the die was then sealed off by pouring molten paraffin wax over the metal plug so that only one surface of the pellet was exposed. The die with the pellet in place was stored in a dessicator over anhydrous calcium sulfate until such time as it was ready for use. The die-pellet combination was mounted in the rotating die holder whose shaft was connected to the drive motor.

4. Dissolution Methodology

All dissolution rate studies were run in triplicate, utilizing the USP rotating basket dissolution apparatus. In order to provide sink conditions for the dissolution, a relatively large volume of 1000 ml of distilled water was employed as the dissolution medium. The temperature of this medium was allowed to equilibrate with the temperature of the constant-temperature bath which was maintained at

37±0.5°C. At time zero, the rotating assembly containing the sample was lowered into the dissolution medium to a depth of 5.0 cm from the bottom of the dissolution flask. Rotation was then commenced at a constant speed of 54±1 r.p.m. Sample aliquots were withdrawn at appropriate time intervals and replaced with an equal volume of fresh dissolution medium maintained at 37°C. The aliquots were immediately filtered through 0.45 micron pore size Millipore filters, using Swinney adapters. After suitable dilution of the clear filtrate, the samples were assayed spectrophotometrically. The cumulative amount of the drug dissolved at any given time was corrected for the dilution effect due to repeated sampling, using the Wurster and Taylor equation (94):

$$Y = X_n + \frac{U}{V} \sum_{t=1}^{n-1} X_t \qquad \text{(Eq. 22)}$$

where:

Y = corrected amount dissolved in the n^{th} sample

X_n = uncorrected amount dissolved in the n^{th} sample

U = size of the sample removed

V = volume of the dissolution medium

X_t = uncorrected amount dissolved at time t

E. ANALYTICAL PROCEDURES FOR BIOLOGICAL FLUIDS

1. Estimation of Methisazone in Whole Blood, Plasma, and Urine

Methisazone, an antiviral drug, is sparingly soluble in water. In view of its limited aqueous solubility and

inherent thermal instability, it was felt that GLC techniques for the quantitative analysis of this drug in biological fluids could pose several problems. On the other hand, spectrophotometric techniques involving extraction of methisazone with toluene had been reported in two rather brief and sketchy communiques (95,96). While the procedures appeared to be in a preliminary stage of development, it was considered advisable to study them more fully since no completely tested method for the measurement of methisazone levels in body fluids had been published. As a consequence, a simple, direct, and rapid method of analysis for methisazone using a spectrophotometric technique was developed independently. The rationale for this methodology was based on the observation that methisazone undergoes a bathochromic shift accompanied by a hyperchromic effect in alkaline medium, giving rise to a chromophore-absorbing maximum at 420 nm.

Calibration Curve for Methisazone in 1,4-Dioxane

A stock solution of methisazone was prepared by dissolving 100.0 mg of methisazone in 500 ml of 1,4-dioxane. The stock solution was then serially diluted with 1,4-dioxane to give standard solutions, containing 2.0, 4.0, 8.0, 12.0, 16.0, 20.0, and 24.0 mcg methisazone/ml, respectively.

The stock and standard solutions were freshly prepared. And color development was achieved by diluting the standard solutions with equal volumes of 1 N NaOH. The color was

found to be stable at room temperature for at least five minutes. Using a 1-cm cell, absorbance of the alkaline standard solution was measured against a reagent blank at 420 nm. A Unicam[1] SP 600 Series 2 single-beam spectrophotometer was employed in the determination, and readings were usually taken within one minute of color formation. The standard curve was then constructed by plotting the absorbance values against the corresponding concentrations of methisazone in 1,4-dioxane.

Extraction Procedure

Two milliliter aliquots of rat whole blood, plasma, or urine containing 12-50 mcg methisazone were transferred to 15-ml glass-stoppered conical centrifuge tubes. To each centrifuge tube 8-ml of 1,4-dioxane was added. The mixtures were horizontally shaken on a reciprocating mechanical shaker[2] for 20 minutes. The tubes were then centrifuged for 10 minutes at 3000 r.p.m. A 5-ml portion of the supernatant liquid was removed by aspiration. This protein-free portion was then transferred to a 10-ml volumetric flask, and diluted to volume with 1 N NaOH. The solution was mixed by gently inverting the flask several times. The absorbance of the alkaline sample was then measured immediately at 420 nm against an appropriate blank treated as above. The concentration of methisazone in the sample was determined by reference to the calibration curve constructed previously.

---

[1]Pye Unicam Ltd., York Street, Cambridge, England

[2]Eberbach & Sons, Ann Arbor, Michigan, U.S.A.

Percent Recovery Studies

Blank blood and urine specimens were obtained for the percent recovery studies. In order to get essentially non-hemolyzed whole blood, arterial blood from the abdominal aorta was collected in a heparinized syringe. A portion of the blood sample was centrifuged to harvest clear plasma. The urine samples were simply diluted five-fold with distilled water. Six reference solutions containing known amounts of methisazone in 1,4-dioxane were placed in 15-ml glass-stoppered conical centrifuge tubes, and 2.0 ml of whole blood, plasma, or diluted urine added to each tube and the volume adjusted to 10 ml with 1,4-dioxane. Simultaneously, a series of six reference solutions of equivalent concentrations was prepared. The samples were extracted as described previously under the extraction procedure. The ratio of the amount of methisazone recovered from biological fluids to the amount of methisazone present in the corresponding reference solutions was determined. The quotient of these ratios multiplied by 100 gave the percent recovery of methisazone. In the case of incomplete recoveries from whole blood, plasma, or urine, calibration curves for methisazone in whole blood, plasma, or urine were constructed so that methisazone levels could be corrected for recovery losses.

Reproducibility of the Extraction Procedure

To obtain an estimate of the error due to variation in the extraction procedure, the reproducibility of the

recovery of methisazone from spiked [illegible]es was determined by analyzing replicate samples to which known amounts of methisazone had been added.

Precision of the Measurement

In order to determine the precision of the method of analysis, nine replicate analyses were run on the same blood sample. The precision expressed in terms of the coefficient of variation was calculated according to the following formula:

$$\text{Coefficient of Variation} = \frac{\text{Standard Deviation} \times 100}{\text{Mean}} \qquad \text{(Eq. 23)}$$

2. Colorimetric Determination of N^1-substituted Sulfonamides in Whole Blood

The most commonly used colorimetric method for the quantitative measurement of N^1-substituted sulfonamides in biological fluids is that of Bratton and Marshall (98). This analytical procedure is specific for aryl amines and is based upon the diazotization of the primary amino group attached to the aromatic ring at the N^4-position. The absorbance of the colored diazonium salt was measured at 545 nm. In the present study, this method was selected as the method of choice for the quantitative determination of sulfonamide levels in blood.

Calibration Curves

One hundred mg each of sulfisoxazole and sulfamethoxazole, previously dried at 105°C for 5 hr. were accurately weighed and quantitatively transferred to 2000-ml volumetric flasks. The powders were then dissolved in a minimum amount of methanol and diluted to volume with distilled water. Suitable aliquots of this stock solution were further diluted with distilled water to obtain standard solutions in the 2.5-100 mcg/ml range. One ml each of the standard solutions was pipetted into 10-ml volumetric flasks. To each flask 0.2 ml of 15% trichloroacetic acid was added followed by 1.0 ml of 0.1% sodium nitrite. The flasks were stoppered and the contents mixed. The mixtures were allowed to stand for 5 minutes before the excess nitrous acid was destroyed by the addition of 1.0 ml of 0.5% ammonium sulfamate. As soon as nitrogen evolution had ceased, 1.0 ml of 0.1% N-(1-naphthyl) ethylenediamine dihydrochloride was added. After the color had developed the volume was adjusted to the mark with distilled water. A reagent blank was also prepared. All the reagents were freshly prepared. The absorbance of the standards was measured in a 1-cm cell against the reagent blank at 545 nm., using the Unicam SP 600 spectrophotometer. Standard curves were then constructed by plotting absorbance as a function of concentration.

Extraction Procedure

One hundred microliter aliquots of rat whole blood were hemolyzed with 1.9 ml of distilled water in 15-ml glass-stoppered conical centrifuge tubes. To each tube 2.0 ml of 15% trichloroacetic acid was added followed by 6.0 ml of distilled water. The stoppered tubes were horizontally shaken on the reciprocating mechanical shaker for 20 minutes after which they were centrifuged for 10 minutes at 3000 r.p.m. The protein-free supernatant liquids were recovered by aspiration and 1.0 to 7.0 ml aliquots of these were analyzed by the colorimetric procedure described previously.

Percent Recovery Studies

Blank blood was hemolyzed by diluting it five-fold with distilled water. Six reference solutions containing known amounts of sulfisoxazole or sulfamethoxazole were placed in 15-ml glass-stoppered conical centrifuge tubes. Two ml of hemolyzed blood was added to each tube followed by 2.0 ml of 15% trichloroacetic acid and the volume was adjusted to 10.0 ml with distilled water. Simultaneously, a series of six reference solutions of equivalent concentrations was prepared. The samples were extracted as described previously. Percent recoveries of sulfisoxazole or sulfamethoxazole from whole blood were determined by the method described under percent recovery studies.

Reproducibility of the Extraction Procedure

The reproducibility of the recovery of sulfisoxazole or sulfamethoxazole from spiked whole blood was determined by the procedure identical to that described for methisazone.

Precision of the Measurement

The precision of the colorimetric method was determined by a procedure identical to that described for methisazone.

F. BIOAVAILABILITY STUDIES

The *in vivo* availability profiles obtained following oral administration of the pure drugs, solid dispersions, and physical mixtures were compared by estimating the rate and extent of absorption in the rat based on the evaluation of blood levels and urinary excretion data.

1. Protocol for Single-Dose Oral Administration to Rats

Adult albino male rats of the Wistar strain weighing between 350-500 g were used as the test animals in this study. The rats were isolated by individually housing them in cages. The rats were fasted for 16 hr. prior to oral administration, but water was accessible for drinking. However, water was removed from the animals one hour before the commencement of the experiment. Blood and urine specimens collected prior to drug administration were treated as the blanks. The animals were given by oral intubation[1] a single dose of 500 mg of the drug or its equivalent per kg body weight as an aqueous suspension. The suspensions were made in a 0.2% aqueous solution of methylcellulose just prior to the time of dosing. All doses were prepared

---

[1] Intubation was carried out by means of a 15-gauge needle which was 7 cm long with an external diameter of 3mm.

as 50 mg/ml and were administered to unanesthetized animals at a constant dosing volume of 10 ml/kg.

2. Blood Level Studies in Rats

Estimation of Methisazone

Twenty-four animals were used in this study. Groups of three rats each were sacrificed at predetermined time intervals of 0.25, 0.5, 1, 2, 3, 4, 5, 6, 7, and 8 hr. following oral administration of a single dose. No drug was detected in the blood 8 hr. after ingestion of methisazone. All animals were anesthetized by injecting urethane (ethyl carbamate) intraperitoneally at the dose level of 1.5 mg/g. Blood samples were drawn into heparinized syringes from the heart by cardiac puncture. A 2.0 ml aliquot of each heparinized blood specimen was immediately analyzed by the method described previously under analytical procedure. Each blood specimen was analyzed in duplicate, using blood obtained from control animals as a blank. As a check on the assay procedure, reference standard solutions of methisazone were assayed concurrently with unknown blood samples.

Estimation of N^1-substituted Sulfonamides

Three animals were used in this study. Each animal was treated as his own control. Blood specimens were obtained prior to and at specified times after oral administration of a single dose. One hundred microliters of whole blood samples were withdrawn from the tail vein into heparinized disposable micro-pipettes[1]. The contents of

[1]Clay Adams, Becton, Dickinson and Company, Parsippany, N.J., U.S.A.

the pipettes were expelled into 15-ml glass-stoppered conical centrifuge tubes containing 1.9-ml distilled water. The inside of the pipettes was rinsed two or three times. Two ml aliquots of 15% trichloroacetic acid were added to each tube. The volume was then adjusted to 10-ml with distilled water. The blood specimens were then analyzed according to the method described previously under analytical procedures.

3. Urinary Excretion Studies

Urinary excretion studies of methisazone were conducted under uncontrolled urinary pH conditions using three animals. The animals were placed in individual metabollic cages, and allowed to fast for 16 hr. Blank urine samples were collected prior to the oral administration of a single dose. Urine samples were collected for 72 hr. except in certain instances where urine was collected for 96 hr. Both the urine and the washings were combined and transferred to 25-ml volumetric flasks. The volume was then adjusted to the mark with distilled water. The diluted urine samples were then centrifuged for 10 minutes at 3000 r.p.m. and 2.0-ml aliquots of these were analyzed by the method described previously under analytical procedure.

RESULTS

A. THERMAL ANALYSIS STUDIES

Sekiguchi et al. (99) have proposed three methods of sample preparation for thermal analysis. These methods may be referred to as the physical mixture, the fusion, and the solvent evaporation methods. The authors also reviewed the merits of these methods with regard to the determination of phase diagrams. In their opinion the presence of a large surface area in both the fused and evaporated mixture samples would cause melting to occur at the correct temperature, and hence data obtained on these mixtures would be more meaningful in constructing phase diagrams. It is believed that samples prepared by the evaporation method may show better thermal stability than those prepared by the fusion method. Certainly in those instances where the components have a tendency to decompose on fusion, the evaporation method would be indicated for thermal analysis. Chiou and Niazi (19) have indicated that the interpretation of phase diagrams constructed from data obtained on physical mixtures alone can be inconclusive or erroneous in confirming the existence of solid solution formation.

1. Calibration of the Instruments

The operating conditions for the Fisher QDTA[1] are listed under Table I. It can be seen from the table that the sen-

---

[1]Quantitative differential thermal analyzer

TABLE I

Operating Conditions for the Fisher Quantitative Differential Thermal Analyzer

Variables	Standards[a]	SX[b]	SM[c]	MZ[d]
Sample Size:	15.0 mg	8.0 mg	5.0 mg	5.0 mg
Reference:	Empty Pan	Empty Pan	Empty Pan	Empty Pan
Atmosphere:	Static Air	Static Air	Static Air	Static Air
Chart Speed:	1 in min^{-1}	0.5 in min^{-1}	0.5 in min^{-1}	0.5 in min^{-1}
Program Rate:	20°C min^{-1}	20°C min^{-1}	10°C min^{-1}	10°C min^{-1}
Sensitivity:				
ΔT -	0.3°C in^{-1}	0.3°C in^{-1}	0.3°C in^{-1}	0.3°C in^{-1}
T -	13.7°C in^{-1}	13.7°C in^{-1}	13.7°C in^{-1}	13.7°C in^{-1}

[a]Fisher calorimetric standards
[b]Sulfisoxazole
[c]Sulfamethoxazole
[d]Methisazone

TABLE II

Calibration Data[a] for the Fisher Quantitative Differential Thermal Analyzer

Calorimetric Standards	Fusion Temperature, °C	Calibration Coefficient, mcal deg^{-1} min^{-1}
Naphthalene	84.0	1.23±0.08
Indium	155.0	1.34±0.04
Tin	230.0	1.40±0.03
Lead	323.0	1.74±0.20
Zinc	471.0	2.07±0.15

[a]Mean values from three thermograms with standard deviation

sitivity of the instrument was kept constant throughout the investigation. The calibration data for the Fisher QDTA are summarized in Table II. The theoretical heats of fusion used in the determination of calibration coefficients were 35.06, 6.79, 14.24, 5.50, and 24.40 cal/g for Naphthalene, Indium, Tin, Lead, and Zinc respectively. The fusion temperature for each standard sample was taken as the extapolated peak temperature of the endothermic peak. The plot of the calibration coefficients versus the fusion temperature is shown in Figure 1. In order to confirm the validity of the calibration, the heats of fusion of two reference substances, benzoic acid and sulfathiazole, were determined. As can be seen from Table III, the observed values were in agreement with reported literature values (92,93).

The data for the calibration of the Thomas-Hoover Capillary Melting Point Apparatus is presented in Table IV and the calibration curve for the instrument is depicted in Figure 2.

2. Construction of Phase Diagrams

The construction of phase diagrams from data obtained by thermal analyses can provide information on the mechanism for solid dispersion formation. Sekiguchi et al. (100) have pointed out that the incidence of either congruent or incongruent melting points in binary systems is usually associated with complex formation between the two components. On the basis of phase diagram studies, they were able to

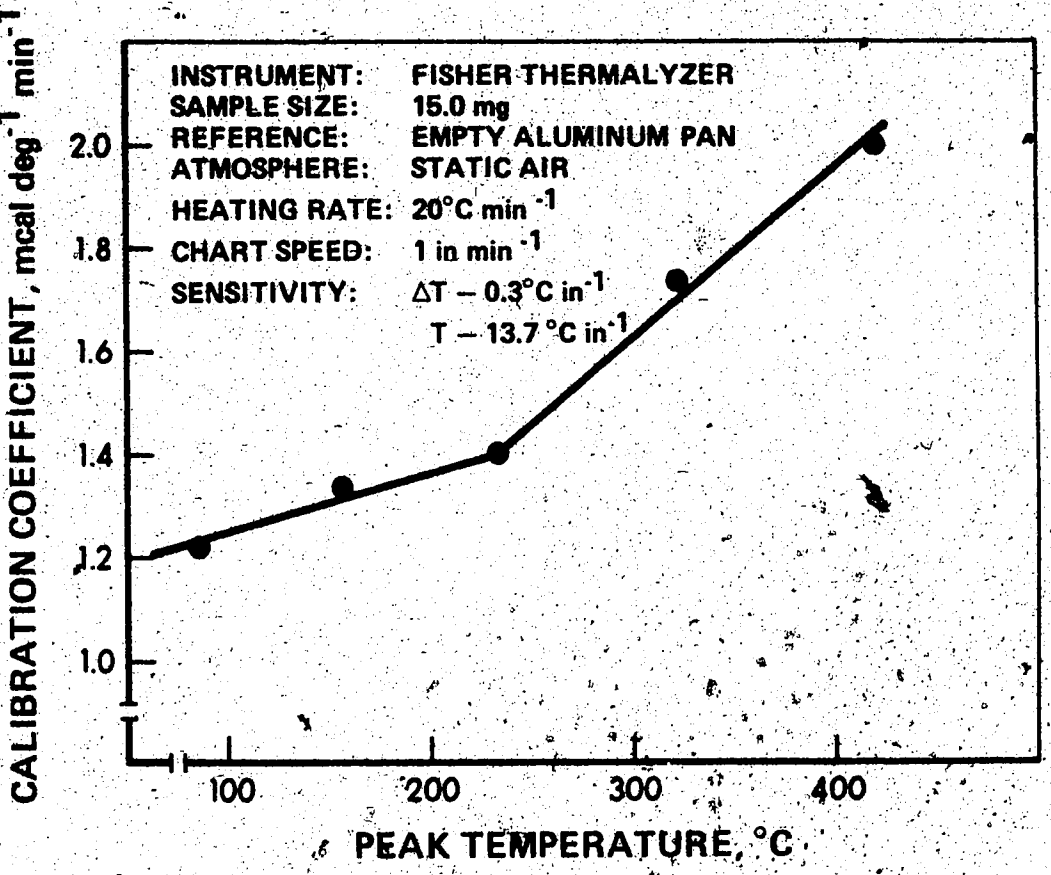

Figure 1 - Calibration Curve for the DTA Instrument

TABLE III

Calorimetric Measurements of Reference Substances

	Observed[a]	Reported
Benzoic Acid[b]		
Fusion Temperature (°C)	126.00	122.40
Heat of Fusion (cal/g)	37.20	33.89
Sulfathiazole[c]		
Transition Temperature (°C)	167.00	161.00
Heat of Transition (Kcal/mole)	1.47	1.42
Fusion Temperature (°C)	203.00	200.00
Heat of Fusion (Kcal/mole)	7.14	5.97

[a]Average of three determinations
[b]Reported literature values (93)
[c]Reported literature values (92)

TABLE IV

Calibration Data for the Thomas-Hoover Capillary Melting Point Apparatus

Reference Standards[a]	Melting Point, °C	
	Expected	Observed[b]
Vanillin	83.0	83.8
Acetanilid	116.0	116.2
Acetophenetidin	136.0	136.7
Sulfanilamide	166.5	165.5
Sulfapyridine	193.0	191.9
Caffeine	237.5	235.3

[a]Arthur H. Thomas Co., Phila., Pa., U.S.A.
[b]Average of nine determinations

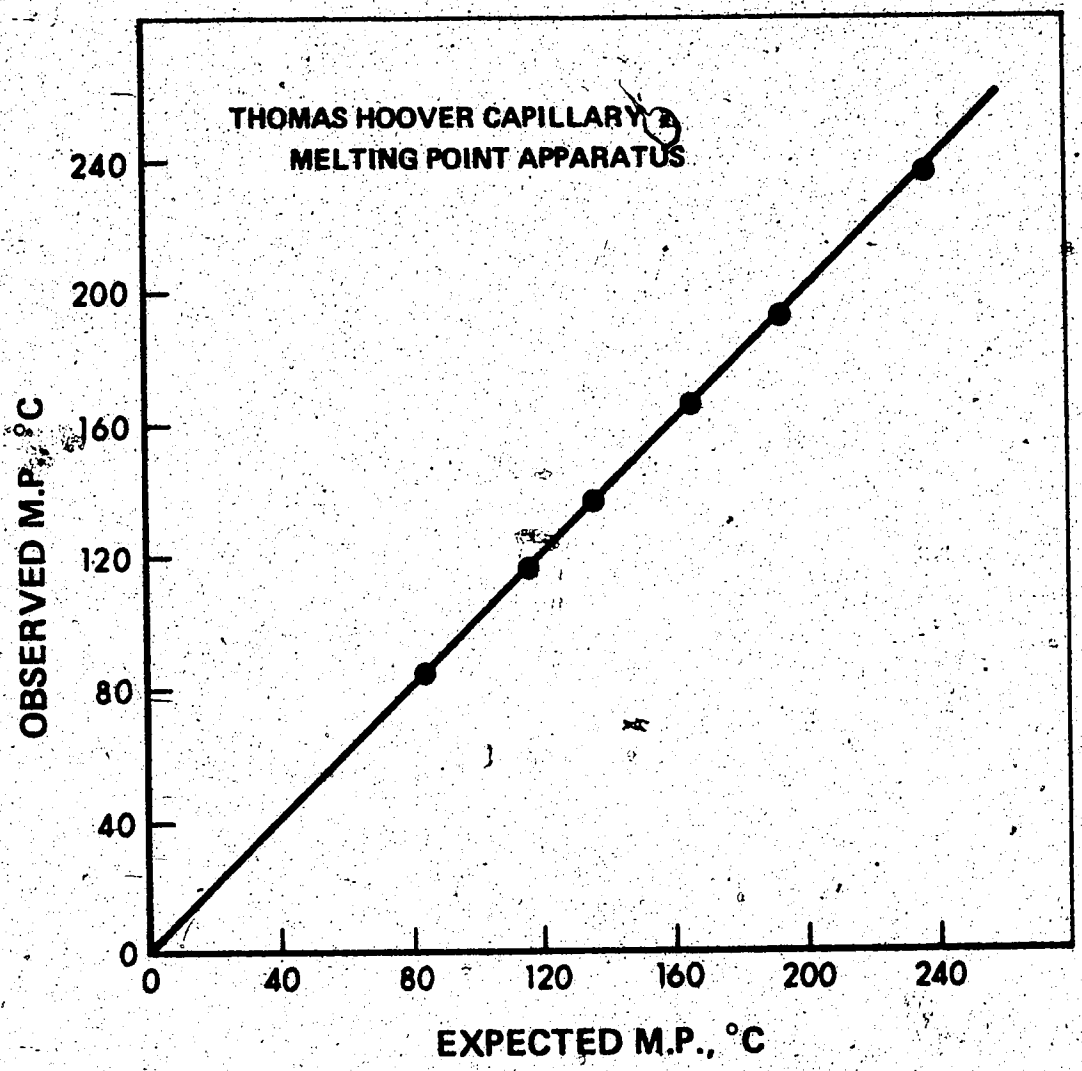

Figure 2 - Calibration Curve for the Capillary Melting Point Apparatus

characterize a sulfisoxazole-aminopyrine binary mixture as a eutectic system in which a complex with incongruent melting point was formed between the components.

During the initial differential thermal analyses, it was found that a re-run of the re-solidified urea samples obtained from the original run yielded thermograms showing an extra endothermic peak at 100°C. In addition to this, a definite shift of the major endotherm to a lower temperature was observed in each case. It can be seen from Figure 3 that, on repeated DTA runs, the thermal effects of the extra endothermic peak are magnified. This implies that urea partially decomposes on melting and subsequently forms a eutectic mixture with its thermally-decomposed fraction. Because of the decomposition of urea on exposure to heat, the use of samples prepared by the fusion method was precluded from this study. Instead, evaporated mixtures were used throughout the present investigation. Phase diagrams were constructed by plotting the thaw and melting point temperatures against corresponding composition of the binary mixtures.

Solid Dispersions containing Urea

The capillary melting point data as shown in Tables V and VI were obtained on the evaporated mixtures. The phase diagrams for the sulfisoxazole-urea and sulfamethoxazole-urea binary systems constructed from the capillary melting

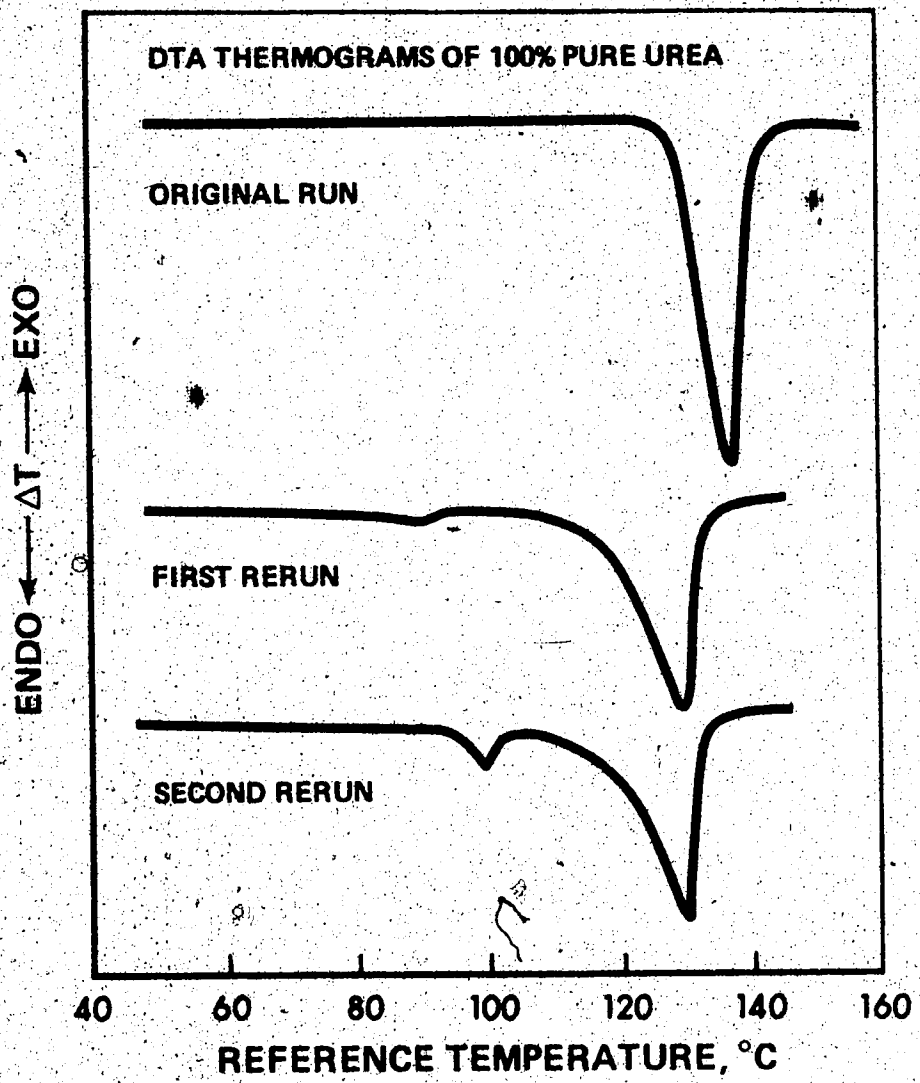

Figure 3 - DTA thermograms of Pure Urea

TABLE V

Capillary Melting Point Data for Phase Diagram of Sulfisoxazole-Urea Binary System

Percent Sulfisoxazole	Temperature[a], °C Thaw Point	Incongruent Melting Point	Melting Point
0.0	135.0		137.0[b]
2.0	132.2		136.0
5.0	132.0		135.0
10.0	131.0		134.0
20.0	131.0		133.0
25.0	131.0		132.2
30.0	131.0		133.0
40.0	132.0	134.0	138.2
50.0	132.0	136.0	143.0
60.0	135.0	139.2	147.0
70.0	138.0	141.20	151.0
80.0	138.0	150.0	168.0
90.0	164.0		181.0
95.0	175.0		189.0
98.0	184.0		195.0
100.0	192.0		200.0[c]

[a]Average of five determinations

[b]Melting point of pure urea

[c]Melting point of pure sulfisoxazole

TABLE VI

Capillary Melting Point Data for Phase Diagram of Sulfamethoxazole-Urea Binary System

Percent Sulfamethoxazole	Temperature[a], °C		
	Thaw Point	Incongruent Melting Point	Melting Point
0.0	135.0		137.0[b]
5.0	124.6		135.0
10.0	120.4		133.4
20.0	119.0		131.0
30.0	119.4		130.0
40.0	118.0	122.0	128.0
50.0	120.0	122.4	126.0
55.0	119.0	122.0	125.0
60.0	118.0	122.0	124.0
65.0	119.0	122.0	128.0
68.0	118.0	122.0	131.0
70.0	119.0	122.0	133.0
75.0	119.4	122.0	138.0
80.0	119.0	122.4	146.0
90.0	120.0		156.0
95.0	123.0		163.8
100.0	167.0		170.0[c]

[a]Average of five determinations

[b]Melting point of pure urea

[c]Melting point of pure sulfamethoxazole

point data are shown in Figures 4 and 5. DTA thermograms of the sulfisoxazole-urea system are depicted in Figures 6 and 7, and those of the sulfamethoxazole-urea system in Figures 8 and 9. The thermograms for 100% urea, 100% sulfamethoxazole, and 100% sulfisoxazole exhibit fusion peaks at 134, 165, and 192°C, respectively. These data compare favorably with literature values of 136°C (19), 166.3°C, and 195°C (101), indicating that these compounds were of satisfactory purity.

A phase diagram of the methisazone-urea binary system was constructed from differential thermal analysis data obtained on the evaporated mixtures. The data for the phase diagram, as shown in Figure 10, are summarized in Table VII. Figures 11 and 12 illustrate DTA thermograms of the methisazone-urea binary system. These thermograms were used in the construction of the subsequent phase diagram.

Solid Dispersions containing PVP

The thermal analysis of binary systems containing PVP indicated that there was no phase relationship between the components involved. The effects of varying amounts of PVP on the melting points of sulfisoxazole, sulfamethoxazole, and methisazone are illustrated in Figures 13, 14, and 15 respectively.

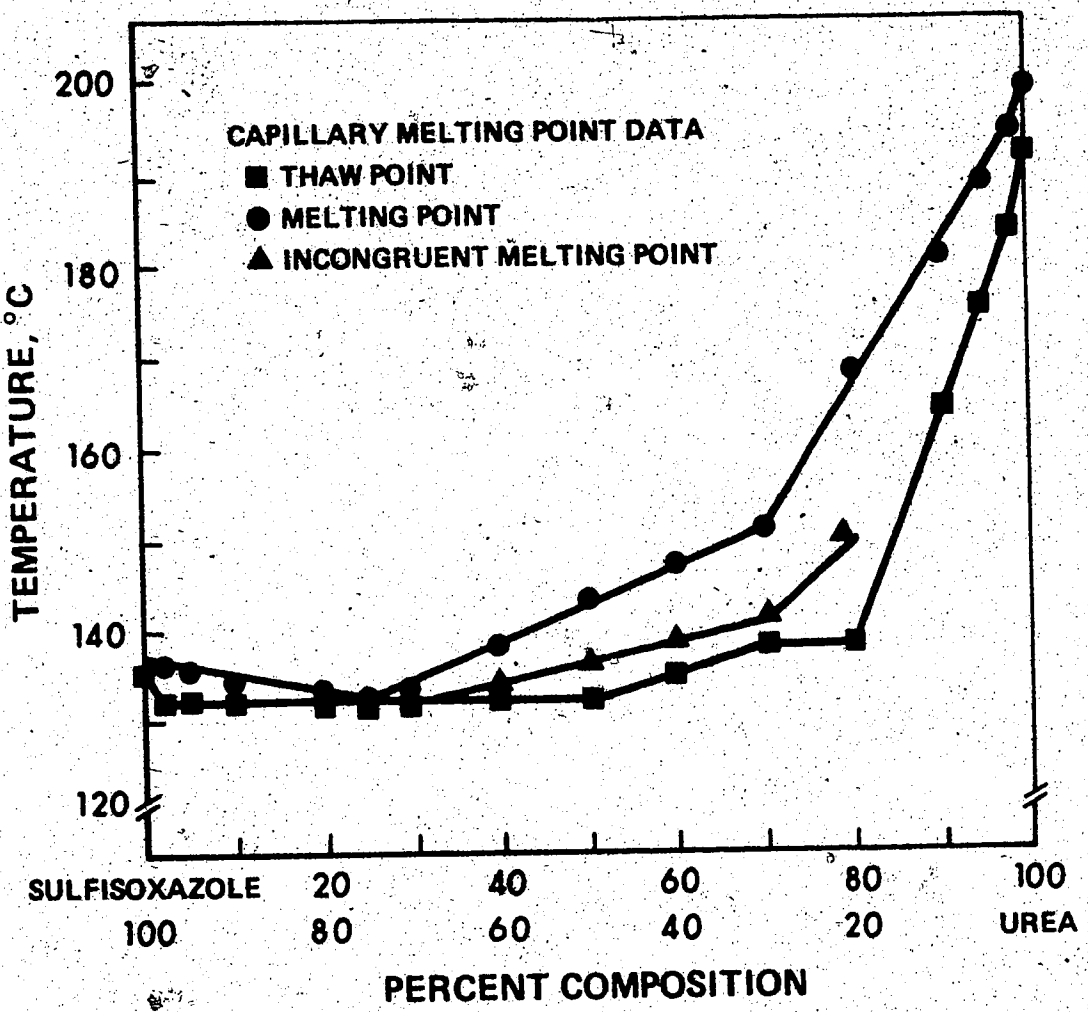

Figure 4 - Phase Diagram of Sulfisoxazole-Urea Binary System

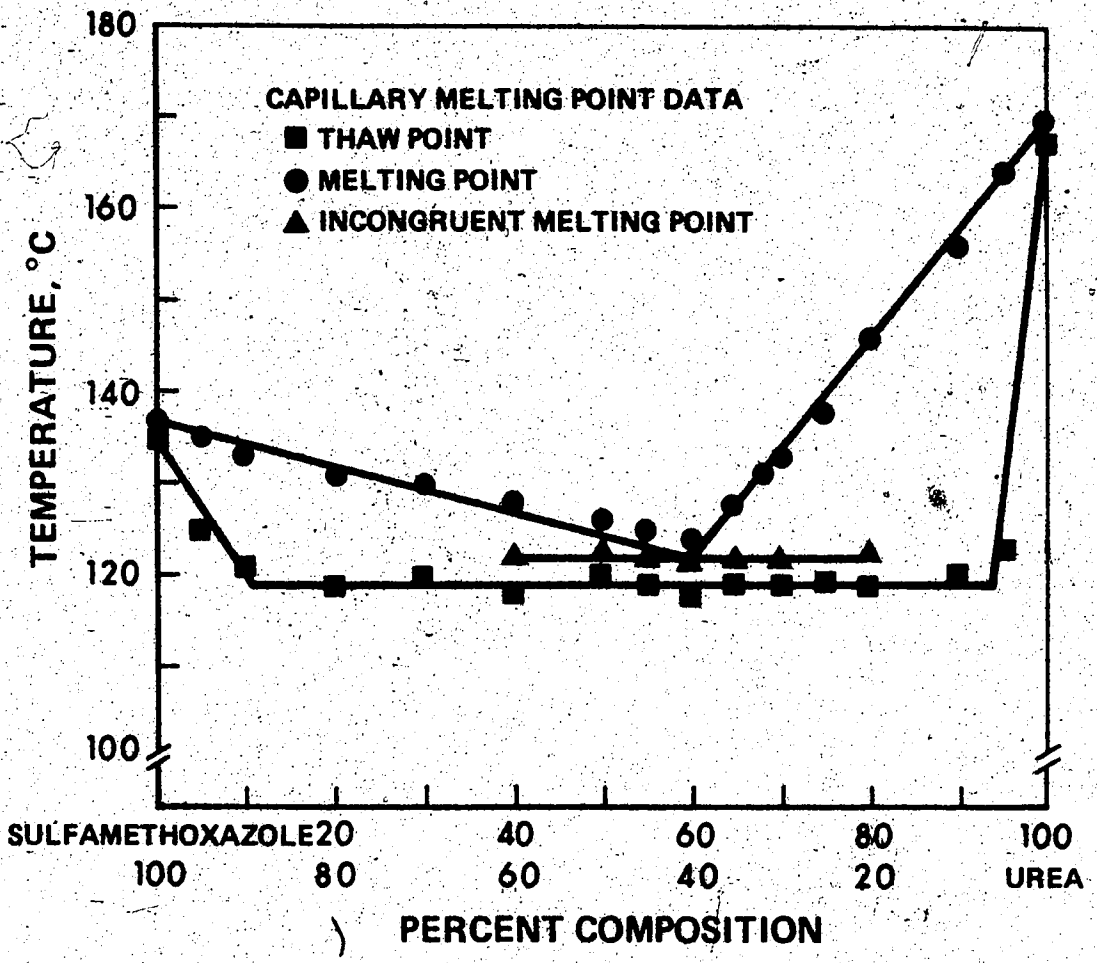

Figure 5 - Phase Diagram of Sulfamethoxazole-Urea Binary System

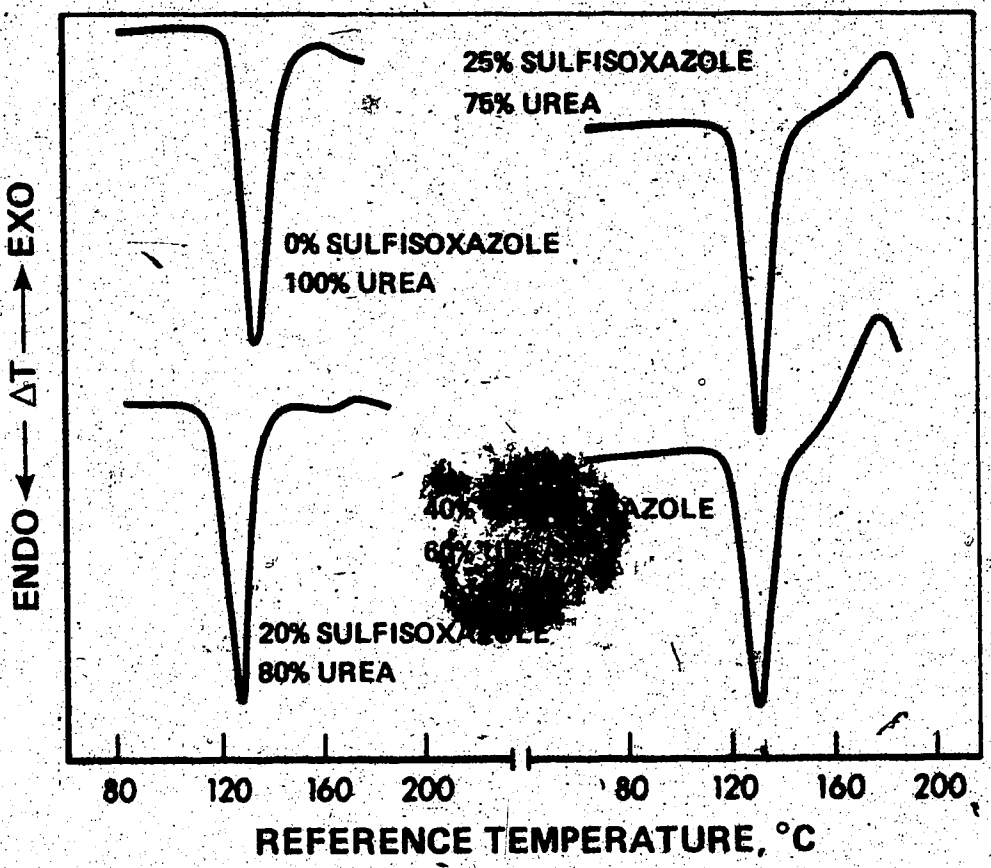

Figure 6 - DTA thermograms for Sulfisoxazole-Urea Binary System

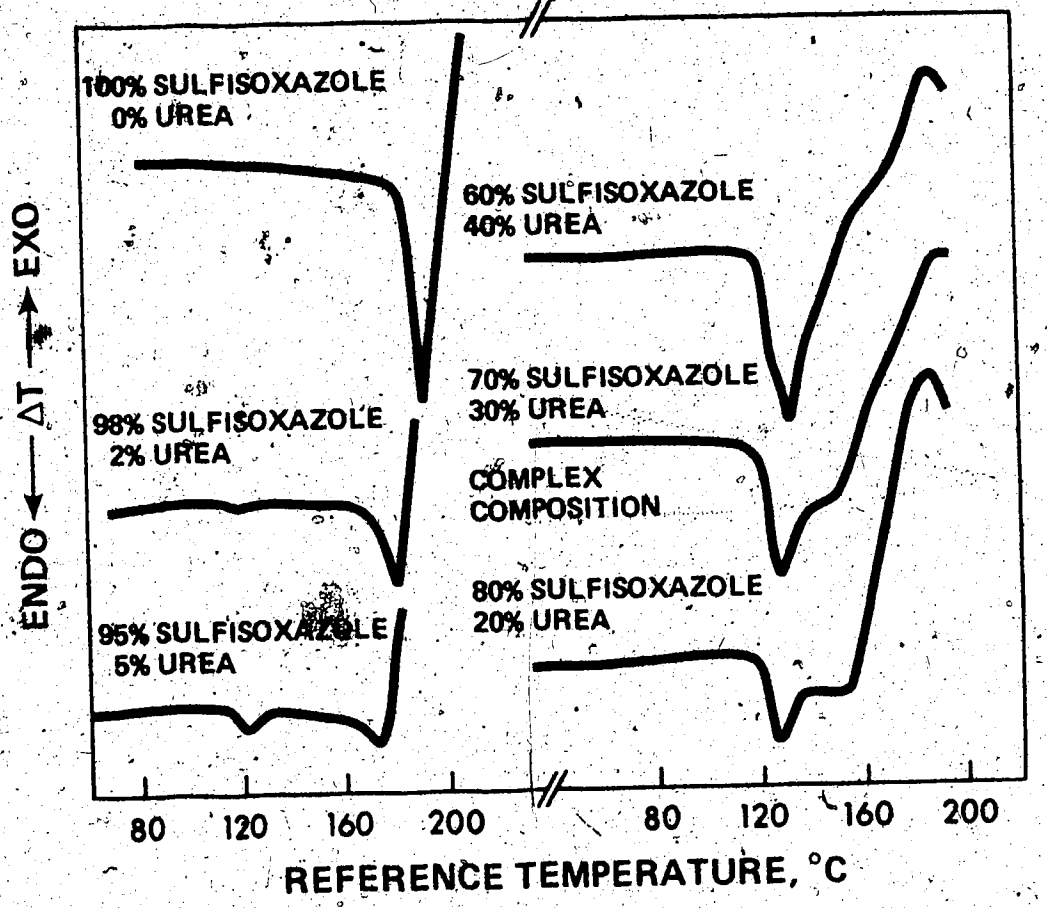

Figure 7 - DTA thermograms for Sulfisoxazole-Urea Binary System

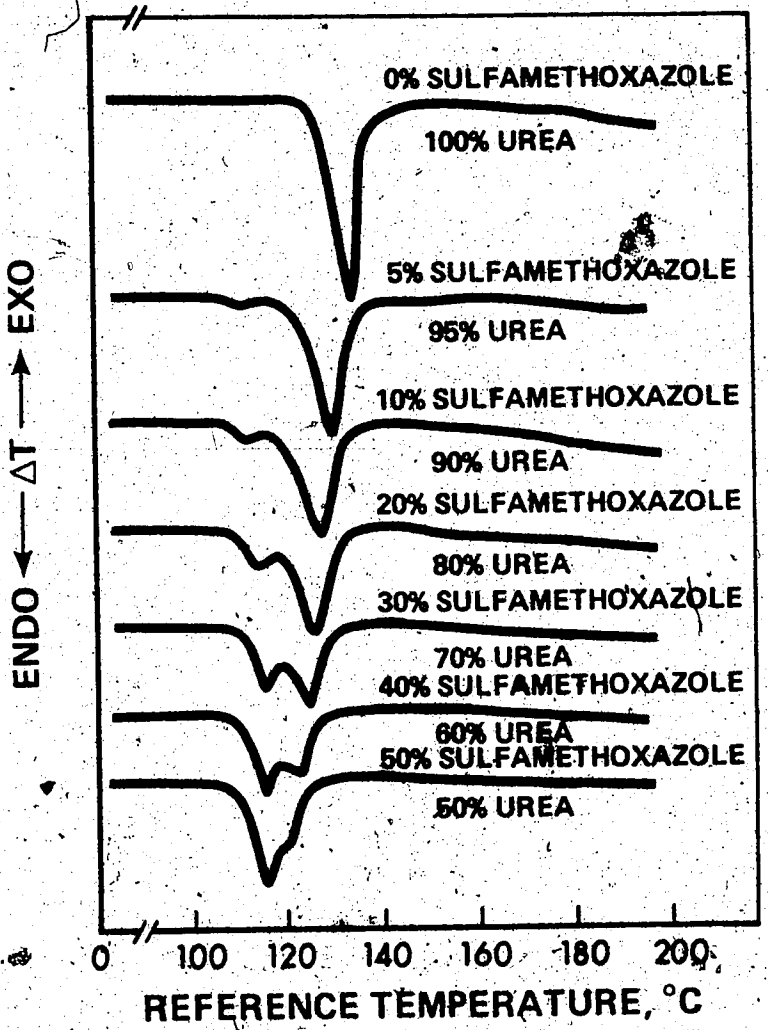

Figure 8 - DTA thermograms for Sulfamethoxazole-Urea Binary System

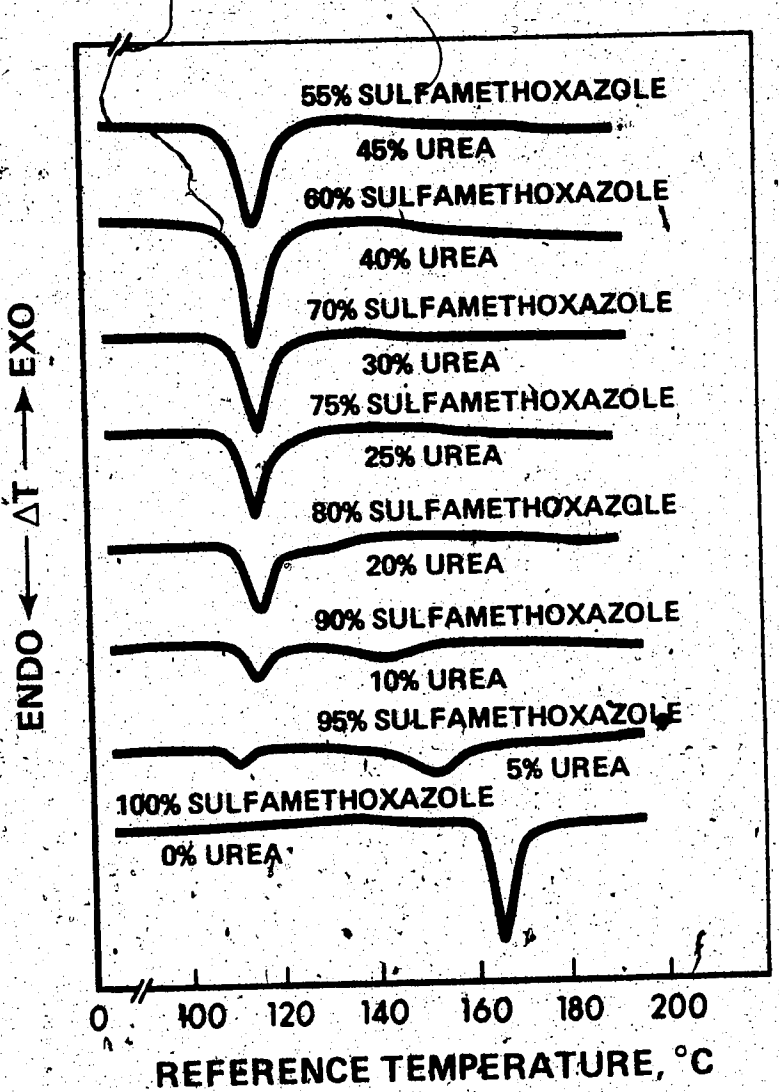

Figure 9 - DTA thermograms for Sulfamethoxazole-Urea Binary System

TABLE VII

Differential Thermal Analysis Data for Phase Diagram of Methisazone-Urea Binary System

Percent Methisazone	Temperature[a], °C		
	Eutectic	Peritectic	Liquidus
0.0	127.0		132.3[b]
2.0	126.0		131.0
5.0	124.0		129.0
	129.0		185.3
10.0	129.0		187.0
15.0	128.0	187.0	198.0
20.0	128.0	187.0	202.0
30.0	127.3	186.6	211.3
40.0	126.3	186.3	215.0
49.0	128.3	190.6	217.3
50.0	126.3	187.3	217.0
51.0		187.3	219.0
55.0		186.0	217.0
60.0		185.3	220.6
70.0		181.3	226.0
90.0		181.0	238.6
100.0		245.0	250.3[c]

[a] Mean values from three DTA thermograms
[b] Melting point of pure urea
[c] Melting point of pure methisazone

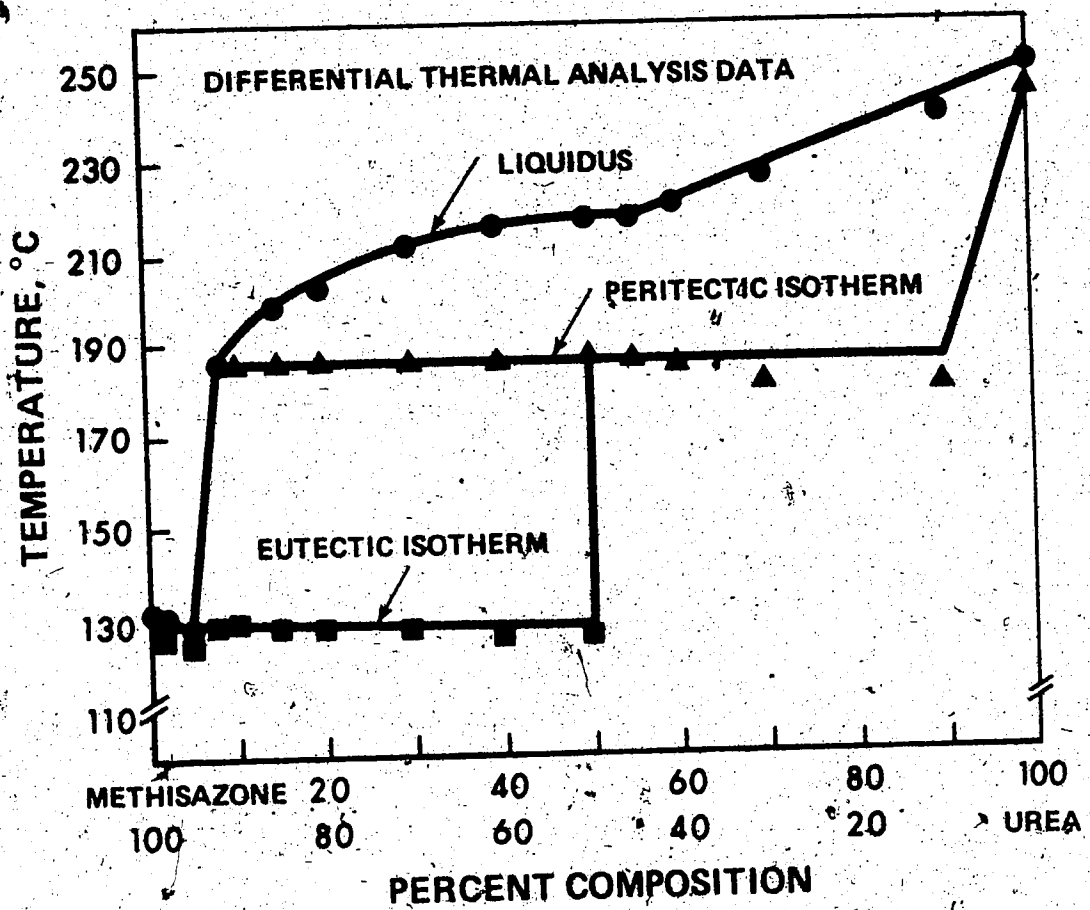

Figure 10 - Phase Diagram of Methisazone-Urea Binary System

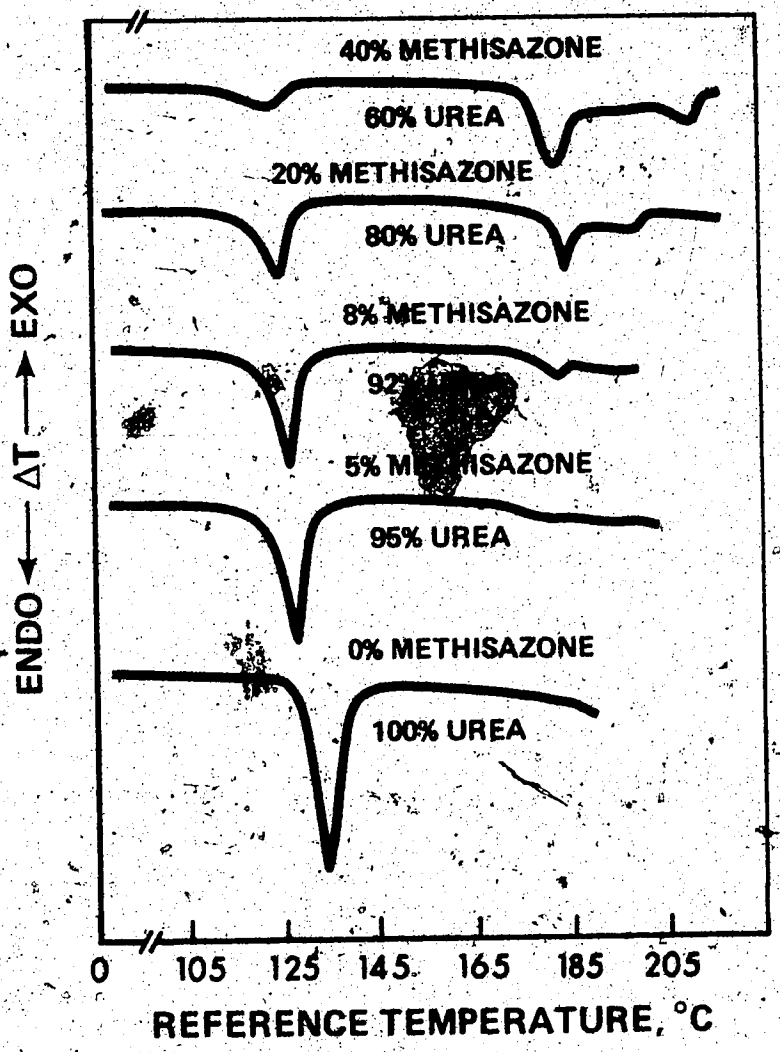

Figure 11 - DTA thermograms for Methisazone-Urea Binary System

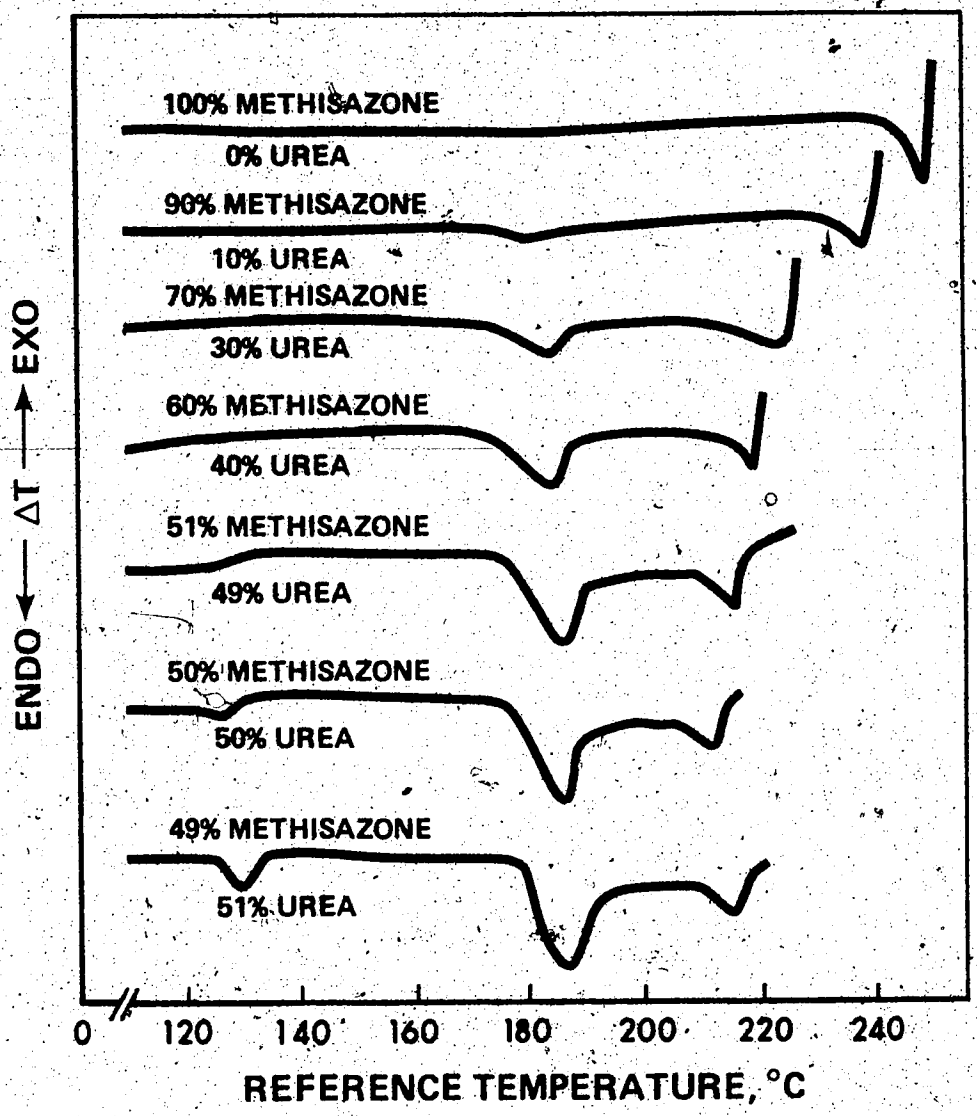

Figure 12 - DTA thermograms for Methisazone-Urea Binary System

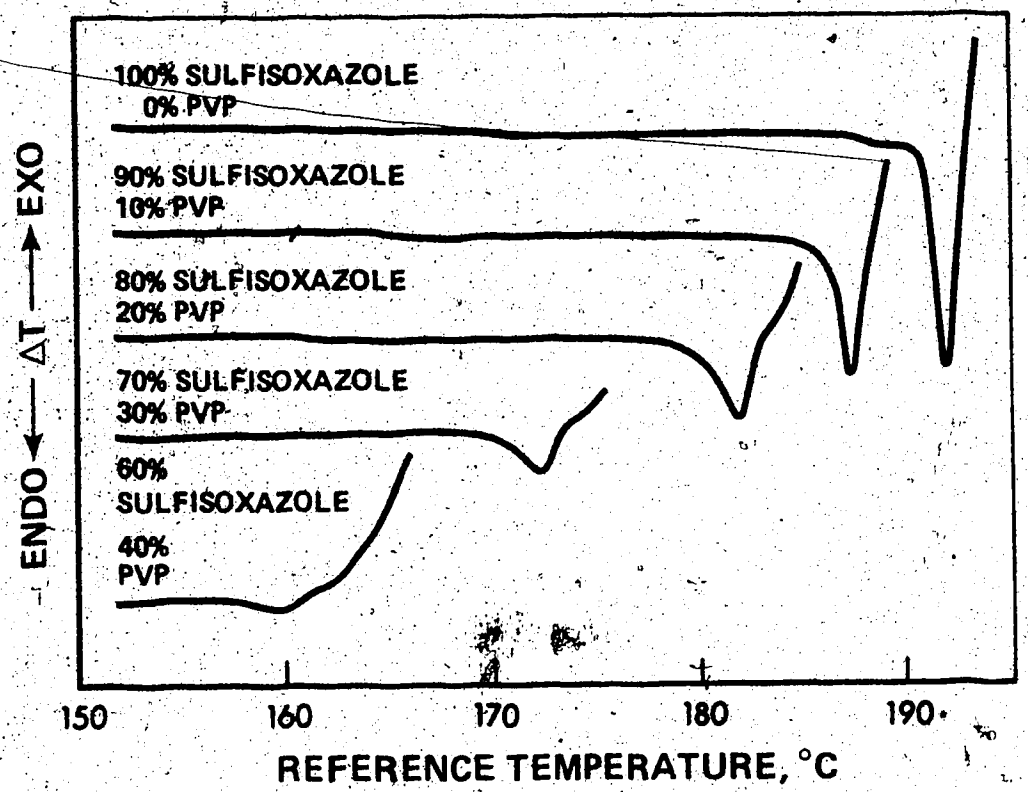

Figure 13 - DTA thermograms for Sulfisoxazole-Polyvinylpyrrolidone Binary System

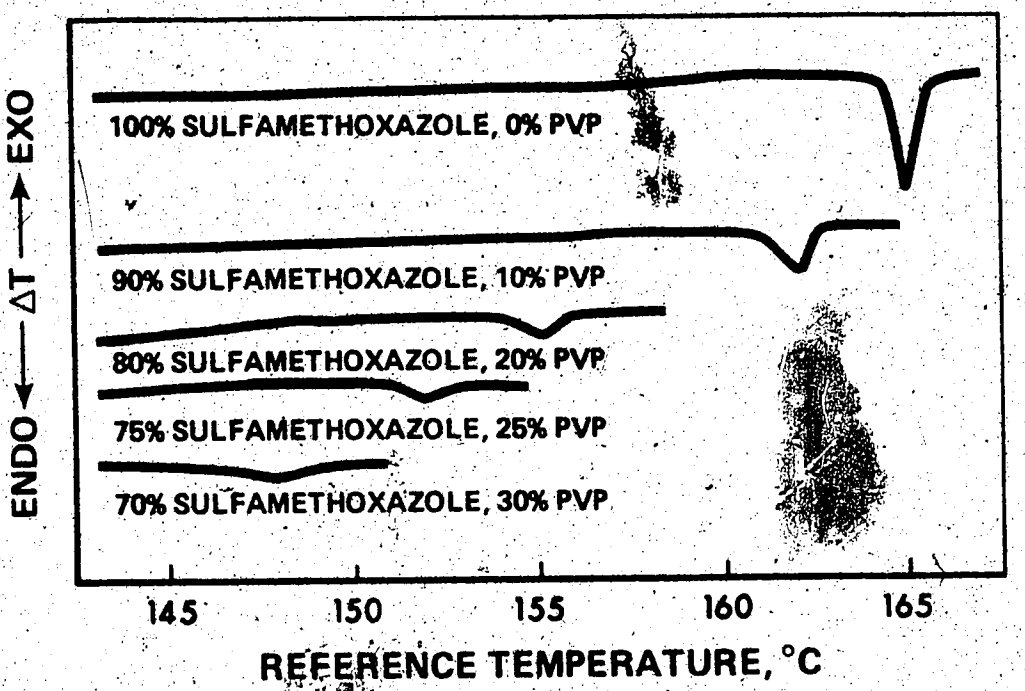

Figure 14 - DTA thermograms for Sulfamethoxazole-Polyvinylpyrrolidone Binary System

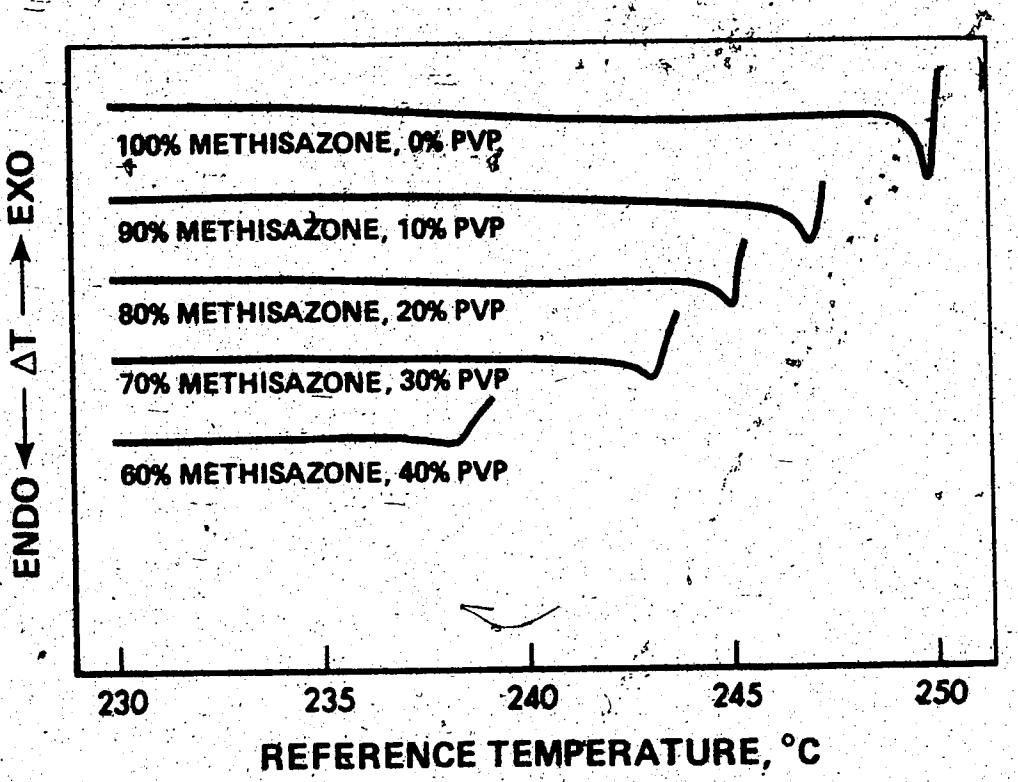

Figure 15 - DTA thermograms for Methisazone-Polyvinylpyrrolidone Binary System

B. EQUILIBRIUM SOLUBILITY STUDIES

Equilibrium solubility studies were conducted with a view to determining any possible interaction between drug and carrier in aqueous solution as well as the significance of the solubilizing effect. The solubility method described by Higuchi and Zuck (31,32,33) was used to determine the thermodynamic parameters for the urea and polyvinylpyrrolidone complexing systems. The average molecular weight of the PVP used in the present study was approximately 40,000.

1. Theoretical Considerations

According to the law of mass action, the bimolecular interaction between drug and carrier may be represented as:

$$mD + C \underset{k_2}{\overset{k_1}{\rightleftharpoons}} D_m{-}C \qquad \text{(Eq. 24)}$$

where D is the drug, C is the carrier, m is the number of moles of drug, k_1 is the association rate constant, and k_2 is the dissociation rate constant. The association equilibrium constant, K_a, for the interaction may be written as:

$$K_a = \frac{k_1}{k_2} = \frac{\left[D_m{-}C\right]}{\left[D\right]^m \left[C\right]} \qquad \text{(Eq. 25)}$$

The nature of complex formation at any given temperature can be investigated by empirically determining the association equilibrium constant for the complex by the use of the following relationship (102):

$$K_a = \frac{(D_c - D_s)}{(D_s)^m \left[mC_o - (D_c - D_s)\right]} \qquad \text{(Eq. 26)}$$

where:

D_c = total molar concentration of drug in presence of carrier

D_s = saturation solubility of drug in moles per liter in absence of carrier

C_o = original molar concentration of carrier added to the system

Dividing both the numerator and the denominator of the second term of Eq. 26 by the original carrier concentration, C_o, we have:

$$K_a = \frac{(D_c - D_s)/C_o}{(D_s)^m \left[m - \frac{(D_c - D_s)}{C_o}\right]} \qquad \text{(Eq. 27)}$$

As can be seen from Eq. 27, the association equilibrium constant, K_a, can be evaluated from solubility measurements by plotting drug solubility against carrier concentration. When a plot of the total molar concentration of drug, D_c, versus the original molar concentration of carrier, C_o, yields a straight line with intercept D_s and slope equal to $(D_c - D_s)/C_o$, Eq. 27 may simply be written as:

$$K_a = \frac{\text{Slope}}{(D_s)^m \ (m - \text{Slope})} \qquad \text{(Eq. 28)}$$

Connors and Mollica (102) have pointed out that, if the slope of the solubility plot is less than one, then the complex formed is of the 1:1 type. However, if the slope is greater than unity, then m is probably equal to 2. Similarly, if the value of the slope is greater than 2, then

value of m is probably equal to 3. These authors have also indicated that the solubility diagrams may show either linearity or positive curvature depending upon whether the complex formed has one or two moles of carrier.

The association equilibrium constant, K_a, is related to the standard free energy change, ΔF^o, by the following relationship:

$$-\Delta F^o = R\,T\,\ln K_a \qquad \text{(Eq. 29)}$$

The dependence of association equilibrium constants on temperature can be represented by the Gibbs-Helmholtz equation:

$$\log K_a = \frac{-\Delta H_f^o}{2.303R} \cdot \frac{1}{T} + \text{Constant} \qquad \text{(Eq. 30)}$$

According to Eq. 30, a plot of log K_a versus 1/T should result in a straight line relationship, assuming that ΔH_f^o is independent of temperature. The heat of formation, ΔH_f^o, then can be calculated from the slope of the line as follows:

$$\Delta H_f^o = -\text{slope} \times 2.303\ R \qquad \text{(Eq. 31)}$$

When the values of K_a at two temperatures are known, the heat of formation, ΔH_f^o, can be determined from the following equation:

$$\log \frac{K_a \text{ at } 25^oC}{K_a \text{ at } 37^oC} = \frac{-\Delta H_f^o}{2.303\ R} \left[\frac{1}{T_{298}} - \frac{1}{T_{310}} \right] \qquad \text{(Eq. 32)}$$

The entropy change, ΔS°, for the interaction can be calculated by substituting ΔH° and ΔF° into the following equation:

$$\Delta S^{\circ} = \frac{\Delta H_f^{\circ} - \Delta F^{\circ}}{T} \qquad \text{(Eq. 33)}$$

2. Calibration Curves, Solubility Data and Thermodynamic Parameters

The data for the calibration curves of sulfisoxazole, sulfamethoxazole, and methisazone in distilled water, as depicted in Figure 16, are summarized in Table VIII. The effects of urea and polyvinylpyrrolidone on the solubility of various drugs in distilled water at 25 and 37°C are reported in Tables A-1 to A-4 (Appendix A). The drug solubilities as a function of carrier concentration at 25 and 37°C were plotted as shown in Figures 17-20. The regression lines were fitted to the solubility data by a computer-programmed least-squares method, using a PDP-8/L minicomputer[1]. The co-ordinate units were converted into molar units and slopes were determined to facilitate comparative evaluation. The association equilibrium constants were then computed by substituting the values of the slopes and D_s in Equation 28. The values of thermodynamic parameters for the interaction were then obtained from association equilibrium constants determined at 25 and 37°C. The free energy change, the heat of formation, and the entropy change were calculated by solving Equations 29, 32, and 33 respectively. The data obtained on these thermodynamic parameters are summarized in Tables IX and X.

[1]Digital Equipment Corporation, Maynard, Massachusetts, U.S.A.

TABLE VIII

Linear Relationship between Absorbance and Drug Concentration in Water

Concentration	Absorbance[a]		
mcg/ml	Sulfisoxazole[b]	Sulfamethoxazole[b]	Methisazone[c]
1.25	--	--	0.070±0.006
2.50	0.150±0.010	0.130±0.010	0.150±0.006
3.75	--	--	0.240±0.000
5.00	0.300±0.015	0.277±0.015	0.330±0.006
6.25	--	--	0.420±0.006
7.50	0.460±0.015	0.433±0.006	0.500±0.006
8.75	--	--	0.590±0.006
10.00	0.630±0.023	0.563±0.012	0.690±0.010
11.25	--	--	0.780±0.006
12.50	0.810±0.017	0.713±0.012	0.880±0.010
13.75	--	--	0.980±0.010
15.00	0.990±0.023	0.853±0.015	1.070±0.012
17.50	1.160±0.021	0.990±0.017	--
20.00	1.330±0.021	1.130±0.030	--

[a]Average of three determinations with standard deviation

[b]Absorbance measured at 258 nm.

[c]Absorbance measured at 380 nm.

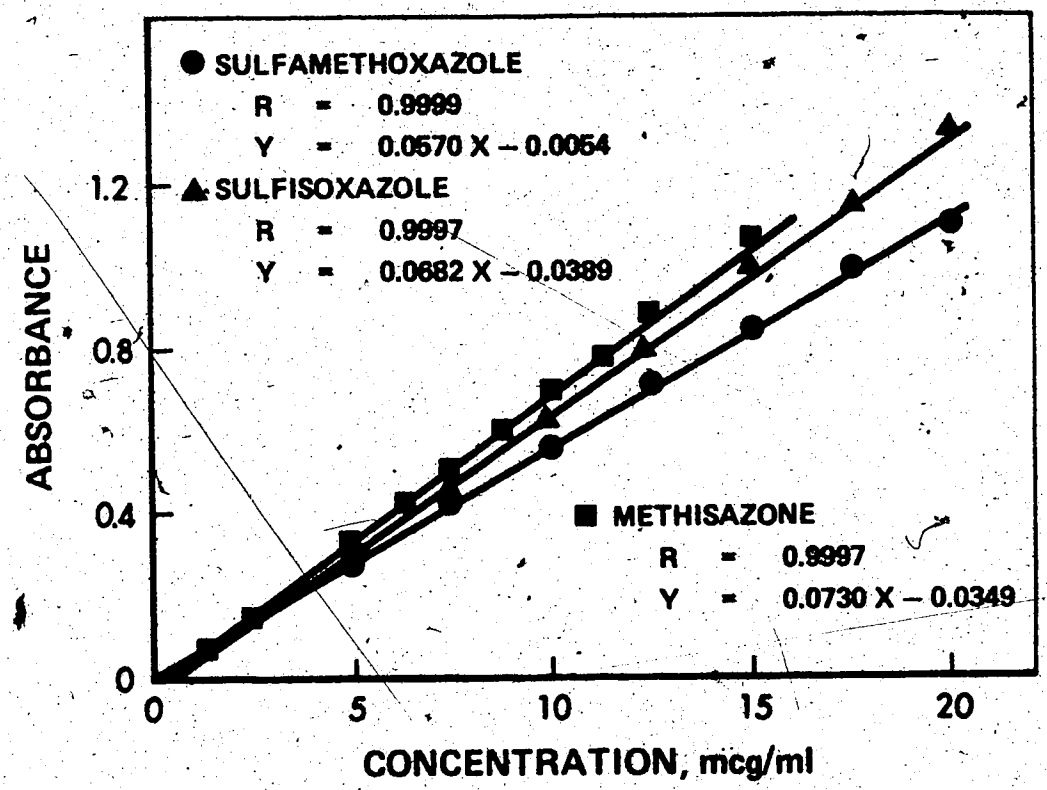

Figure 16 - Linear Relationship between Absorbance and Concentration of Sulfisoxazole, Sulfamethoxazole, and Methisazone in Water

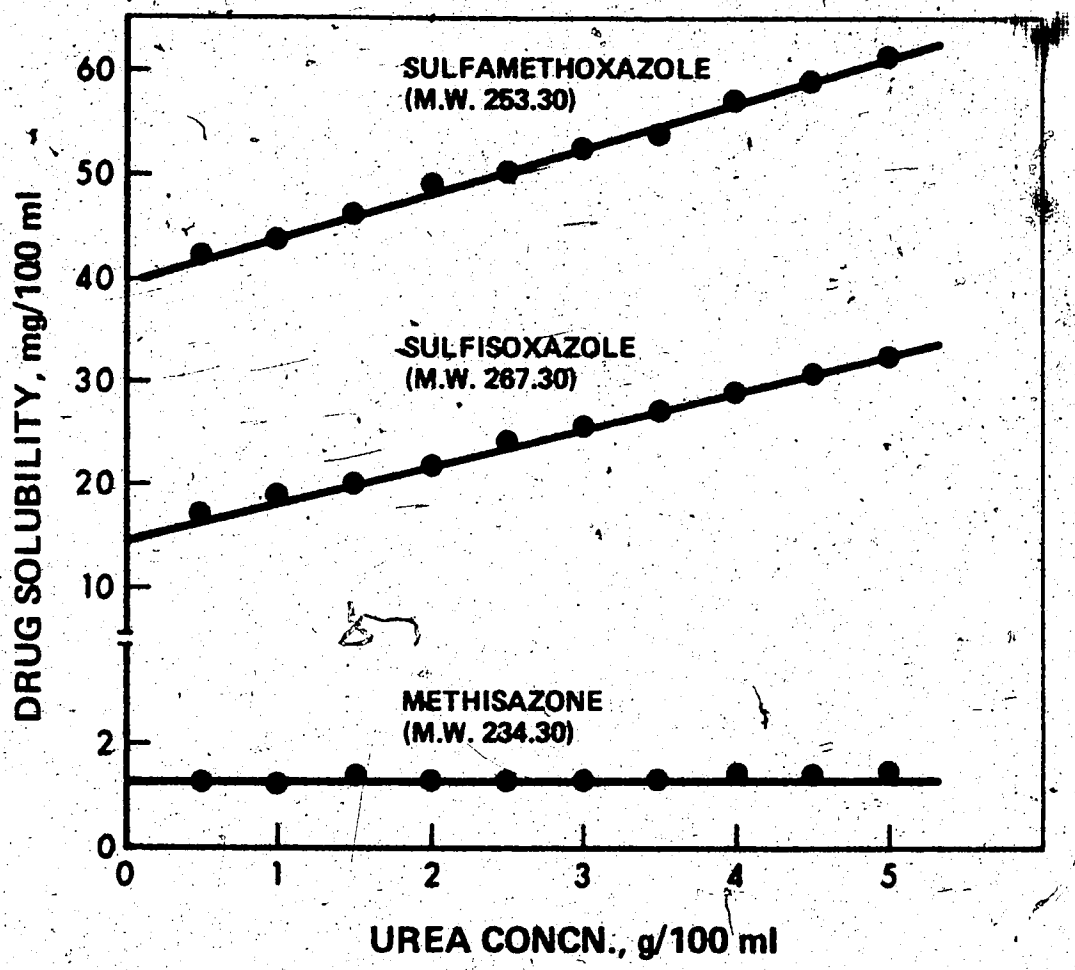

Figure 17 - Aqueous Solubility of Sulfamethoxazole, Sulfisoxazole, and Methisazone as a Function of Urea Concentration at 25°C

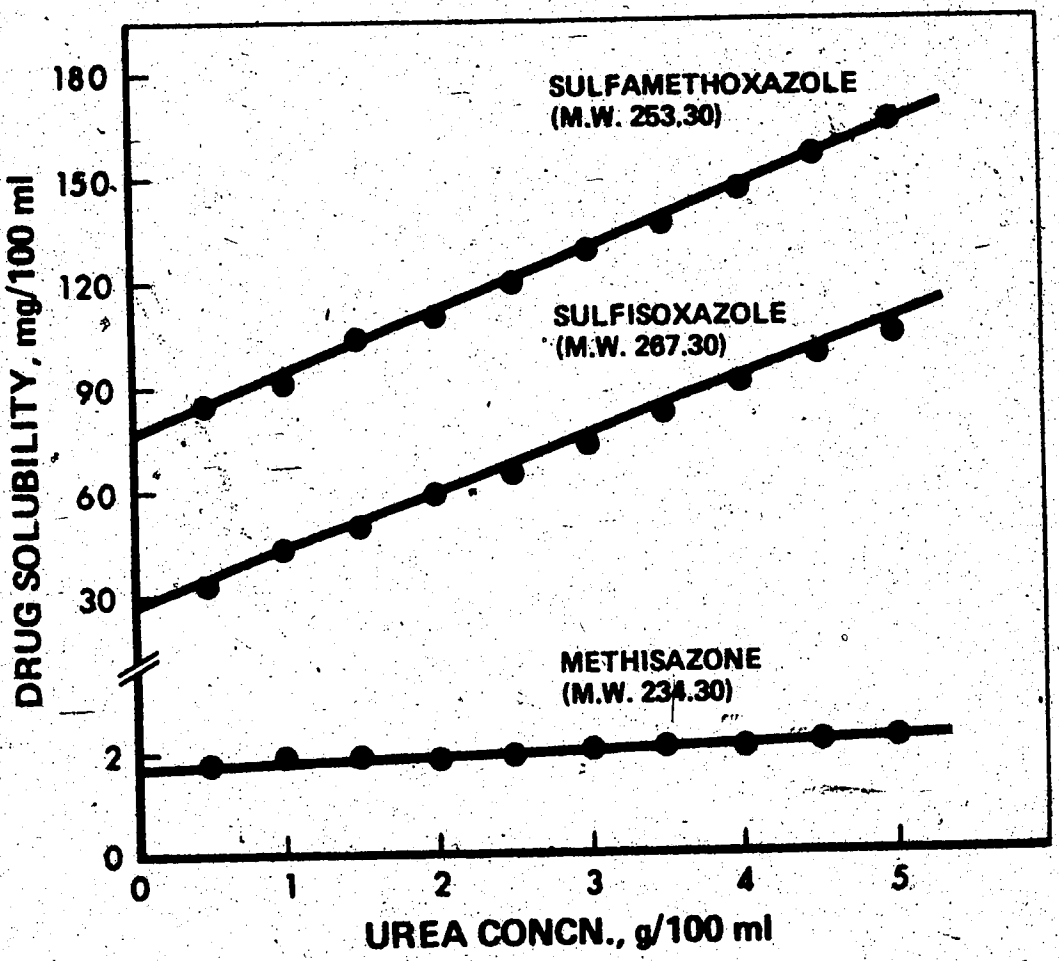

Figure 18 - Aqueous Solubility of Sulfamethoxazole, Sulfisoxazole, and Methisazone as a Function of Urea Concentration at 37°C

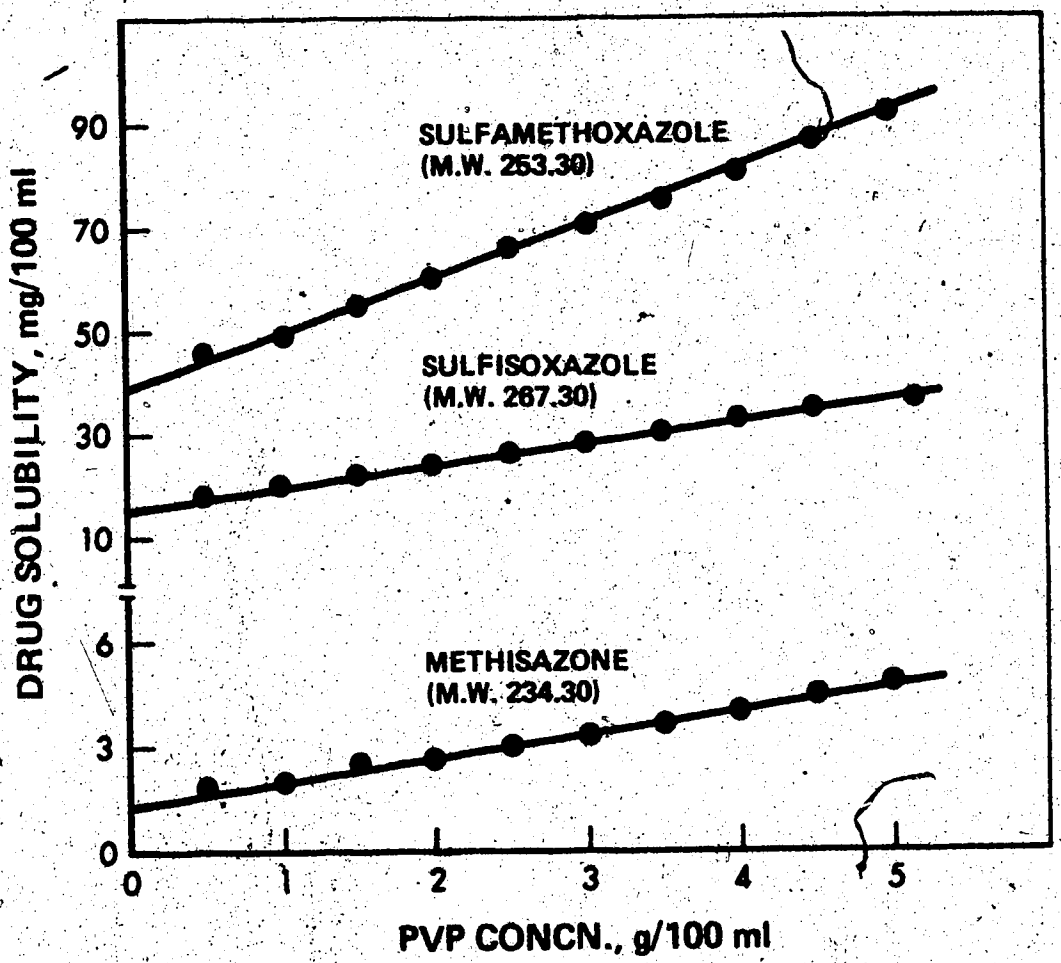

Figure 19 - Aqueous Solubility of Sulfamethoxazole, Sulfisoxazole, and Methisazone as a Function of PVP Concentration at 25°C

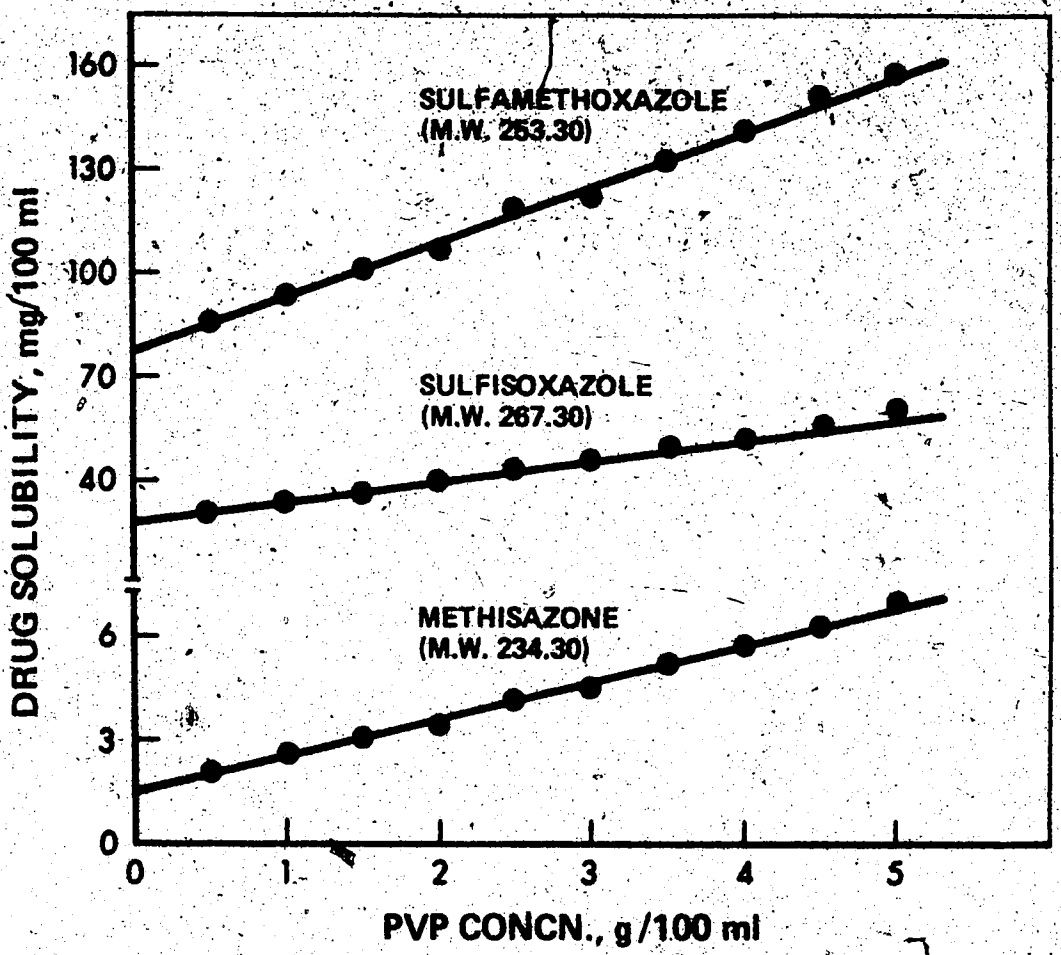

Figure 20 - Aqueous Solubility of Sulfamethoxazole, Sulfisoxazole, and Methisazone as a Function of PVP Concentration at 37°C

TABLE IX

Thermodynamic Data[a] for the Interaction of Sulfamethoxazole, Sulfisoxazole, and Methisazone with Urea

	Slope[b]	K_a	ΔF^o	ΔH_f^o	ΔS^o
Sulfamethoxazole					
25°C	10.0×10^{-4}	0.66	+248	11214	36.80
37°C	42.0×10^{-4}	1.36	-191		36.79
Sulfisoxazole					
25°C	7.8×10^{-4}	1.40	-203	14799	50.34
37°C	36.0×10^{-4}	3.66	-804		50.33
Methisazone					
25°C	6.8×10^{-6}	--	--	--	--
37°C	3.0×10^{-5}	0.44	+509		--

[a]Average of three determinations

[b]Slope of the linear plot determined by the method of least squares

TABLE X

Thermodynamic Data[a] for the Interaction of Sulfamethoxazole, Sulfisoxazole, and Methisazone with PVP.

	Slope[b]	K_a	ΔF^o	ΔH_f^o	ΔS^o
Sulfamethoxazole					
25°C	1.68	2.20×10^6	-8706	69794	263.43
37°C	2.54	1.98×10^8	-11846		263.36
Sulfisoxazole					
25°C	0.630	2909	-4754	32934	126.46
37°C	0.990	24691	-6272		126.47
Methisazone					
25°C	0.116	2393	-4638	1984	22.22
37°C	0.178	2722	-4904		22.21

[a]Average of three determinations

[b]Slope of the linear plot determined by the method of least squares

C. DISSOLUTION RATE STUDIES

All pellets used in the dissolution studies were compressed at a constant pressure and their hardness was measured. The physical characteristics were determined and are listed in Table XI. Pellets prepared from binary systems containing urea were practically non-disintegrating, and, consequently, the dissolution characteristics of such systems were evaluated by the rotating-basket method. In contrast, the pellets prepared from binary systems containing PVP were relatively fast-disintegrating. In order to be able to detect subtle differences in the dissolution characteristics of the fast-disintegrating pellets, the disintegrating time was delayed by exposing only one surface of the pellet to the dissolution medium. This necessitated the use of the rotating-disc method.

Results of the dissolution studies are summarized in Tables A-5 to A-22. Figure 21 illustrates the effects of methodology on the percent of methisazone dissolved from pellets containing PVP. The plots of percent dissolved versus time for methisazone, sulfisoxazole, and sulfamethoxazole are depicted in Figures 22-24. The slopes for both sulfamethoxazole and sulfisoxazole were calculated by the method of least squares. The rate constants were then determined from these slopes according to Eq. 10. A summary of the dissolution rate constants is given in Table XII. The percent undissolved-time plots of the drugs are pre-

TABLE XI

Physical Characteristics of Various Pellets used in Dissolution St[redacted]

Drug	Carrier	System	Pressure, kg./cm.^{2}	[redacted]a
Sulfamethoxazole	--	Pure Drug	907	6.5
Sulfamethoxazole (60%)	Urea (40%)	Solid Dispersion	907	13.0
Sulfamethoxazole (60%)	Urea (40%)	Physical Mixture	907	8.0
Sulfamethoxazole (25%)	PVP. (75%)	Solid Dispersion	907	2.0
Sulfamethoxazole (25%)	PVP. (75%)	Physical Mixture	907	15.0
Sulfisoxazole	--	Pure Drug	1588	2.5
Sulfisoxazole (70%)	Urea (30%)	Solid Dispersion	1588	14.0
Sulfisoxazole (70%)	Urea (30%)	Physical Mixture	1588	2.0
Sulfisoxazole (25%)	PVP. (75%)	Solid Dispersion	1588	9.0
Sulfisoxazole (25%)	PVP. (75%)	Physical Mixture	1588	7.0
Methisazone	--	Pure Drug	1134	11.0
Methisazone (50%)	Urea (50%)	Solid Dispersion	1134	6.0
Methisazone (50%)	Urea (50%)	Physical Mixture	1134	12.0
Methisazone (25%)	PVP. (75%)	Solid Dispersion	1134	16.0
Methisazone (25%)	PVP. (75%)	Physical Mixture	1134	19.0

[a]Measured in Strong Cobb Hardness Units

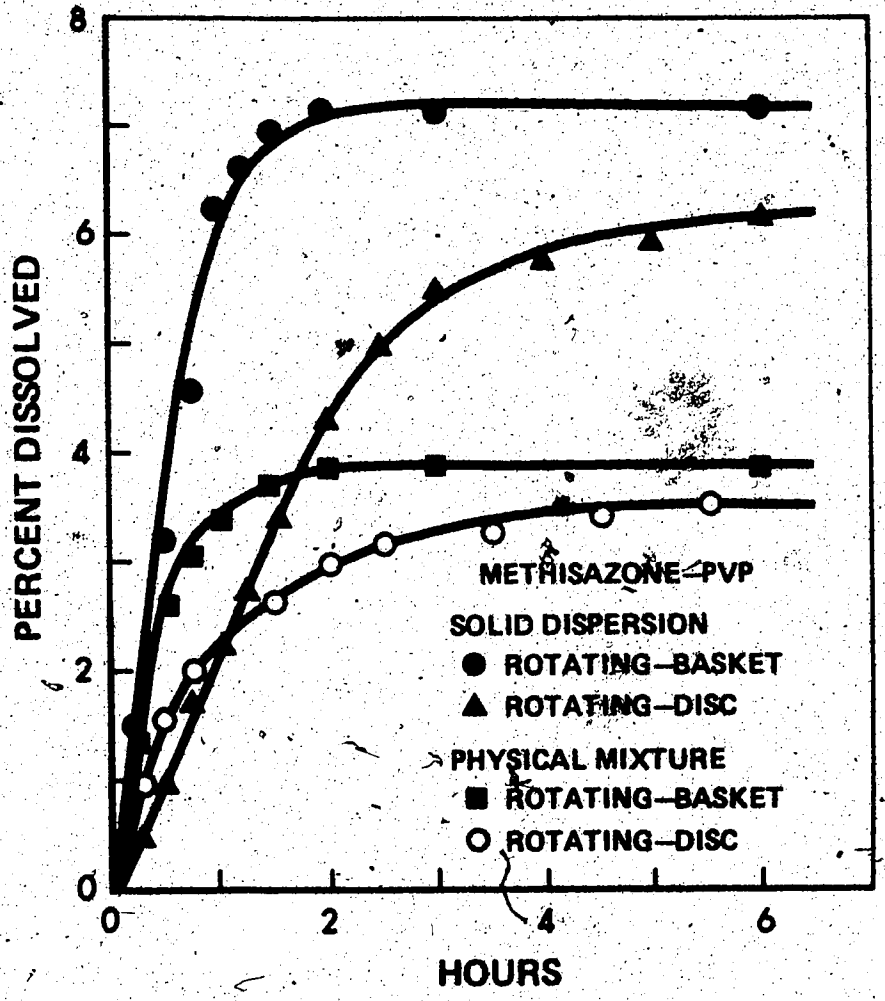

Figure 2F - Dissolution Rates of Methisazone-Polyvinylpyrrolidone Binary Systems

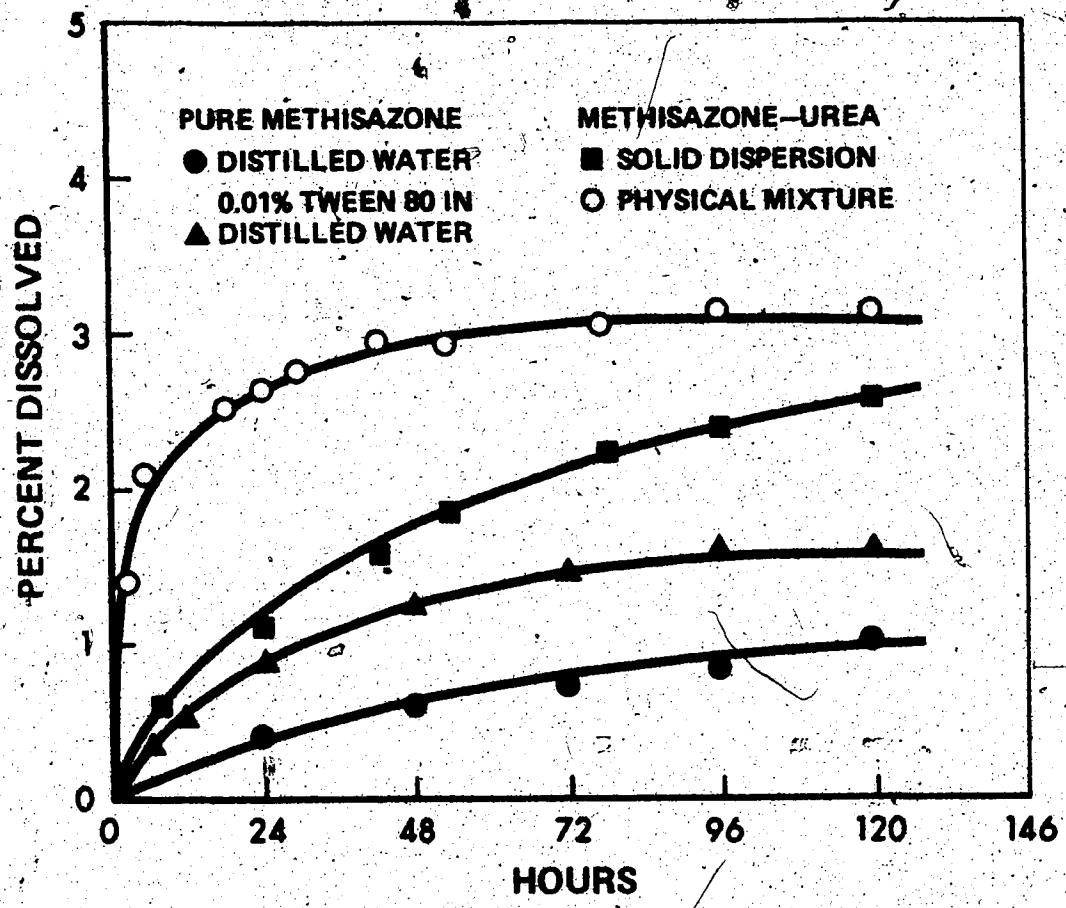

Figure 22 - Dissolution Rates of Pure Methisazone and Preparations containing Urea. Data Obtained by the Rotating-Basket Method.

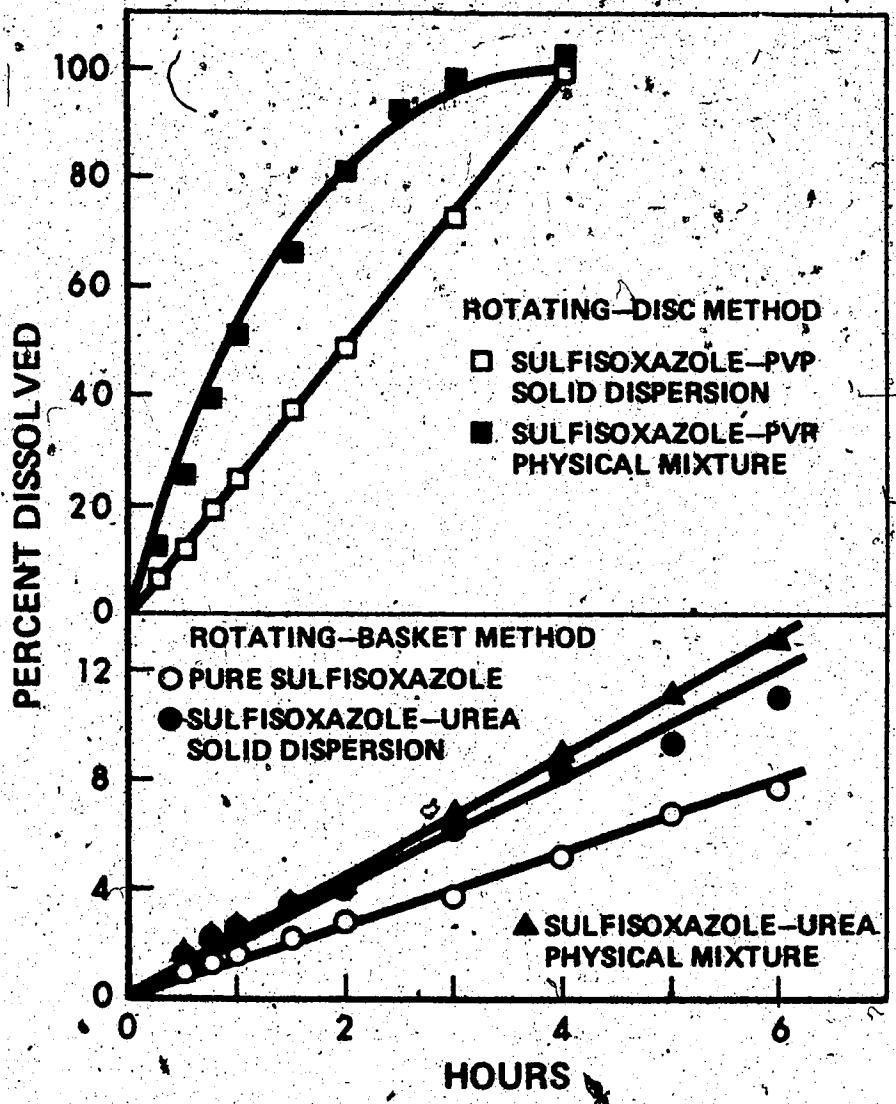

Figure 23 - Dissolution Rates of Pure Sulfisoxazole and Preparations containing Urea or Polyvinylpyrrolidone

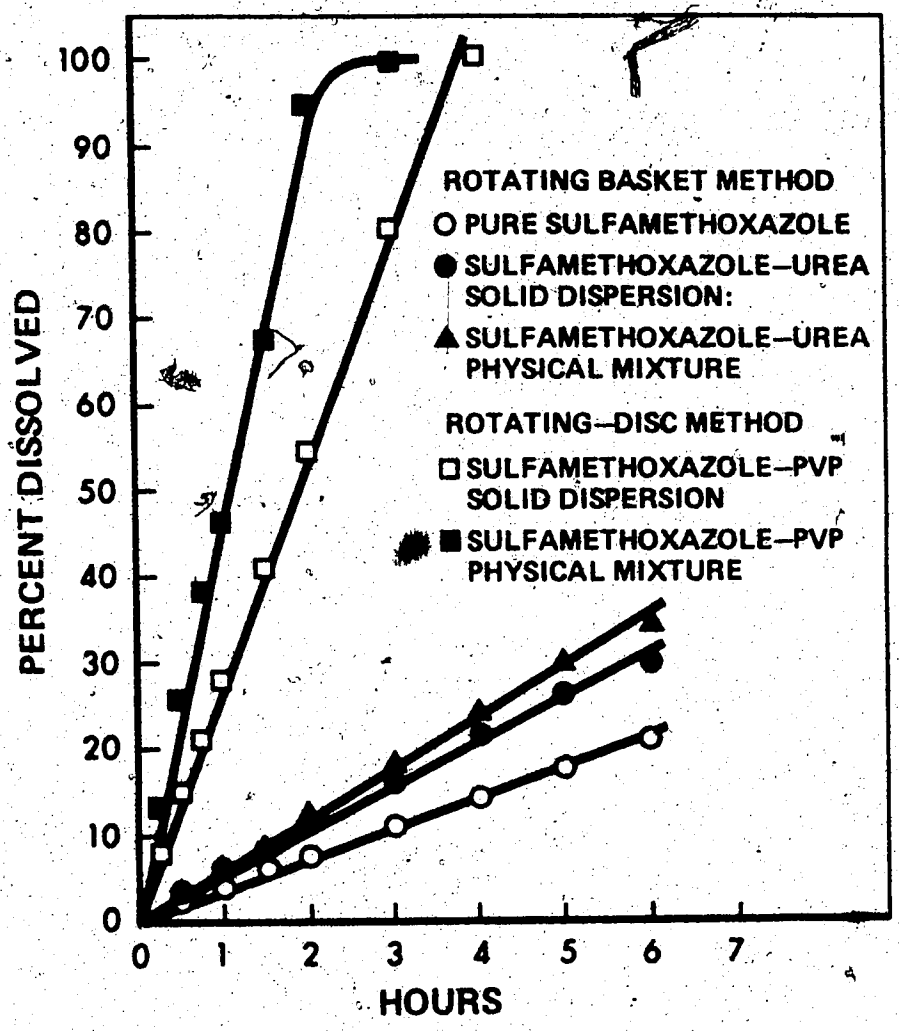

Figure 24 - Dissolution Rates of Pure Sulfamethoxazole and Preparations containing Urea or Polyvinylpyrrolidone

TABLE XII

Rate Constants for Dissolution of Sulfamethoxazole and Sulfisoxazole in Distilled Water at 37°C

Drug	Carrier	System	S, $cm.^2$	V, $cm.^3$	k, $hr.^{-1}$	K, $cm.\ hr^{-1}$
Sulfamethoxazole	--	Pure Drug	5.00	1000	3.36	6.72×10^2
Sulfamethoxazole	Urea	Solid Dispersion	5.00	1000	4.93	9.86×10^2
Sulfamethoxazole	Urea	Physical Mixture	5.00	1000	5.62	11.24×10^2
Sulfamethoxazole	PVP.	Solid Dispersion	--	1000	25.00	--
Sulfisoxazole	--	Pure Drug	5.00	1000	1.28	2.56×10^2
Sulfisoxazole	Urea	Solid Dispersion	5.00	1000	1.78	3.56×10^2
Sulfisoxazole	Urea	Physical Mixture	5.00	1000	2.16	4.32×10^2
Sulfisoxazole	PVP.	Solid Dispersion	--	1000	24.62	--

sented in Figures 25-27. In those instances where both the percent dissolved and percent undissolved-time plots were non-linear, the percent dissolved-time data were plotted on a logarithmic-probability graph paper so that percent dissolution times could be determined. Figures 28-31 illustrate these log-normal probability plots. The percent dissolution times data obtained from these plots is tabulated in Table XIII. In order to test the diffusion-controlled model for the dissolution of methisazone, the amount dissolved-time data were plotted on a logarithmic graph paper. The plots of the logarithm of the amount dissolved versus the logarithm of time are shown in Figure 32.

D. ANALYTICAL PROCEDURES FOR BIOLOGICAL FLUIDS

Estimation of Methisazone Levels

The reliable estimation of methisazone in whole blood, plasma, or urine depends upon the efficiency of solvent extraction. The relatively high solubility of methisazone in 1,4-dioxane warrants its use as a solvent for extraction. In the present study, 1,4-dioxane was selected as the solvent of choice because: (a) it does not absorb in either ultra-violet or visible region between 220 and 500 nm, (b) it is miscible with water in all proportions, (c) it causes precipitation of proteins by dehydration, and (d) it is often used as a standard solvent to solubilize biological materials such as plasma, serum and urine.

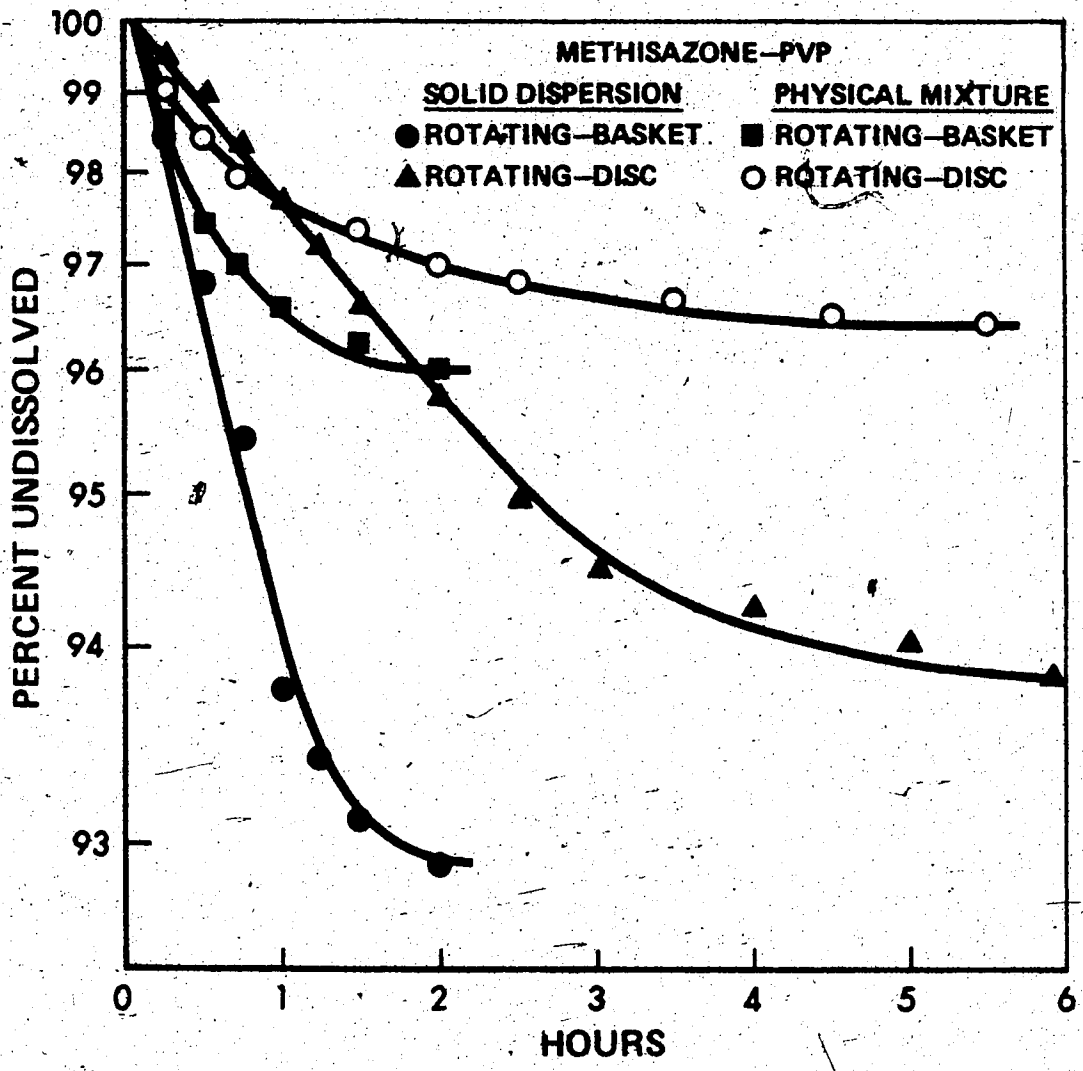

Figure 25 - Semilogarithmic Plots of Percent Methisazone Undissolved from Methisazone-Polyvinylpyrrolidone Binary Systems

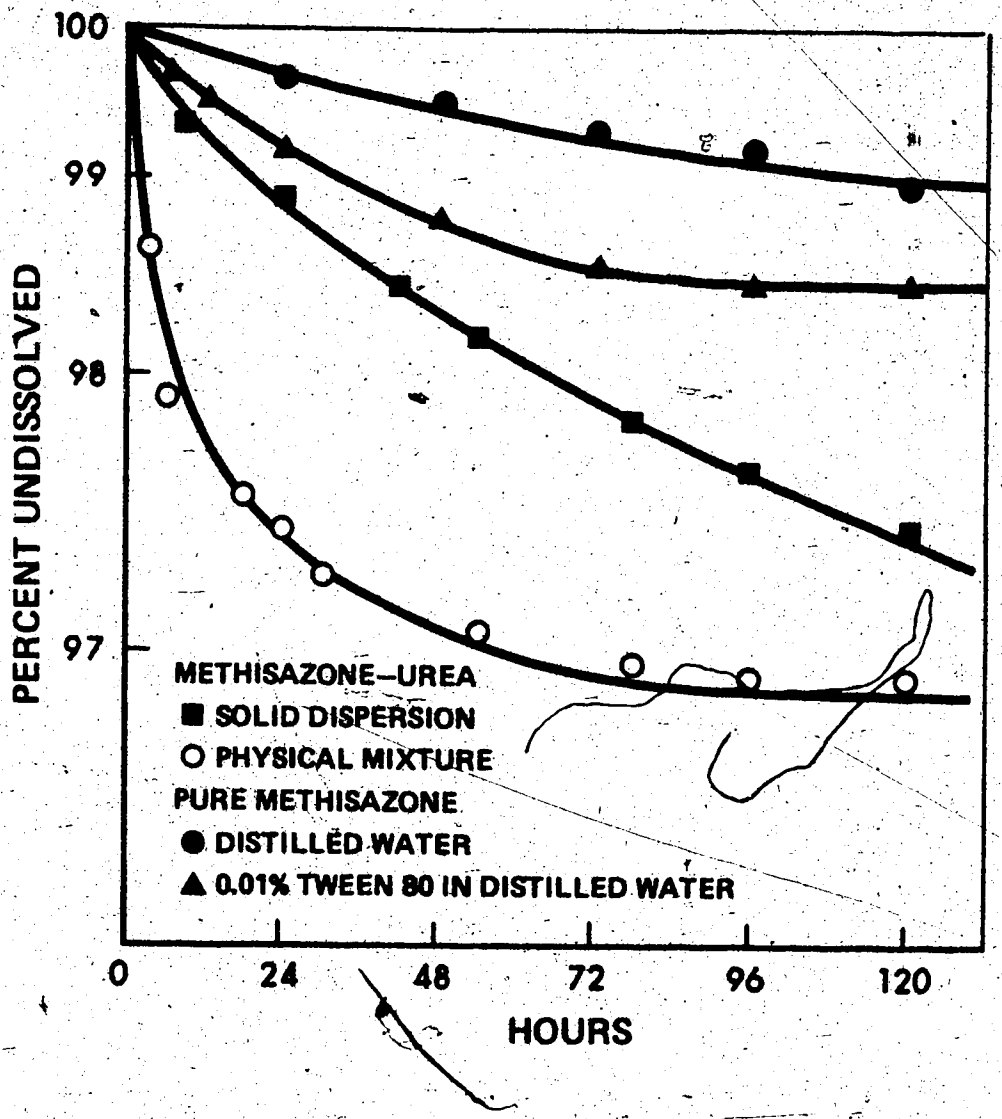

Figure 26 - Semilogarithmic Plots of Percent Methisazone Undissolved for Pure Methisazone and Preparations containing Urea. Data Obtained by the Rotating-Basket Method.

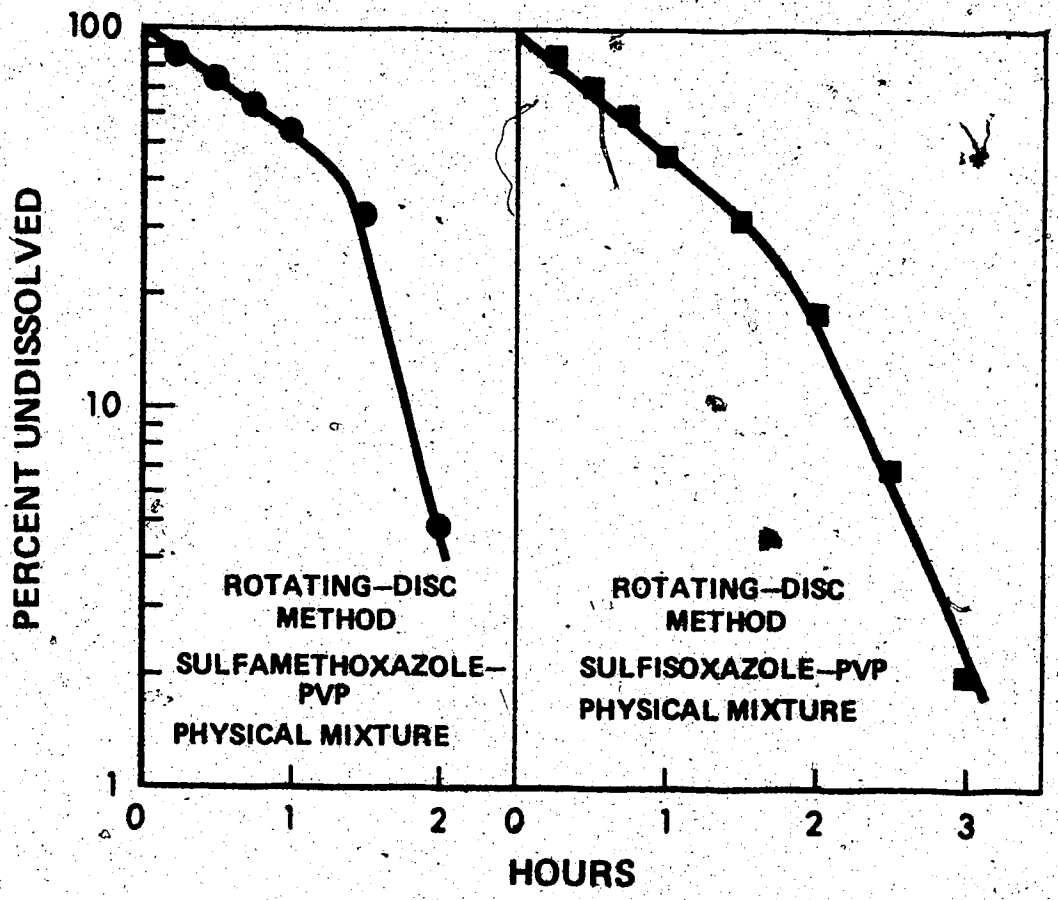

Figure 27 - Semilogarithmic Plots of Percent Undissolved as a Function of Time for Sulfamethoxazole and Sulfisoxazole Physical Mixtures Containing PVP.

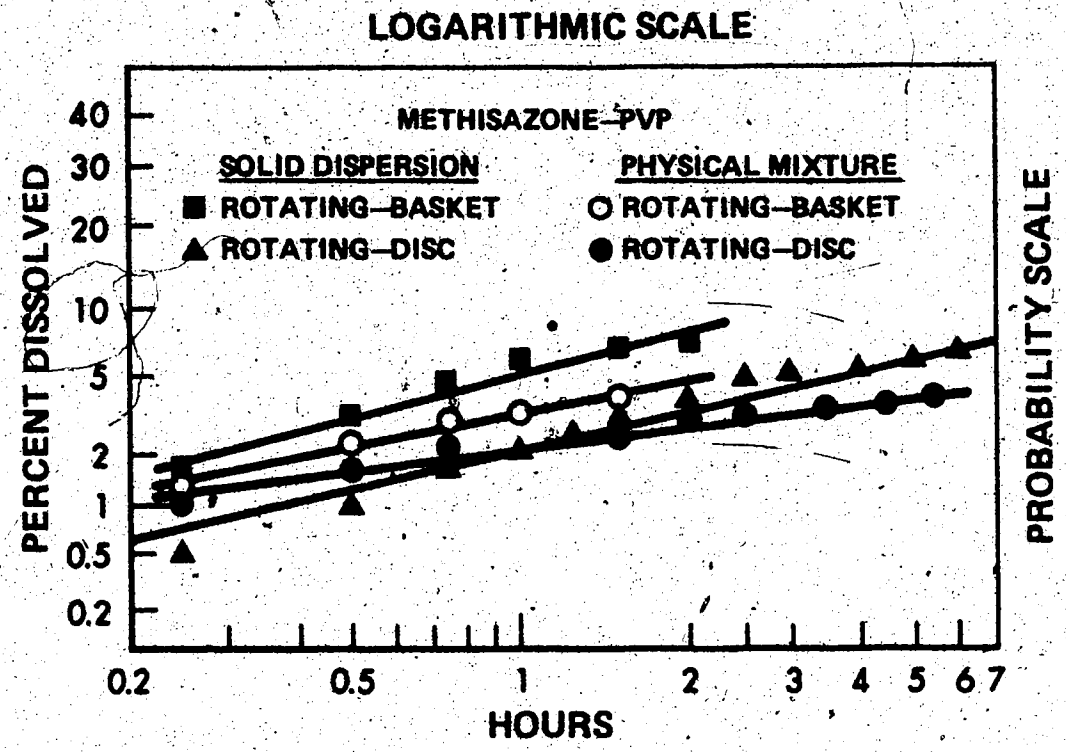

Figure 28 - Log-Normal Probability Plots of Dissolution Data from Methisazone-Polyvinylpyrrolidone Binary Systems

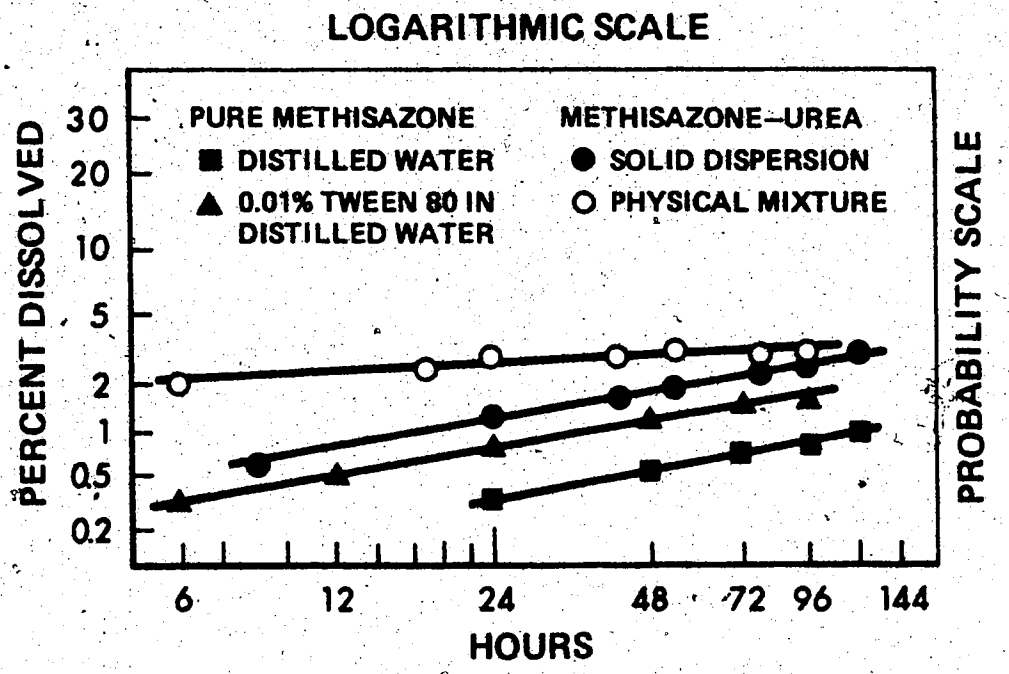

Figure 29 - Log-Normal Probability Plots of Pure Methisazone and its Preparations containing Urea. Data Obatined by the Rotating-Basket Method.

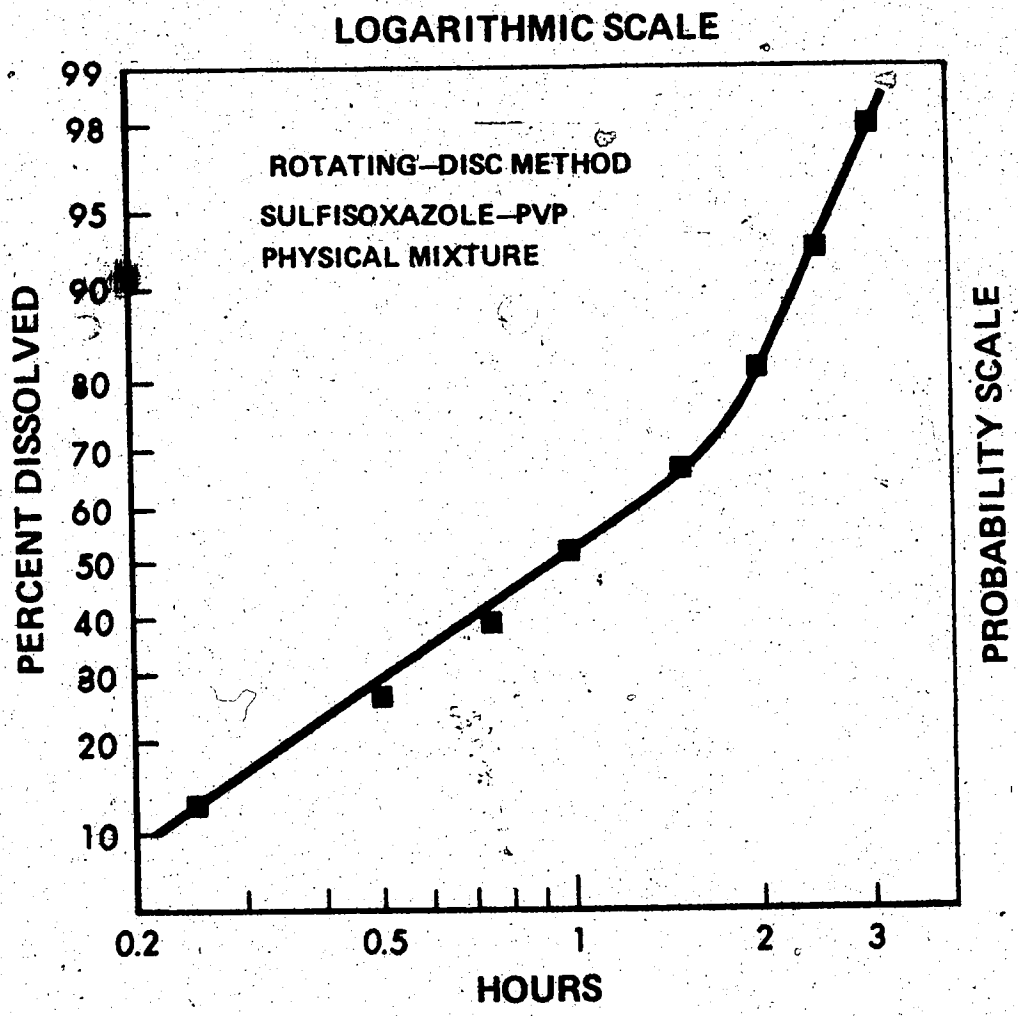

Figure 30 - Log-Normal Probability Plot of Sulfisoxazole-Polyvinylpyrrolidone Physical Mixture

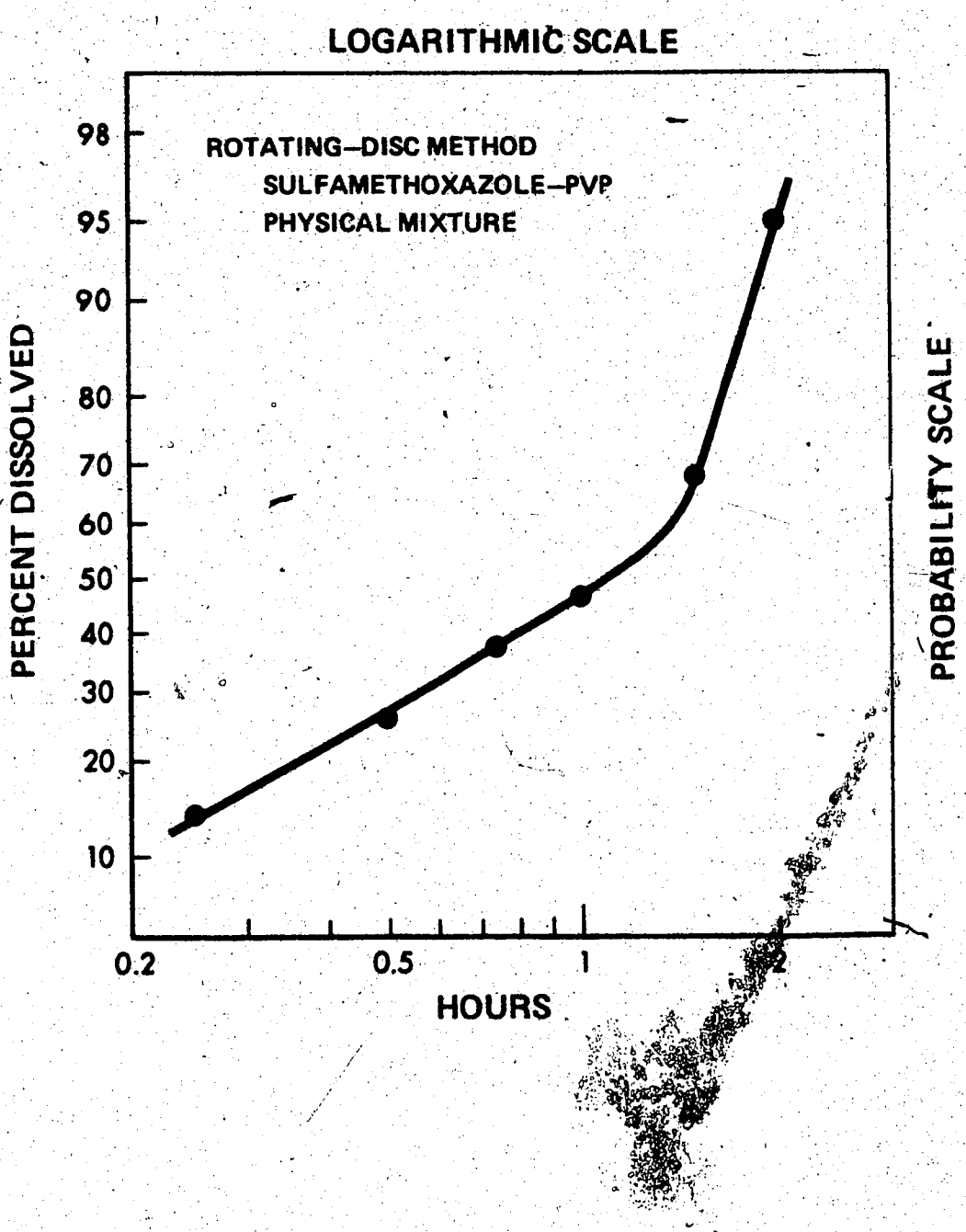

Figure 31 - Log-Normal Probability Plot of Sulfamethoxazole-Polyvinylpyrrolidone Physical Mixture

TABLE XIII

Fifty, Four, Two, and One Percent Dissolution Times for Drug Systems in Distilled Water[a] at 37°C

Drug	Carrier	System	Dissolution Time in Hours			
			T_{50}	T_4	T_2	T_1
Sulfamethoxazole	PVP.	Solid Dispersion	2.00			
Sulfamethoxazole	PVP.	Physical Mixture	1.25			
Sulfisoxazole	PVP.	Solid Dispersion	2.00			
Sulfisoxazole	PVP.	Physical Mixture	1.00			
Methisazone	--	Pure Drug				120.00 36.00[g]
Methisazone	Urea	Solid Dispersion			52.00	
Methisazone	Urea	Physical Mixture			<6.00[f]	
Methisazone	PVP.	Solid Dispersion		2.75[b] 0.75[c]		
Methisazone	PVP.	Physical Mixture		5.50[d] 1.50[e]		

[a] Volume = 1000 cm.^{3}

[b,d] Rotating-Disc Method

[c,e] Rotating-Basket Method

[f] Pellets disintegrated into fragments

[g] Distilled Water containing 0.01% Tween 80

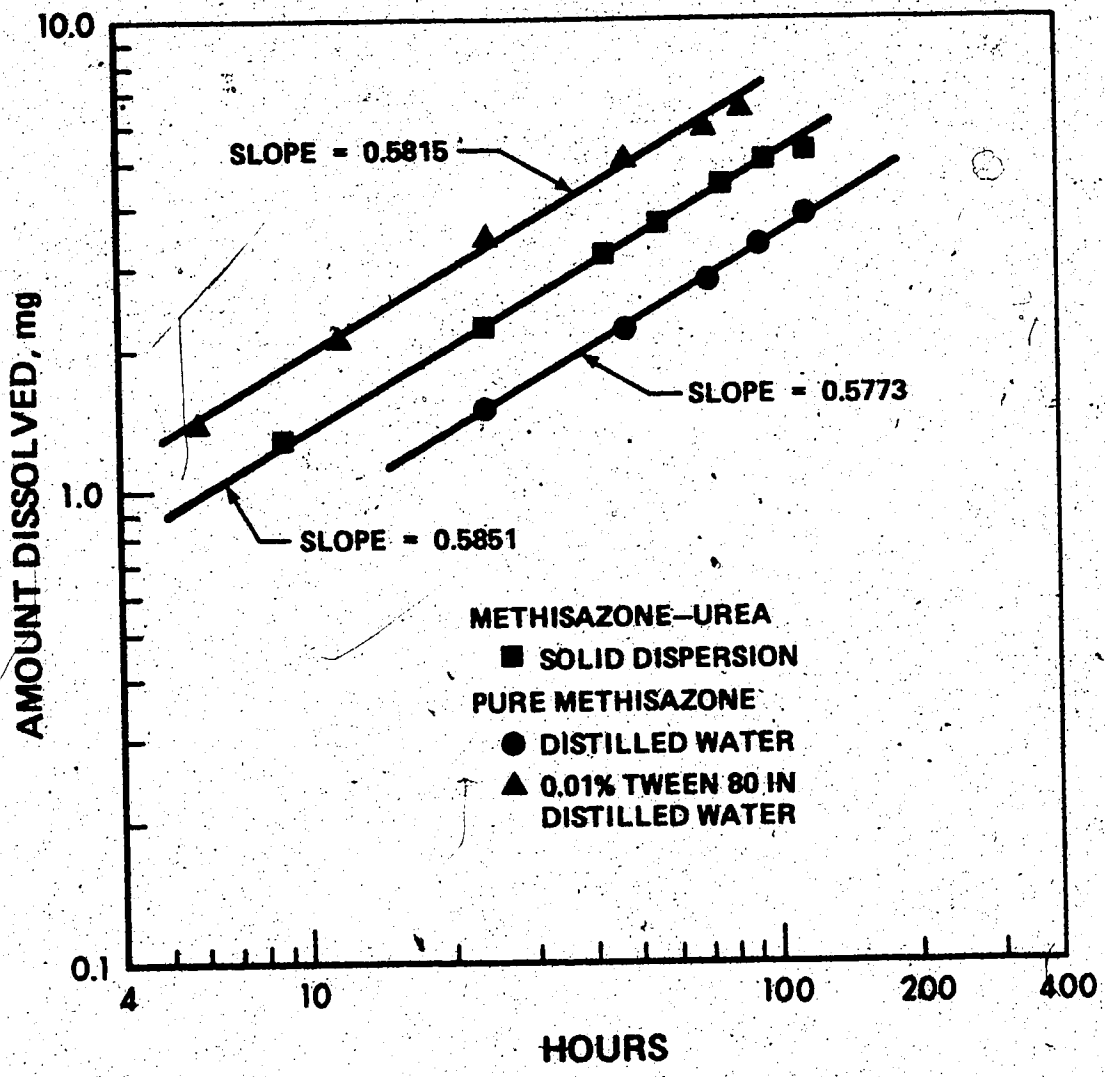

Figure 32 - Relationship Between Logarithm of Methisazone Dissolved and Logarithm of Time. Data Obtained by the Rotating-Basket Method.

It has been reported (97) that, as a result of intramolecular hydrogen bonding, methisazone exerts its antiviral activity in the form of a resonance-stabilized, hydrogen-bonded structure. The chemical structure of methisazone is shown in Figure 33. As shown in Table XIV spectrophotometric investigation on absorption characteristics of methisazone in chloroform, toluene, and 1,4-dioxane solvents revealed that maximum molar absorptivity values, ε_{max}, for methisazone in 1 N NaOH-dioxane (50:50) solvent system and in chloroform are comparable.

TABLE XIV

Molar Absorptivity of Methisazone at Maximum Absorption in Different Solvents

Solvent	λ_{max}	ε_{max}
Chloroform	370 nm	22960
Toluene	370 nm	17689
Dioxane	360 nm	17689
1 N NaOH-dioxane (50:50)	420 nm	20384

It was found that a solution of methisazone in 1,4-dioxane developed a maximum color intensity immediately when mixed with 1 N NaOH solution in equal proportions. The color showed an absorption maximum at 420 nm and was found to be stable for at least five minutes. Methisazone in 1 N NaOH-dioxane (50:50) solvent system obeyed Beer's law over the concentration range 0.5 - 12 mcg/ml. Spectral scans of absorbance for methisazone are depicted in Figure 34. The reproducibility and recovery data of known amounts of methisazone added to blank whole blood, plasma, and urine are summarized in Table XV.

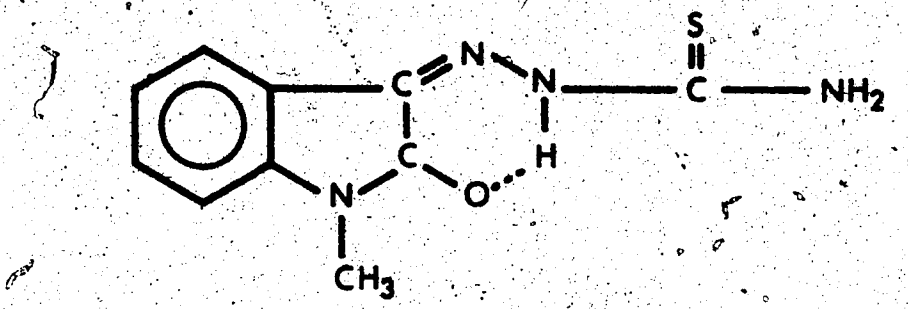

METHISAZONE

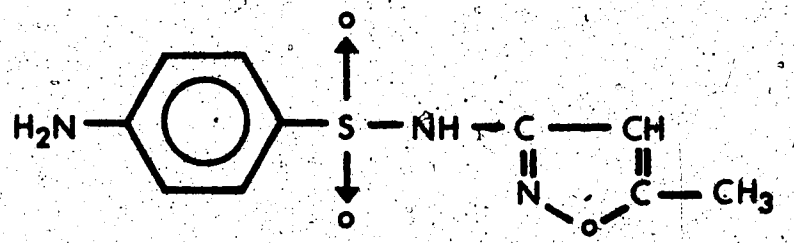

SULFAMETHOXAZOLE

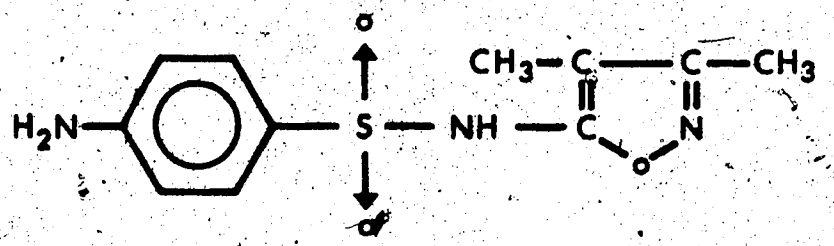

SULFISOXAZOLE

Figure 33 - Chemical Structures of Methisazone, Sulfamethoxazole, and Sulfisoxazole

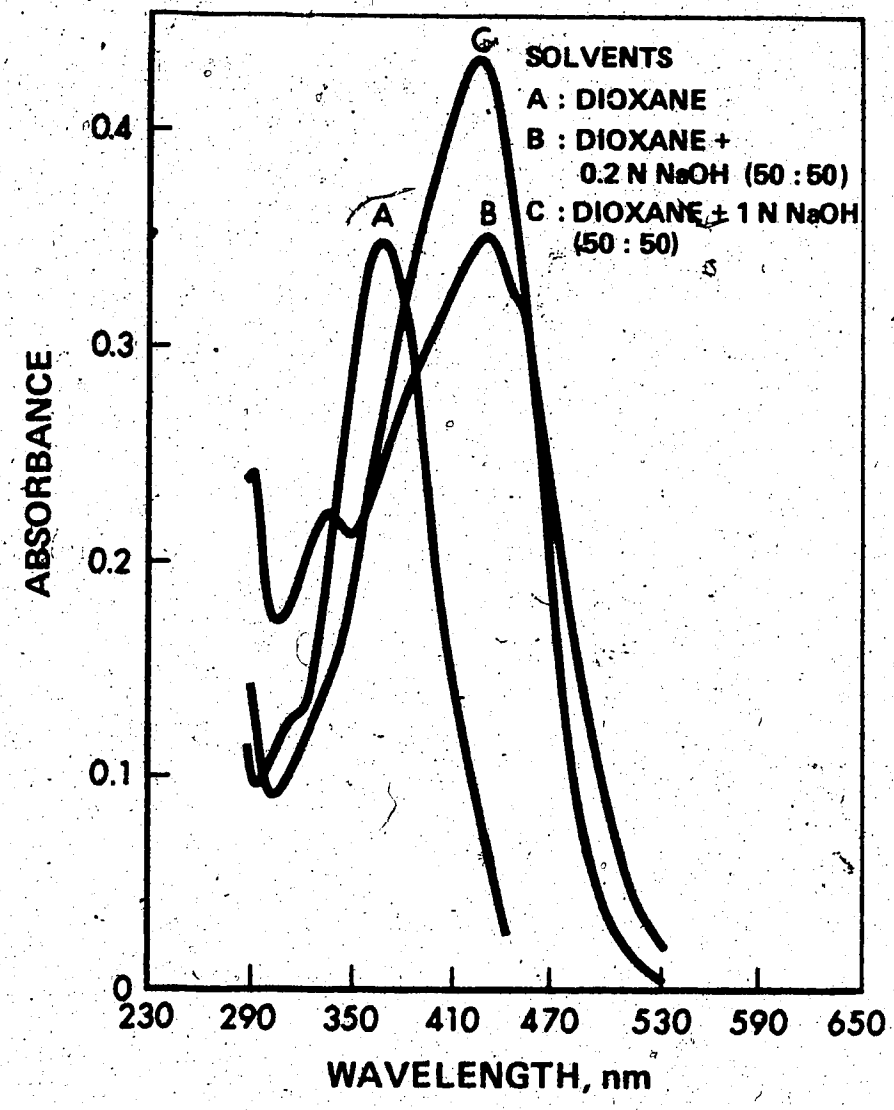

Figure 34 - Spectral Absorbance Curves for Methisazone

TABLE XV

Recoveries of Known Amounts of Methisazone Added to Blank Whole Blood, Plasma, and Urine

Added, mcg/ml	Recovered, %		
	Blood[a]	Plasma[a]	Urine[b]
2.00	61.45±3.36	70.30±8.10	88.24±2.95
4.00	69.00±1.20	73.95±4.95	95.52±1.80
6.00	74.14±2.78	78.12±6.33	96.00±1.20
8.00	73.94±2.17	77.50±4.14	97.00±1.50
10.00	76.30±1.43	78.78±3.13	97.60±1.20
12.00	78.40±1.00	79.66±2.25	98.00±0.60

[a]Average of seven replicates with standard deviation

[b]Average of three replicates with standard deviation

The low values of standard deviation indicate that reproducibility of the extraction process is reliable. The data for the standard curve of methisazone in 1,4-dioxane are presented in Table XVI. The calibration curves for spiked whole blood, plasma, and urine samples were constructed. Figure 35 shows the calibration curves for methisazone and linear regression equations with correlation coefficients. In all instances, the calibration curves showed good linearity. However, they did not pass through the origin. This indicates that error due to loss of added methisazone is fairly constant. Apart from minor differences in slope, the calibration curves of methisazone in whole blood and plasma were quite similar.

Determination of N^1-substituted Sulfonamides in Whole Blood

The Bratton-Marshall colorimetric method was employed for the determination of sulfisoxazole and sulfamethoxazole in whole blood. The data for the calibration curves of sulfisoxazole and sulfamethoxazole are presented in Tables XVII and XVIII. When the absorbance was plotted as a function of concentration, a straight-line relationship was obtained, indicating adherence to Beer's law. Typical Beer's law plots of both sulfisoxazole and sulfamethoxazole are depicted in Figure 36. The reproducibility and recovery data of sulfonamides added to whole blood are presented in Tables

TABLE XVI

Data for the Calibration Curve of Methisazone in 1,4-Dioxane

Concentration, mcg/ml	Absorbance[a]	Transmittance, %	100 - % T[b]
0.50	0.040±0.004	91.199	8.801
1.00	0.083±0.002	82.604	17.396
2.00	0.163±0.017	68.705	31.295
4.00	0.333±0.018	46.451	53.549
6.00	0.503±0.019	31.405	68.595
8.00	0.666±0.020	21.577	78.423
10.00	0.835±0.019	14.622	85.378
12.00	1.006±0.025	10.000	90.000

[a]Average of six determinations with standard deviation.

[b]T: Transmittance

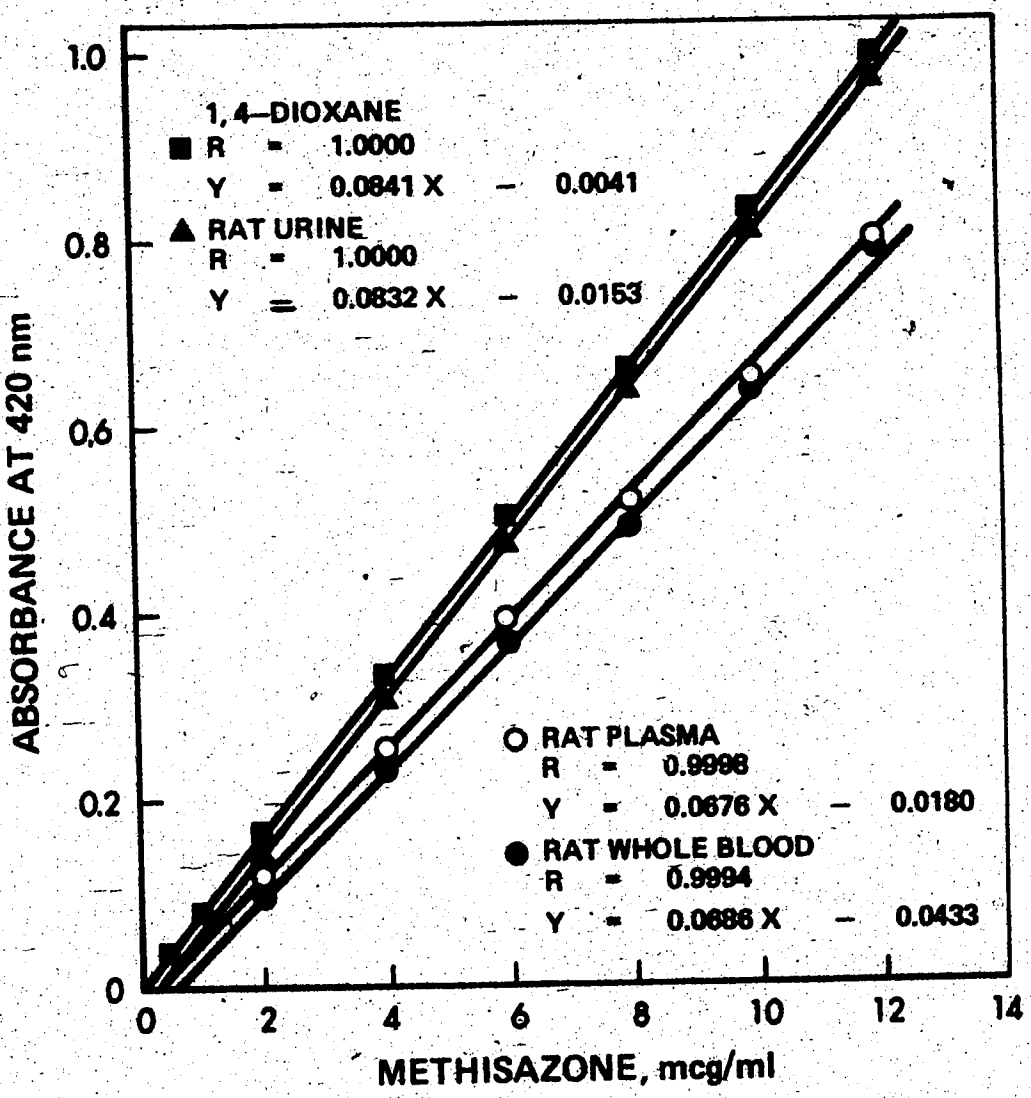

Figure 35 - Calibration Curves for Methisazone in Biological Fluids

TABLE XVII

Data for the Calibration Curve of Sulfisoxazole

Concentration, mcg/ml	Absorbance[a]	Transmittance, %	100 - % T[b]
0.25	0.046±0.004	89.952	10.048
0.50	0.099±0.009	79.618	20.382
0.75	0.135±0.006	73.282	26.718
1.00	0.159±0.005	69.343	30.657
1.50	0.219±0.007	60.394	39.606
2.00	0.278±0.008	52.723	47.277
2.50	0.324±0.004	47.425	52.575
3.00	0.395±0.005	40.272	59.728
4.00	0.500±0.009	31.623	68.377
5.00	0.630±0.006	23.442	76.558
6.00	0.750±0.009	17.783	82.217
7.00	0.870±0.006	13.490	86.510
8.00	0.980±0.008	10.471	89.529
9.00	1.100±0.018	8.000	92.000
10.00	1.190±0.016	6.000	94.000

[a]Average of six determinations with standard deviation.

[b]T: Transmittance

TABLE XVIII

Data for the Calibration Curve of Sulfamethoxazole

Concentration, mcg/ml	Absorbance[a]	Transmittance, %	100 - % T[b]
0.25	0.042±0.003	90.785	9.215
0.50	0.090±0.005	81.281	18.719
0.75	0.135±0.005	73.282	26.718
1.00	0.178±0.003	66.375	33.625
1.50	0.272±0.005	53.456	46.544
2.00	0.363±0.006	43.352	56.548
2.50	0.458±0.003	34.833	65.167
3.00	0.530±0.009	29.512	70.488
4.00	0.730±0.007	18.621	81.379
5.00	0.920±0.005	12.023	87.977
6.00	1.080±0.012	8.250	91.175
7.00	1.260±0.014	5.500	94.500

[a]Average of six determinations with standard deviation

[b]T: Transmittance

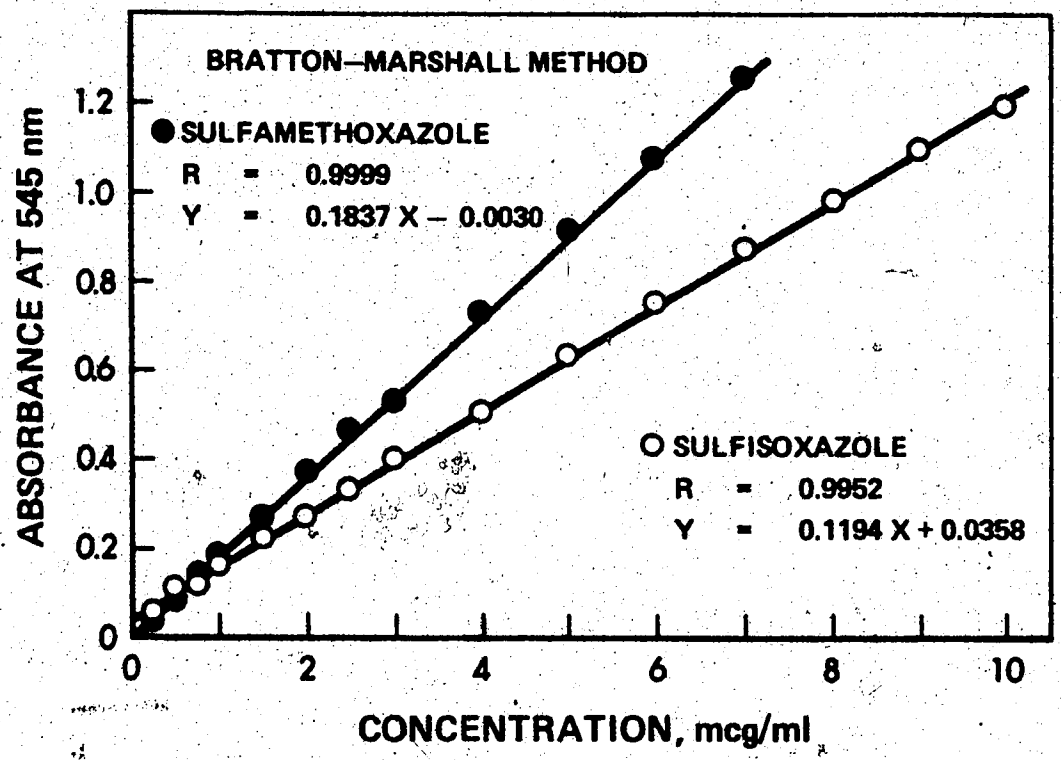

Figure 36 - Beer's Plots for Sulfamethoxazole and Sulfisoxazole

XIX and XX. The results of the standard addition-recovery studies indicated that there is essentially no loss of sulfonamides at the extraction step.

Accuracy and Precision of the Measurements

It is well known that the sensitivity range for spectrophotometric measurements is usually between 20-80% transmittance, and that the error of the measurement is minimized at about 37% transmittance. According to the Ringbom (103) derivation based on Beer's law, a plot of the % transmittance versus the logarithm of the concentration should result in a sigmoid curve. If the system obeys Beer's law, the inflection point should occur at about 37% transmittance. This implies that, for best accuracy, the slope of the curve should be a maximum. From this plot, concentration range for the accuracy of measurement can be determined.

Ringbom's plots for sulfamethoxazole, sulfisoxazole, and methisazone are depicted in Figure 37. These plots indicate that the concentration limits for the accurate measurement of these drugs are 2 and 8 mcg/ml.

The precision of the measurement for methisazone, sulfisoxazole, and methisazone was determined. The precision data for the analysis of these drugs in whole blood are presented in Table XXI. The coefficients of variation for the three drugs ranged from 2.95 to 5.5%, indicating that the error due to variation in analysis would not influence the determination of drug levels in blood.

TABLE XIX

Recoveries of Known Amounts of Sulfisoxazole Added to Blank Whole Blood

Added, mcg/ml	Recovered,[a] %
0.25	92.50±7.20
0.50	91.30±9.70
1.00	91.10±5.10
1.50	94.00±4.50
2.00	90.50±5.50
2.50	102.90±1.40

[a]Average of seven replicate runs with standard deviation

TABLE XX

Recoveries of Known Amounts of Sulfamethoxazole Added to Blank Whole Blood

Added, mcg/ml	Recovered,[a] %
0.25	93.25±6.33
0.50	97.43±3.21
1.00	99.16±1.44
1.50	97.52±2.10
2.00	97.83±1.10
2.50	108.00±1:00

[a]Average of seven replicate runs with standard deviation

TABLE XXI

Precision Data for the Analysis of Methisazone, Sulfisoxazole, and Sulfamethoxazole in Whole Blood

Drug	Added, mcg/ml	Recovered,[a] mcg/ml	CV[b], %
Methisazone	60.0	45.0± 1.33	2.95
Sulfisoxazole	500.0	462.0±25.60	5.50
Sulfamethoxazole	1000.0	1007.0±35.50	3.50

[a]Average of nine replicates with standard deviation
[b]Coefficient of Variation

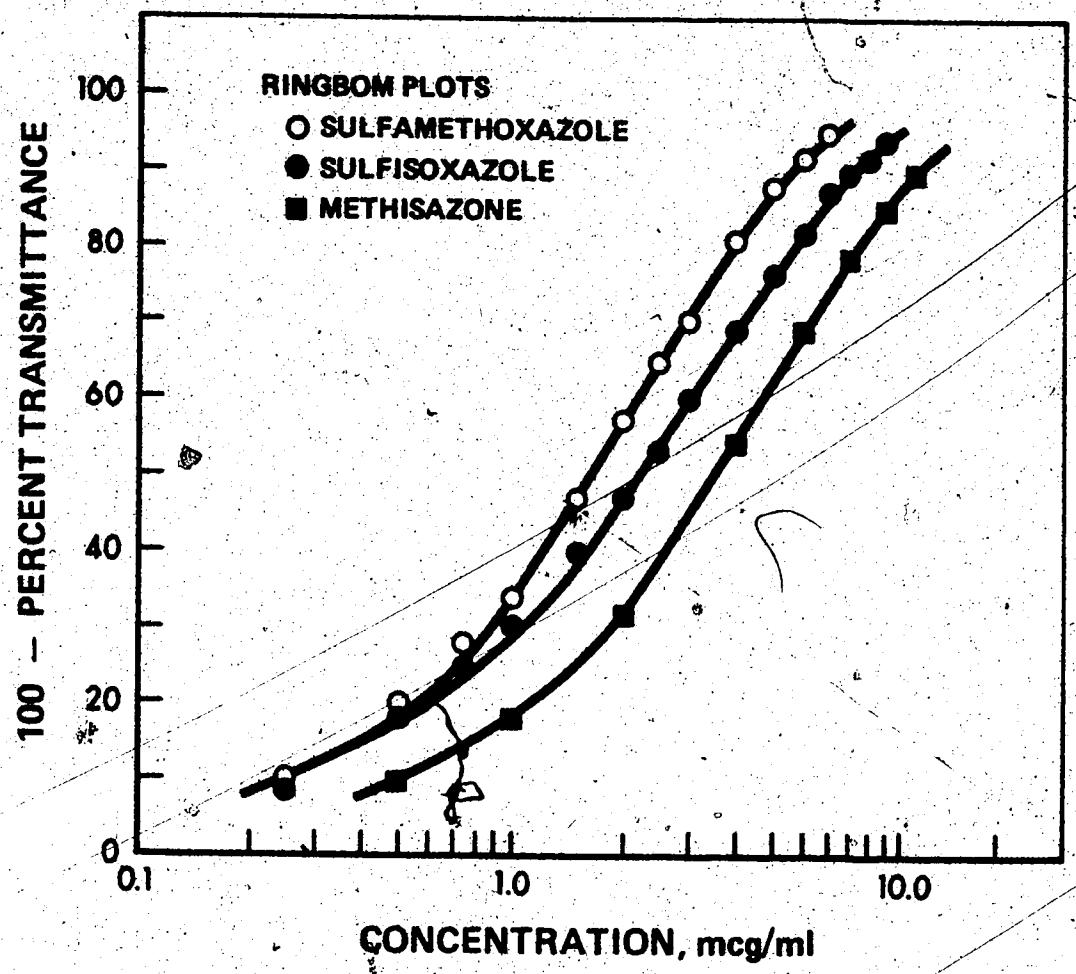

Figure 37 - Ringbom's Plots for Sulfamethoxazole, Sulfisoxazole, and Methisazone

E. BIOAVAILABILITY STUDIES

Blood level Studies

The area under the blood concentration-time curve (AUC) can be used to assess relative absorption of orally administered drugs. On the basis of the AUC, it is possible to determine whether the absorption follows dose-dependent or dose-independent kinetics. Therefore, a preliminary study was instituted to investigate the kinetics of drug absorption. In this study, 250-, 500-, and 1000-mg/kg doses of pure sulfisoxazole and sulfamethoxazole were orally administered to rats, and the blood levels were determined at various time intervals. The mean data are presented in Tables XXII and XXIII. The blood level-time profiles for sulfisoxazole and sulfamethoxazole at three dose levels are depicted in Figures 38 and 39. The areas under the blood level curve were measured by means of a planimeter. The plots of the AUC versus the dose, mg/kg, are depicted in Figure 40. The linearity of the plots is indicative of dose-independent kinetics for both sulfisoxazole and sulfamethoxazole over the dose range examined. The blood levels following single-dose oral administration of sulfisoxazole, sulfamethoxazole, and methisazone are illustrated in Tables A-23 to A-36.

The use of compartmental models in the statistical analysis of pharmacokinetic parameters has been reviewed by many (104-109). The integrated equation for the one-compartment open model is expressed as:

TABLE XXII

Blood Level Data for Pure Sulfisoxazole following Oral Administration of Single Doses in Male Wistar Rats

Hours	Blood Concentration[a], mcg/ml		
	250-mg/kg Dose	500-mg/kg Dose	1000-mg/kg Dose
0.25	82.83± 6.00	116.85±13.86	84.00± 20.00
0.50	116.85± 9.00	182.87±27.00	163.30± 35.00
1.00	176.87± 6.90	312.92±21.00	293.70± 25.00
2.00	224.89±18.34	364.94±24.00	515.00± 70.00
3.00	170.87± 3.46	304.92±31.80	611.00±108.98
4.00	116.85±18.30	198.87±38.12	553.82± 97.00
6.00	65.63±18.00	90.84±21.10	345.74± 48.00
8.00	20.00± 3.00	35.21± 9.70	210.48± 48.64
12.00	12.80± 1.40	10.40± 1.40	51.22± 13.00
Rats weighed:	440±10 g	370±10 g	360±17 g

[a]Mean values from three rats with standard deviation

TABLE XXIII

Blood Level Data for Pure Sulfamethoxazole following Oral Administration of Single Doses in Male Wistar Rats

Hours	Blood Concentration[a], mcg/ml		
	250-mg/kg Dose	500-mg/kg Dose	1000-mg/kg Dose
0.25	182.54±31.75	182.54±20.99	243.40± 24.25
0.50	280.42±43.70	310.85±19.60	407.41± 64.20
1.00	399.50±44.00	484.13±41.24	693.12± 51.00
2.00	497.35±36.60	724.87±45.82	1116.40± 80.00
3.00	481.48±36.66	802.00±20.99	1354.50±102.00
4.00	457.67±30.00	788.36±18.33	1375.70± 92.00
6.00	417.99±24.25	701.06±23.00	1396.80±110.00
8.00	357.14±36.40	661.40±33.00	1343.90± 97.00
12.00	208.99±30.00	412.70±47.60	1015.90± 84.00
20.00	56.88± 6.00	140.20±16.50	328.00± 48.50
28.00	30.42± 2.30	67.50± 3.90	132.30± 37.00
Rats weighed:	437±6 g	390±18 g	460±5 g

[a]Mean values from three rats with standard deviation

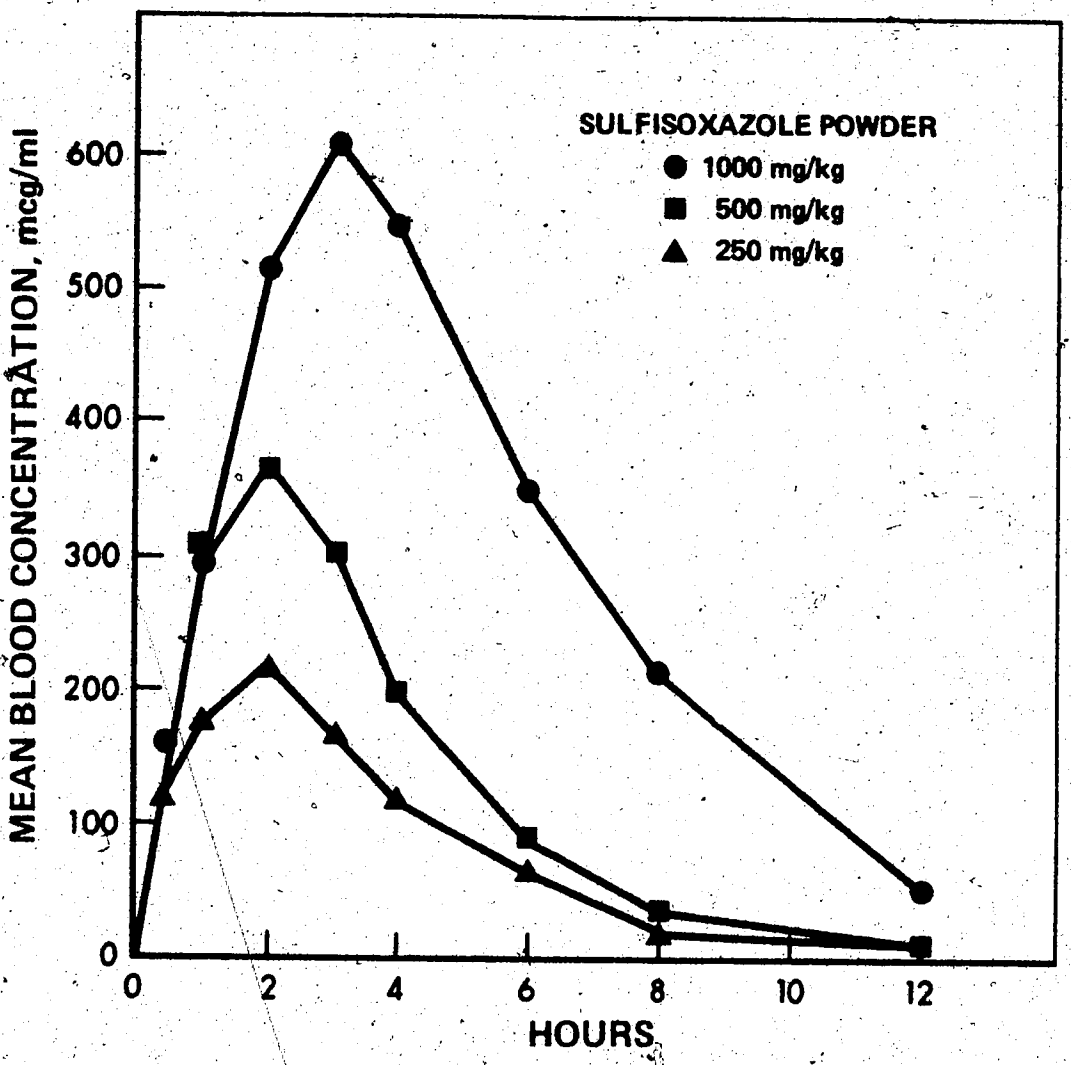

Figure 38 - Blood Concentration-Time Profiles for Sulfisoxazole following Single-Dose Oral Administration to Three Rats.

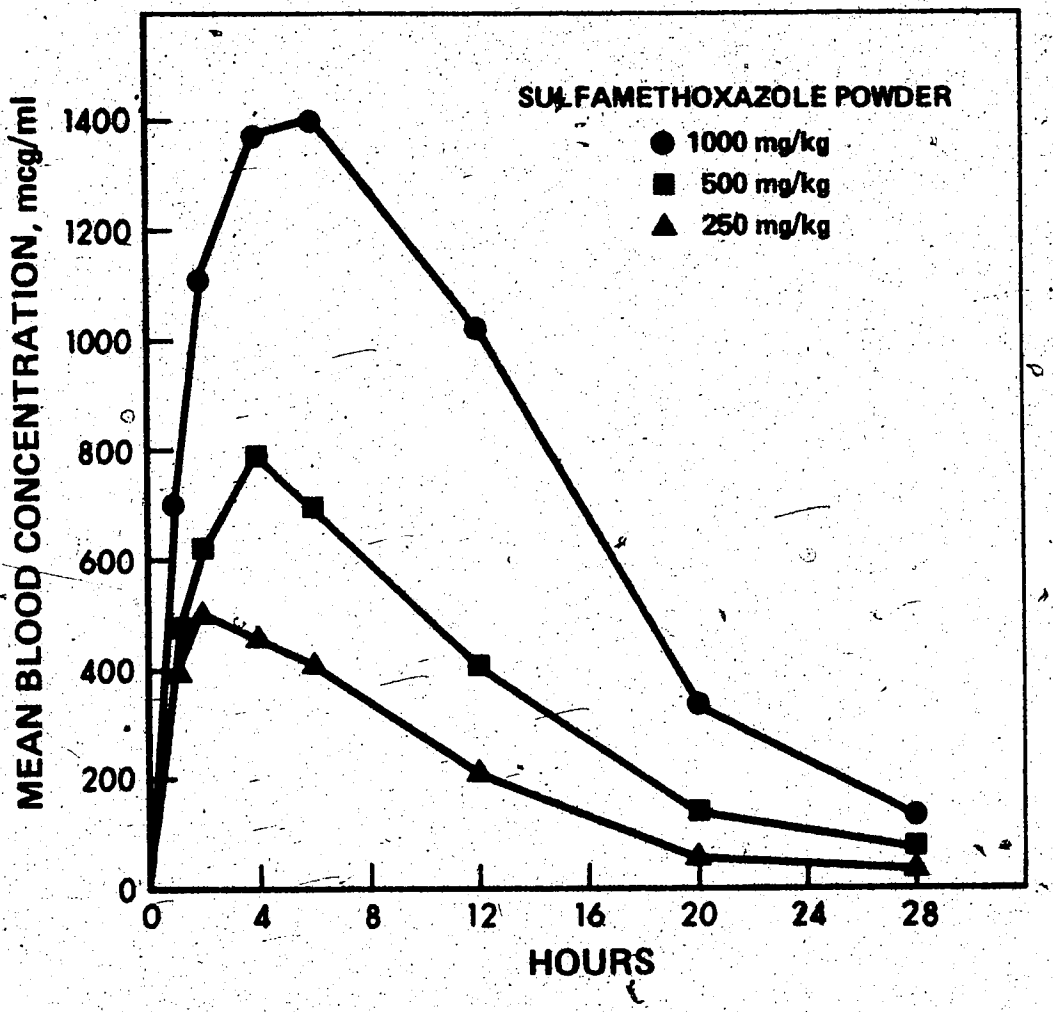

Figure 39 - Blood Concentration-Time Profiles for Sulfamethoxazole following Single-Dose Oral Administration to Three Rats.

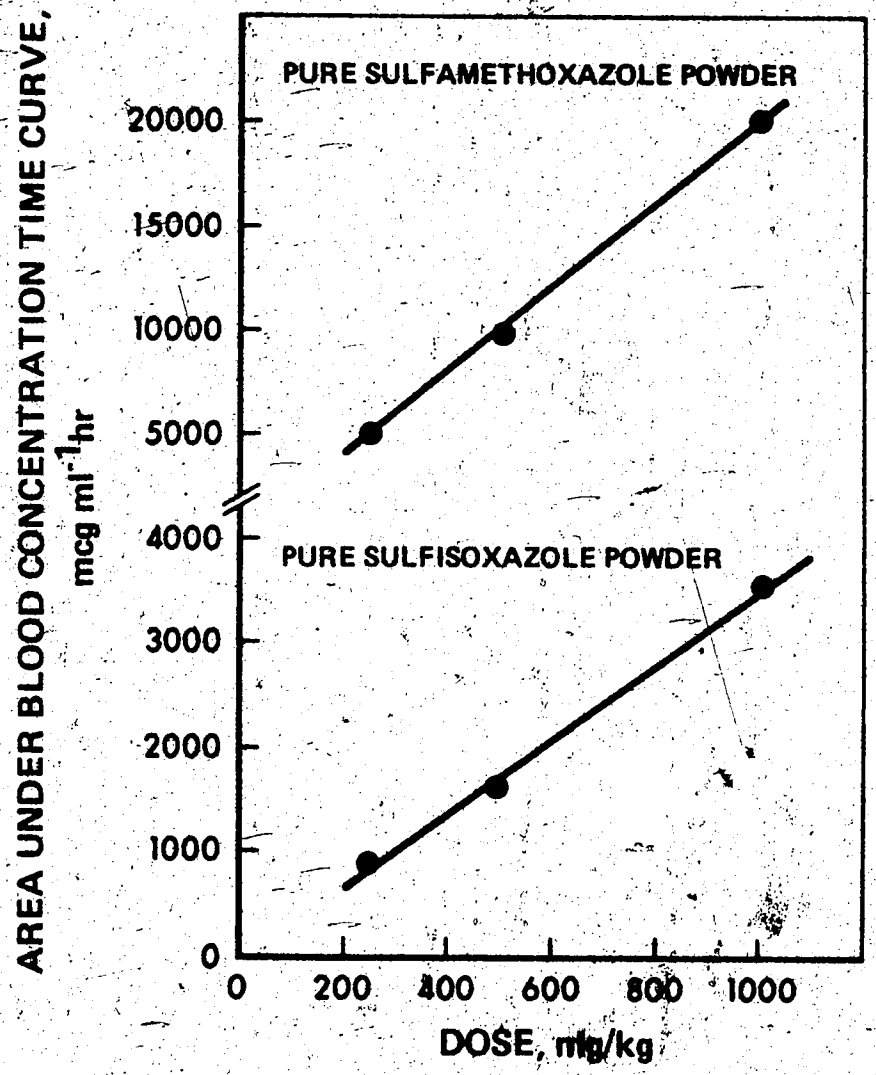

Figure 40 - Dependence of Area under the Curve on Dose Administered for Pure Sulfamethoxazole and Sulfisoxazole Powders

$$B_t = \frac{FD}{V}\left(\frac{K_A}{K_A - K_E}\right)\left(e^{-K_E t} - e^{-K_A t}\right) \qquad \text{(Eq. 34)}$$

In the present study, the blood level data for each drug were analyzed by the one-compartment open model. Typical semilogarithmic plots of the time course of drug concentration in blood for sulfisoxazole and sulfamethoxazole are shown in Figures 41 and 42. Since the ascending portion of the curve is usually associated with the absorption as well as the elimination process, the absorption rate constants, K_A, were calculated by graphical analysis using the feathering technique. The elimination rate constants, K_E, were calculated from the slope of the descending portion of the curve. The calculations were based on the first-order kinetics. The value of the unknown constant, FD/V, was determined from the y intercept of the extrapolated line. The mean blood level data for sulfisoxazole, sulfamethoxazole, and methisazone preparations were plotted on rectilinear coordinates, as shown in Figures 43-49. The measured areas under the curves were then compared statistically.

Analog Computer Fitting

As can be seen from Figure 49, methisazone levels in the blood beyond an 8 hr. period could not be detected. This was attributed to the sensitivity limits of the method used. Based on these observations, it was anticipated that the lack of sensitivity of the method would result in the overestimation of the elimination rate constant. Therefore, it became necessary to fit the blood level curves by analog

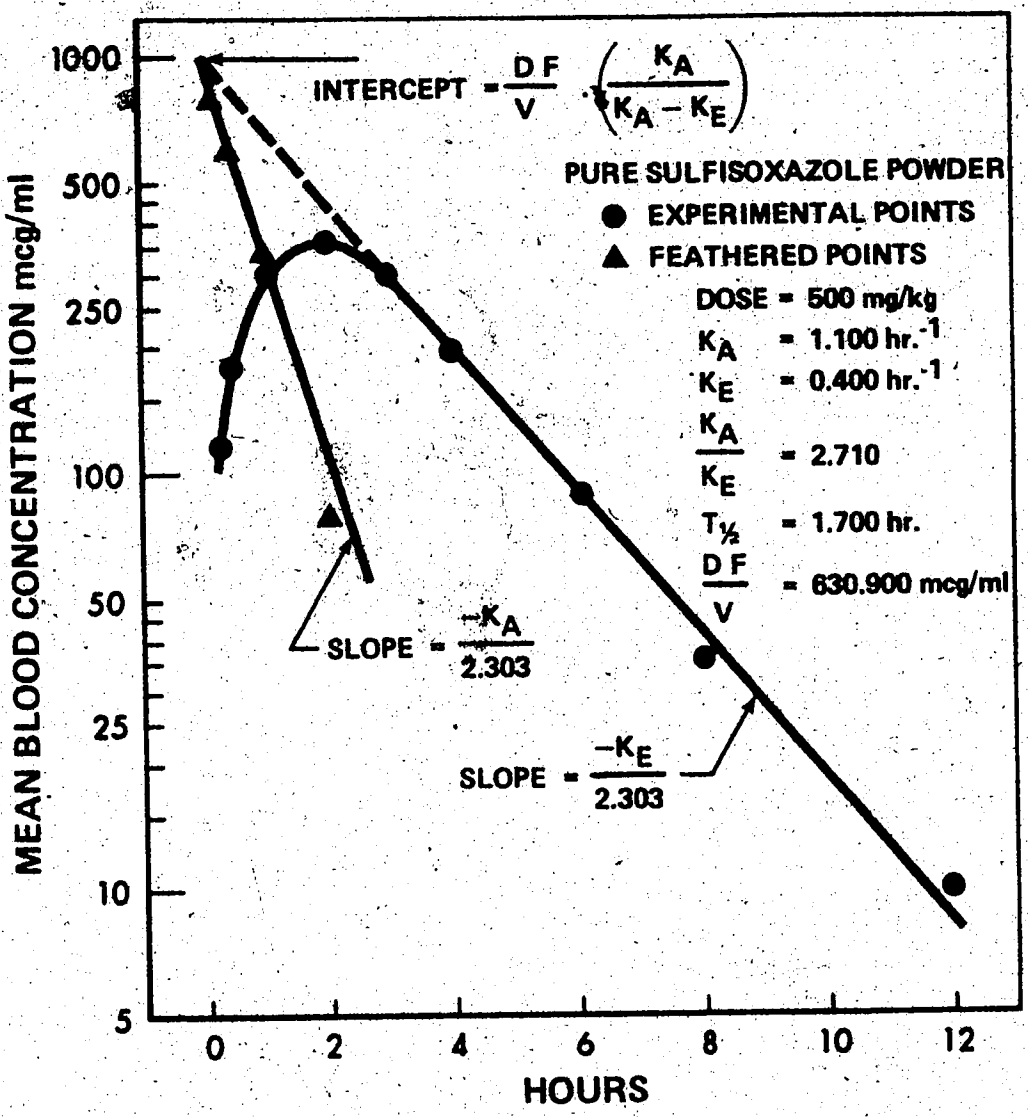

Figure 41 - Semilogarithmic Plot of Blood Levels follwoing Single-Dose Oral Administration of Sulfisoxazole to Three Rats.

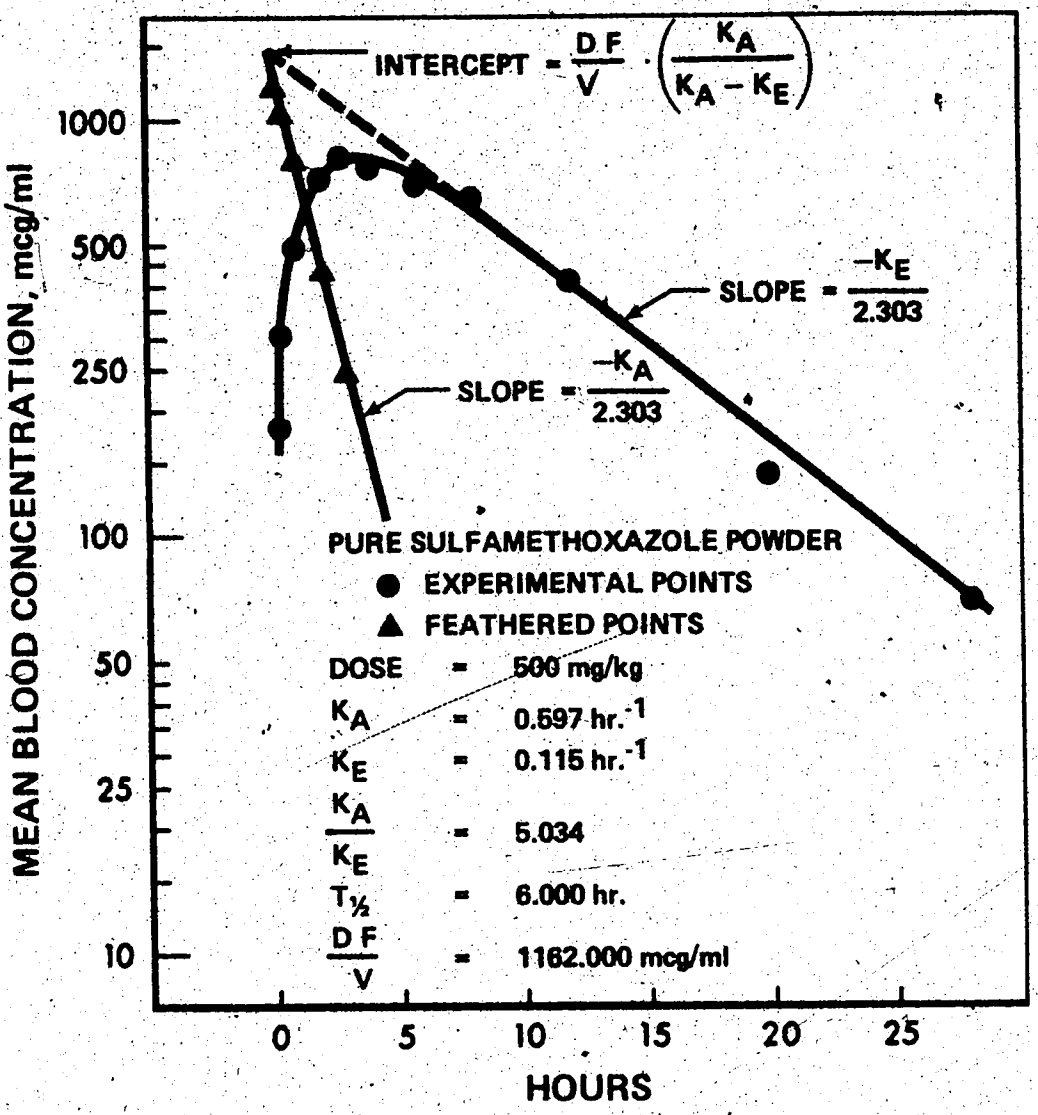

Figure 42 - Semilogarithmic Plot of Blood Levels following Single-Dose Oral Administration of Sulfamethoxazole to Three Rats

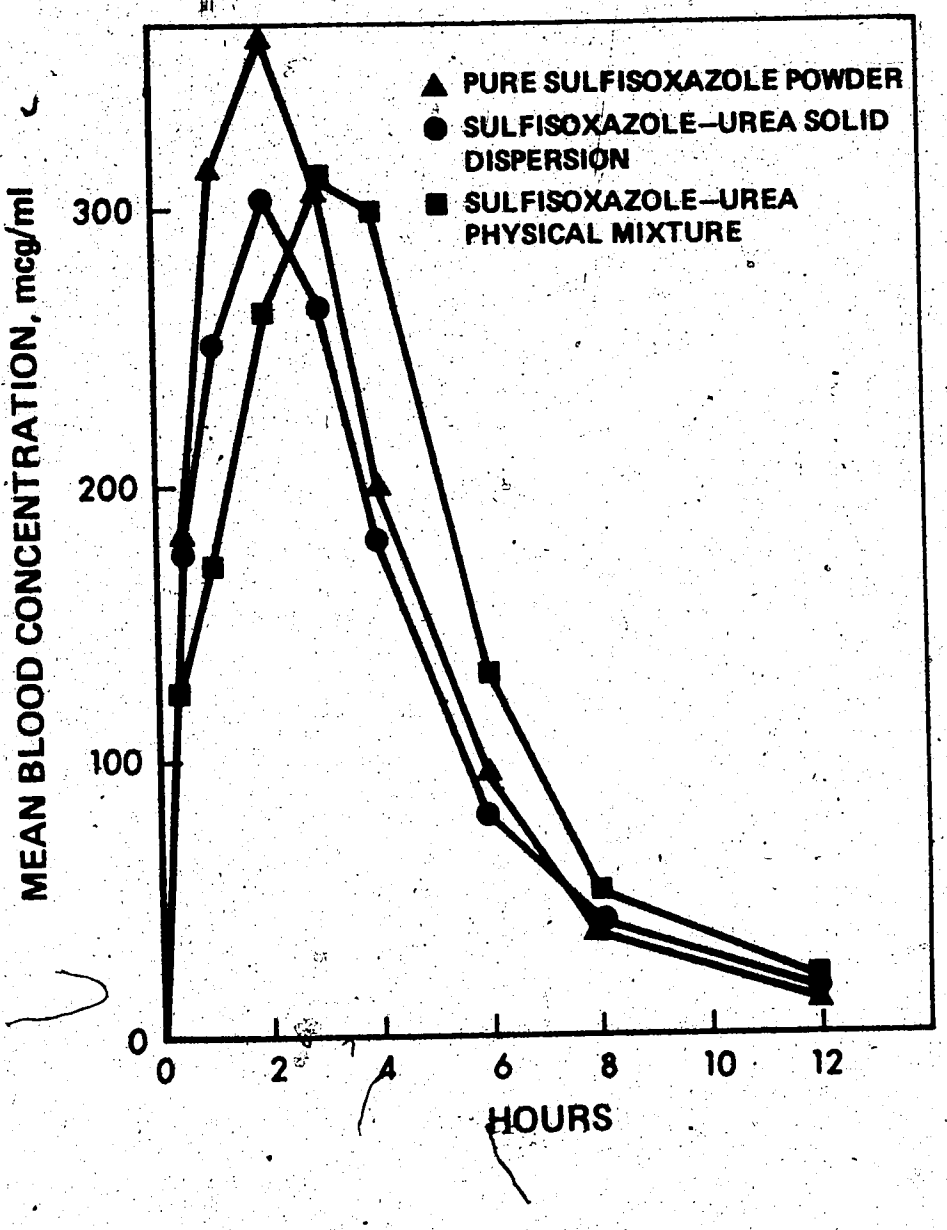

Figure 43 - Sulfisoxazole Blood Level Curves in Three Rats following Single-Dose Oral Administration of Pure Sulfisoxazole and Preparations containing Urea. Dose used was Equivalent to 500 mg/kg of Sulfisoxazole.

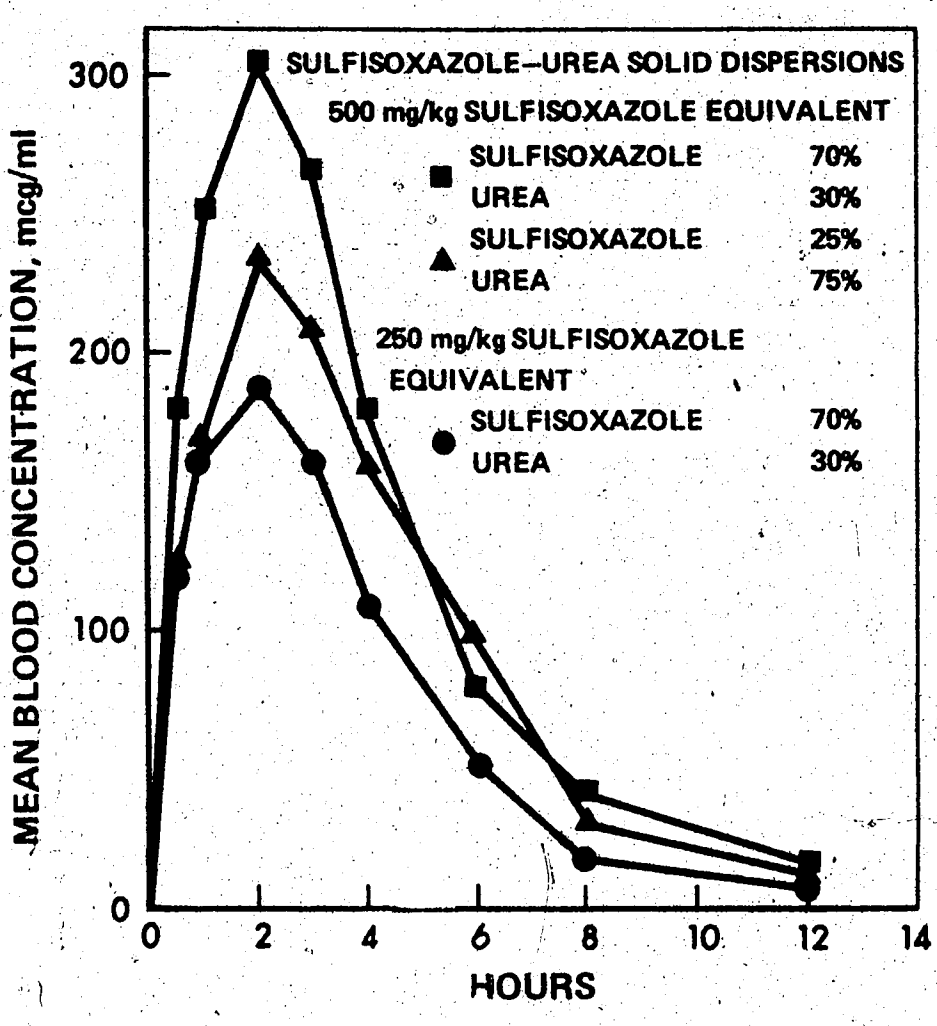

Figure 44 - Sulfisoxazole Blood Level Curves in Three Rats following Single-Dose Oral Administration of Sulfisoxazole-Urea Solid Dispersions.

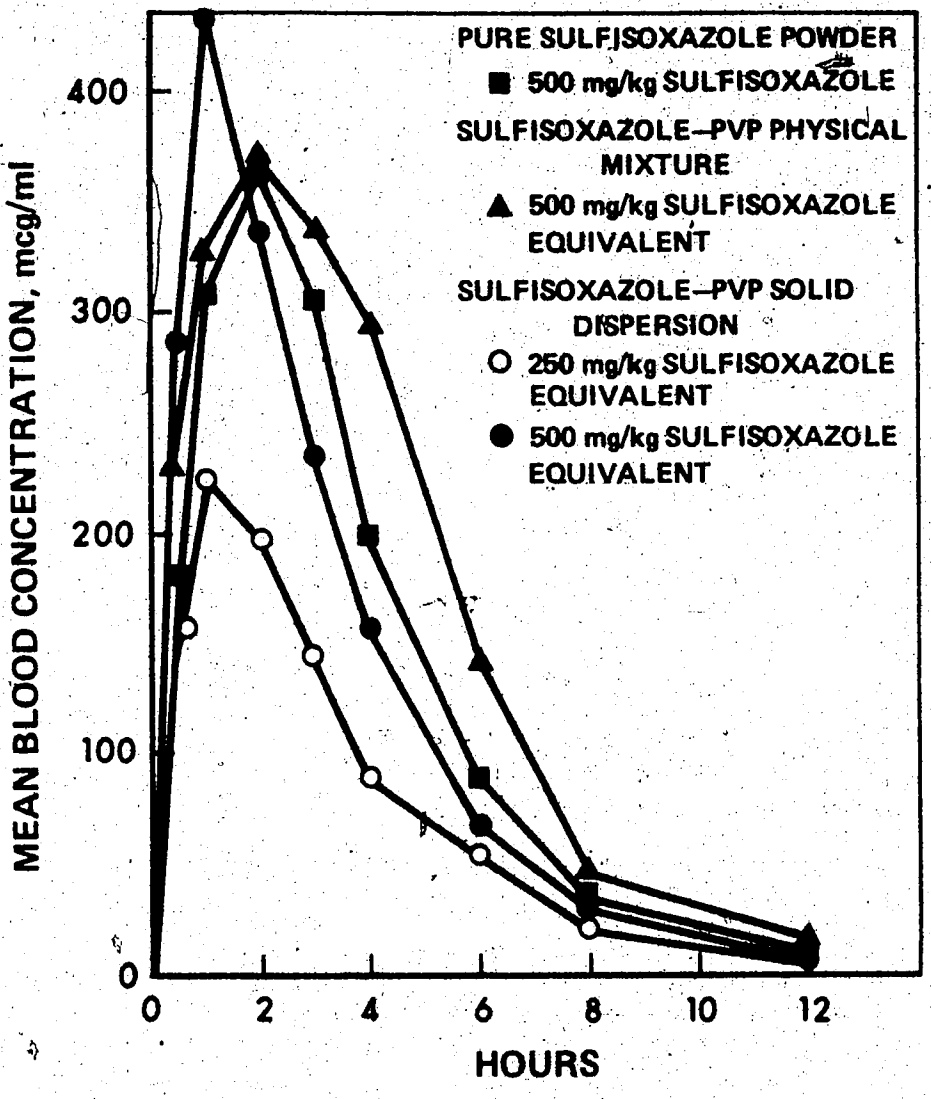

Figure 45 - Sulfisoxazole Blood Level Curves in Three Rats following Single-Dose Oral Administration of Pure Sulfisoxazole and Preparations containing PVP.

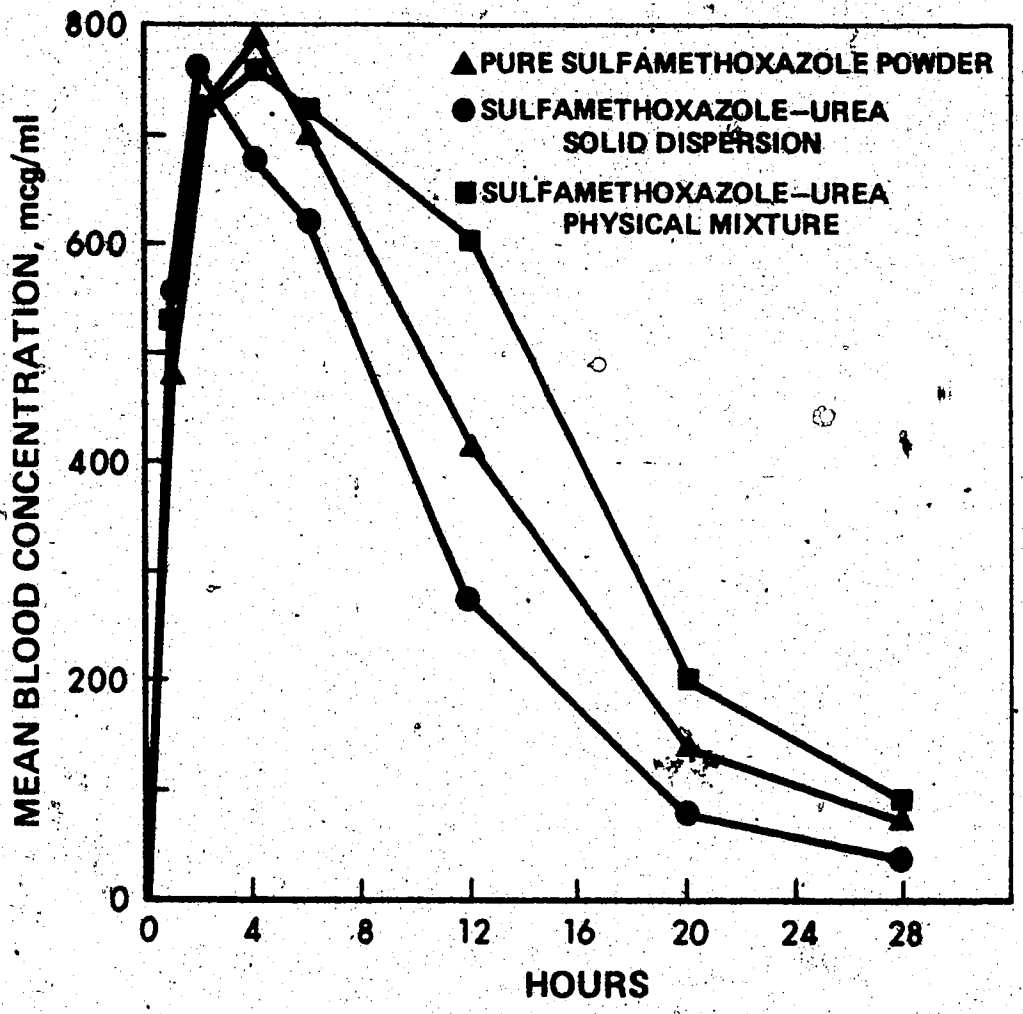

Figure 46 - Sulfamethoxazole Blood Level Curves in Three Rats following Single-Dose Oral Administration of Pure Sulfamethoxazole and Preparations containing Urea. Dose used was Equivalent to 500 mg/kg of Sulfamethoxazole.

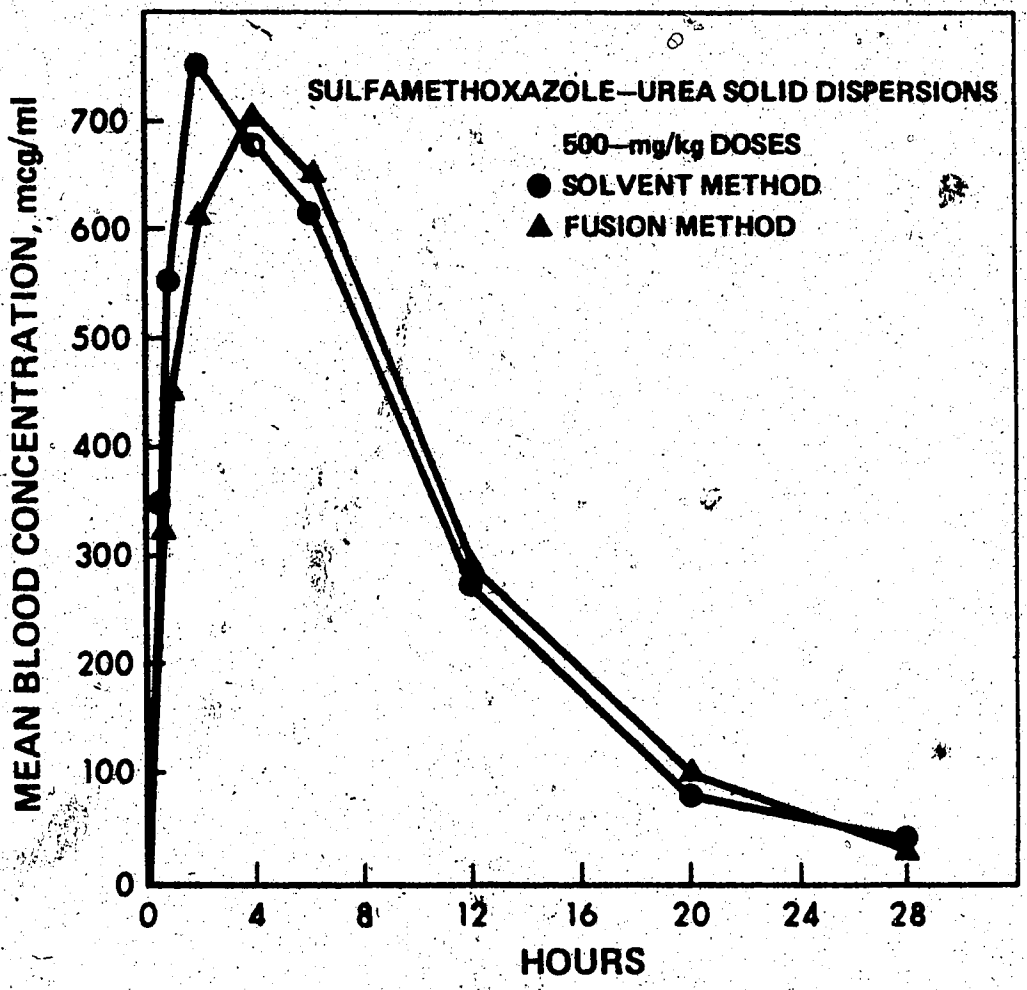

Figure 47 - Sulfamethoxazole Blood Level Curves in Three Rats following Single-Dose Oral Administration of Sulfamethoxazole-Urea Solid Dispersions.

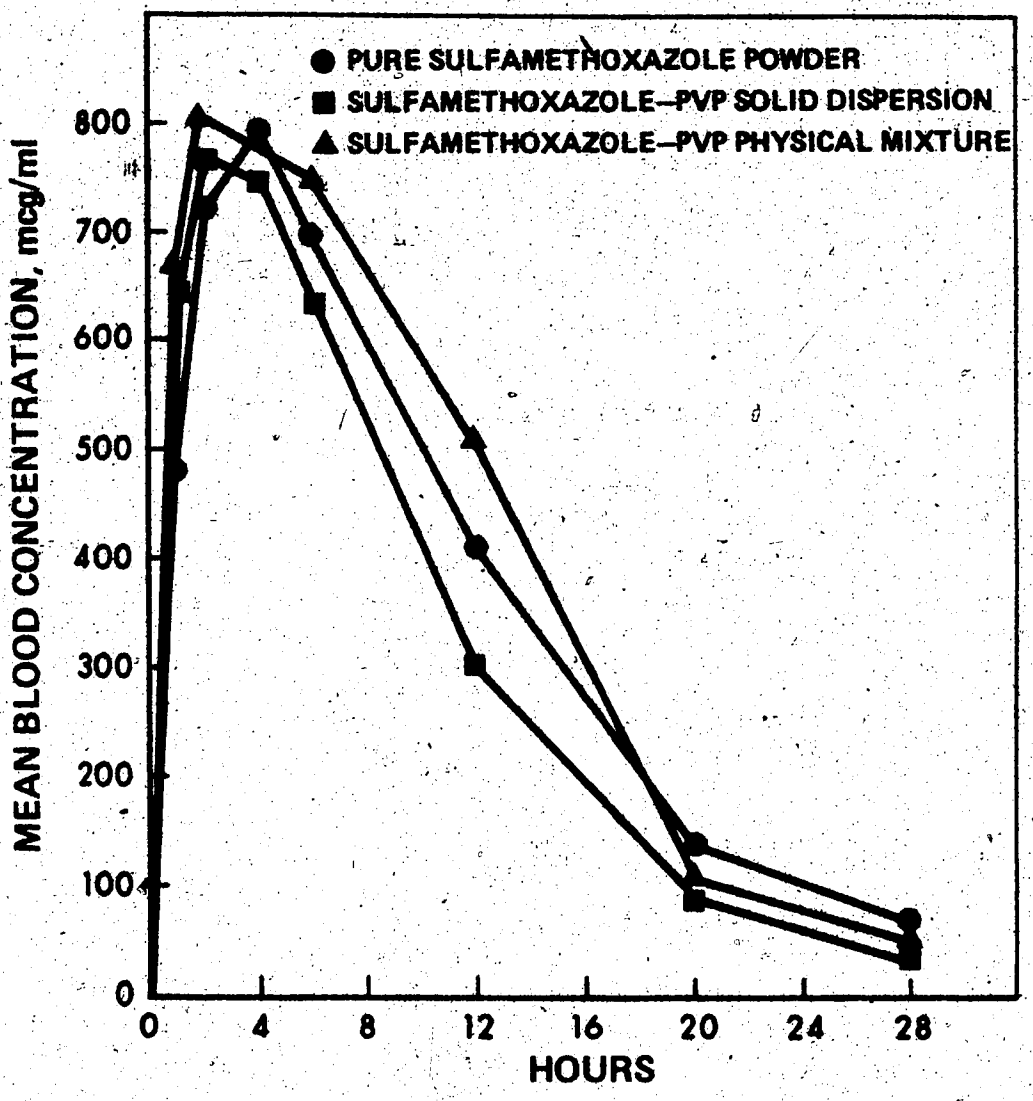

Figure 48 - Sulfamethoxazole Blood Level Curves in Three Rats following Single-Dose Oral Administration of Pure Sulfamethoxazole and Preparations containing PVP. Dose used was Equivalent to 500 mg/kg of Sulfamethoxazole.

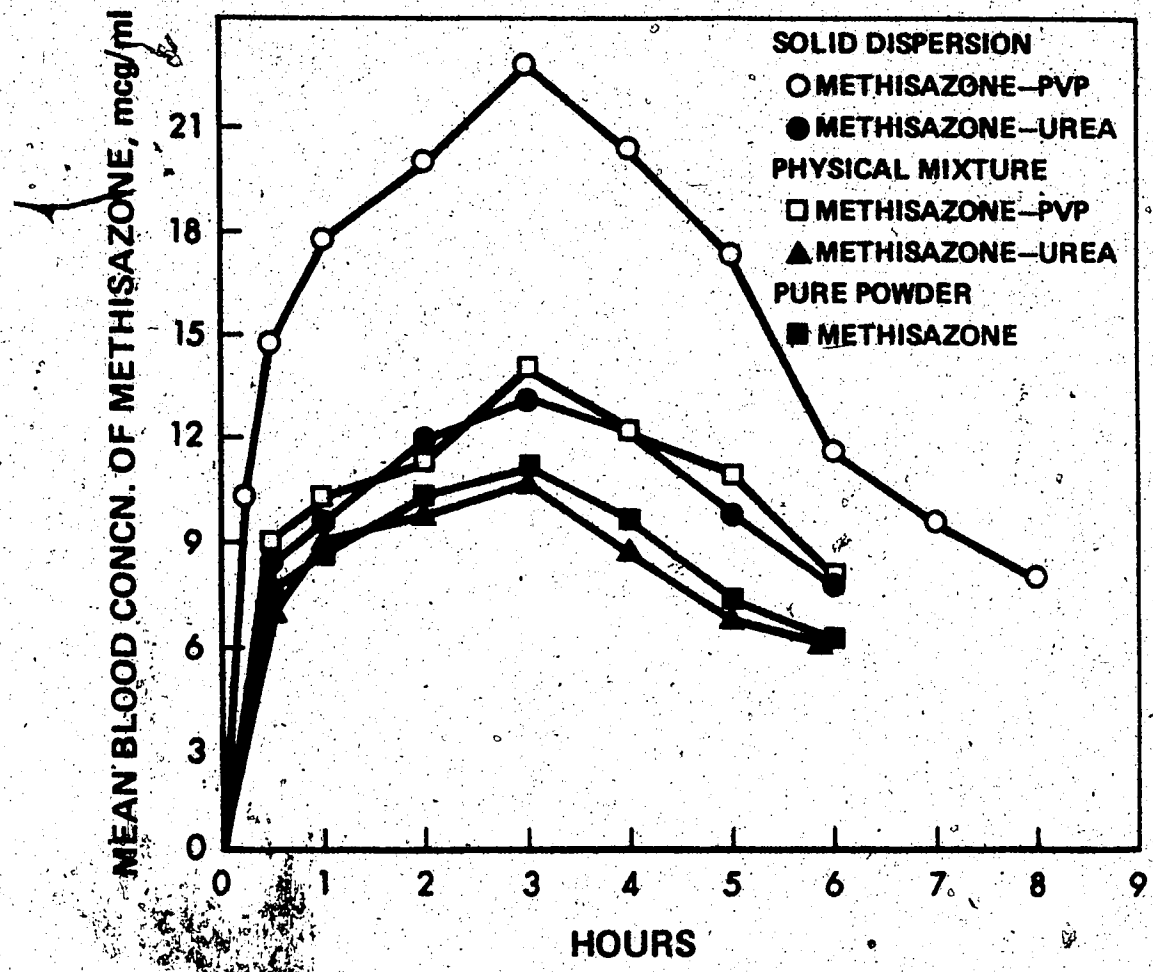

Figure 49 – Methisazone Blood Level Curves in Three Rats following Single-Dose Oral Administration of Pure Methisazone and Preparations containing Urea or Polyvinylpyrrolidone. Dose used was Equivalent to 500 mg/kg of Methisazone.

simulation techniques so that true estimates of the rate constants could be obtained. For this purpose, a TR-20 analog computer[1] was programmed with the one-compartment open model (Scheme I):

$$G \xrightarrow{K_A} B \xrightarrow{K_E} E$$

Scheme I

where G is the quantity of drug remaining in the gut and E is the quantity of drug eliminated. The differential equations describing the model are:

$$\frac{-dG}{dt} = K_A G \qquad \text{(Eq. 35.1)}$$

$$\frac{dB}{dt} = K_A G - K_E B \qquad \text{(Eq. 35.2)}$$

$$\frac{dE}{dt} = K_E B \qquad \text{(Eq. 35.3)}$$

The analog computer program for the model based on equations 35.1, 35.2, 35.3, and 15 is shown in Figure 50. Figure 51 shows the results of a typical analog simulation of blood data in accordance with the one-compartment open model. It can be seen from the analog simulation that the computer-generated curve fits the experimental data reasonably well. However, in order to test the agreement between the experi-

[1]Electronic Associates, Inc., West Long Branch, N.J., U.S.A.

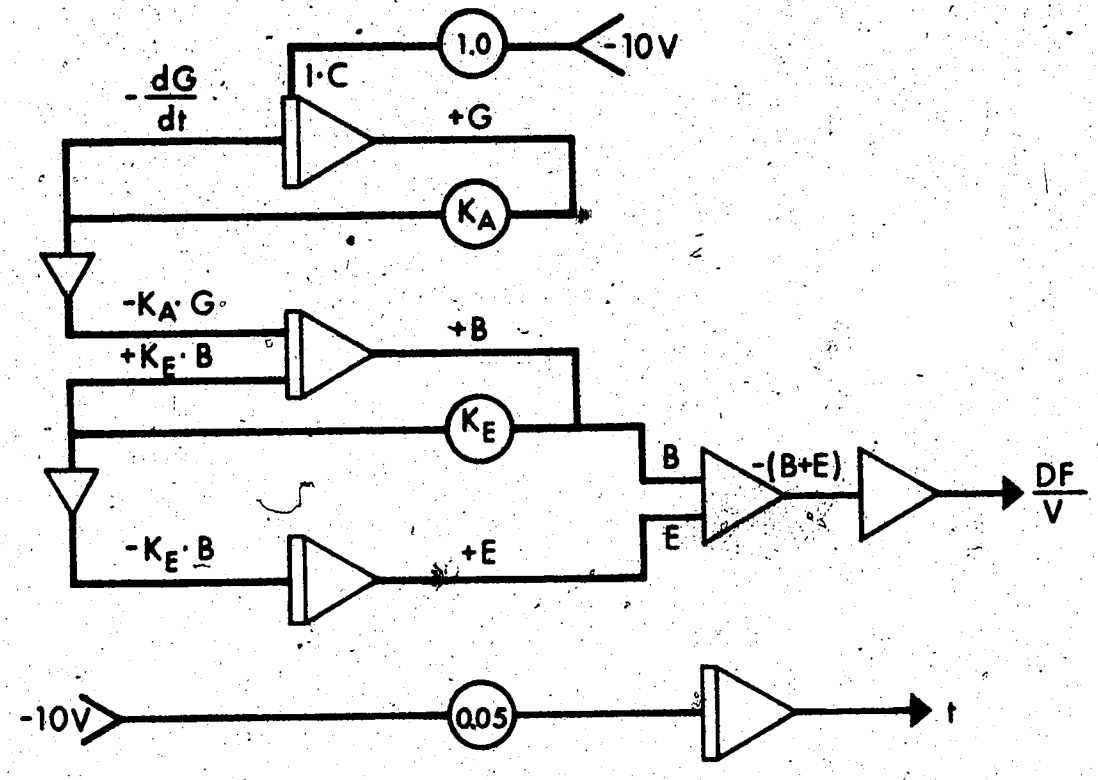

Figure 50 - Analog Computer Program for a One-Compartment Open Model

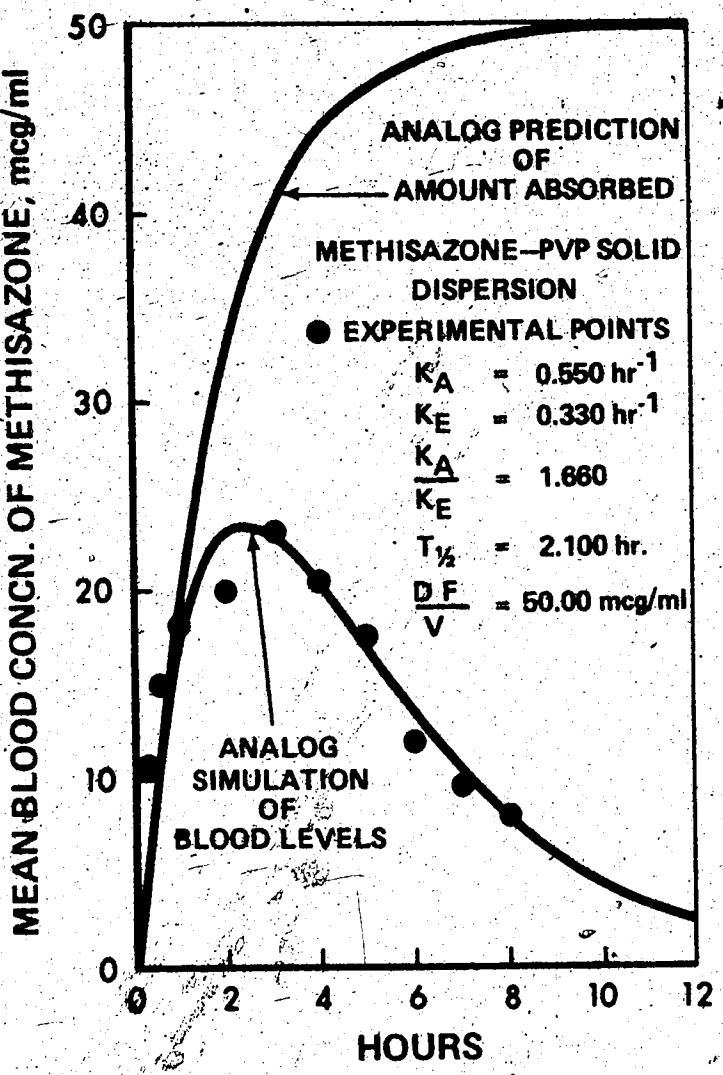

Figure 51 - Analog Computer Fitting of Blood Data in accordance with a One-Compartment Open Model

mental data and the rate constants estimated by the analog computer, urinary excretion studies under uncontrolled urinary pH conditions were conducted.

Urinary Excretion Studies

Urinary excretion studies can be used to evaluate the bioavailability of drugs (110). Assuming that excretion rate parallels blood levels of a drug, both the maximum urinary excretion rate and the time of the maximum urinary excretion rate will reflect the rate of absorption, and the cumulative amount excreted will reflect the extent of drug absorption. Recently, Khalafallah et al. (111) have demonstrated the use of urinary excretion data as an alternative to the use of blood level data in the evaluation of bioavailability of sulfameter.

In the present study, the cumulative excretion of methisazone in urine was calculated as mg/kg and the excretion rate as mg/kg/hr. The mean urinary excretion data for methisazone and its preparations following single-dose oral administration in rats are shown in Tables A-37 to A-41. The plots showing the cumulative amounts of methisazone excreted in the urine as a function of time are illustrated in Figure 52. The semilogarithmic plots of the urinary excretion rate as a function of time are depicted in Figures 53 and 54. The elimination rate constant, K_E, was calculated from the slope of the descending segment of

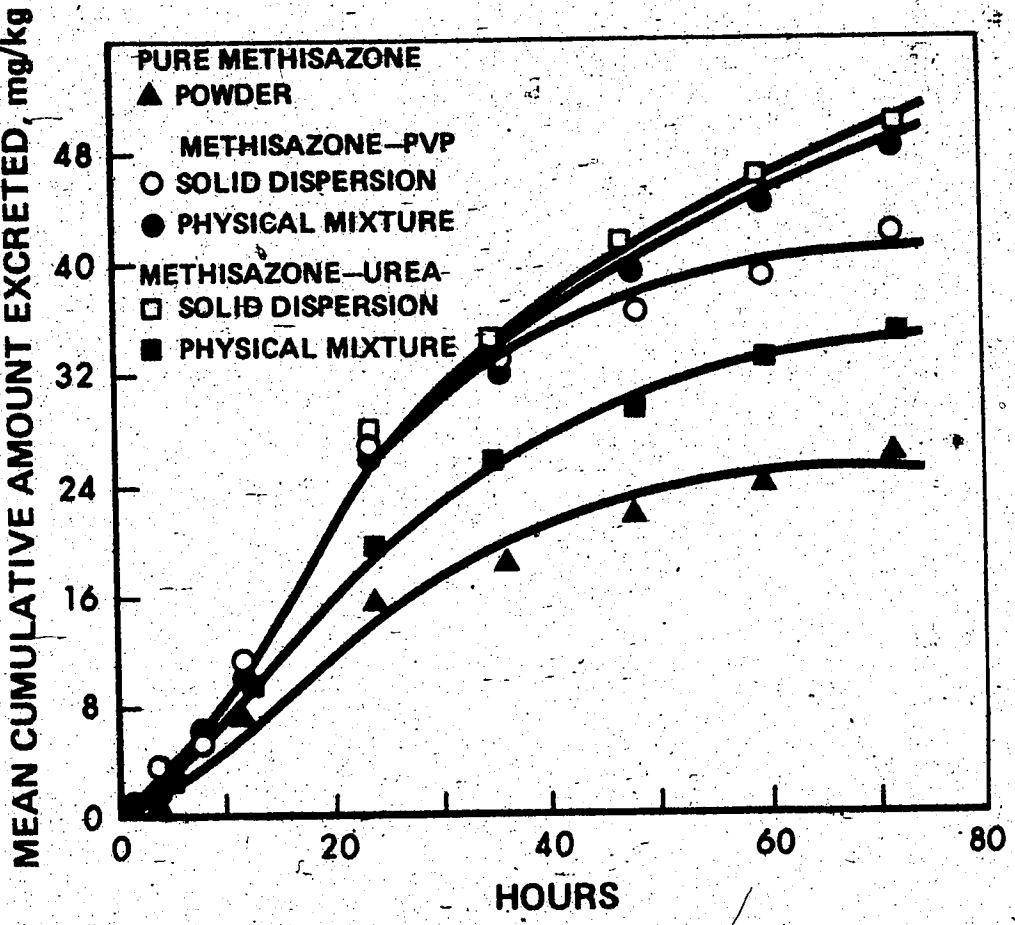

Figure 52 - Cumulative Amounts of Methisazone Excreted in Urine following Single-Dose Oral Administration to Three Rats. Dose used was Equivalent to 500 mg/kg of Methisazone.

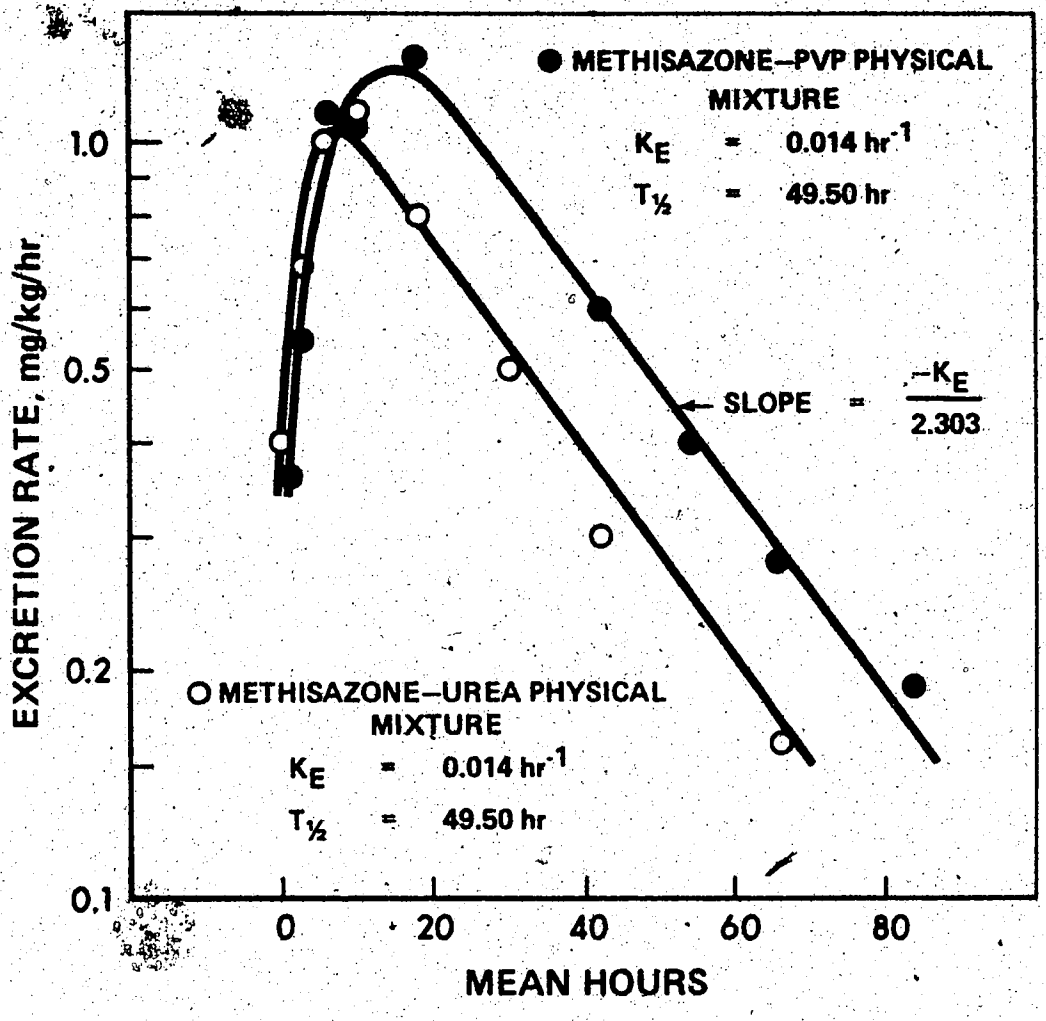

Figure 53 - Semilogarithmic Plots of Urinary Excretion Rate as a function of Time following Single-Dose Oral Administration to Three Rats. Dose used was Equivalent to 500 mg/kg of Methisazone.

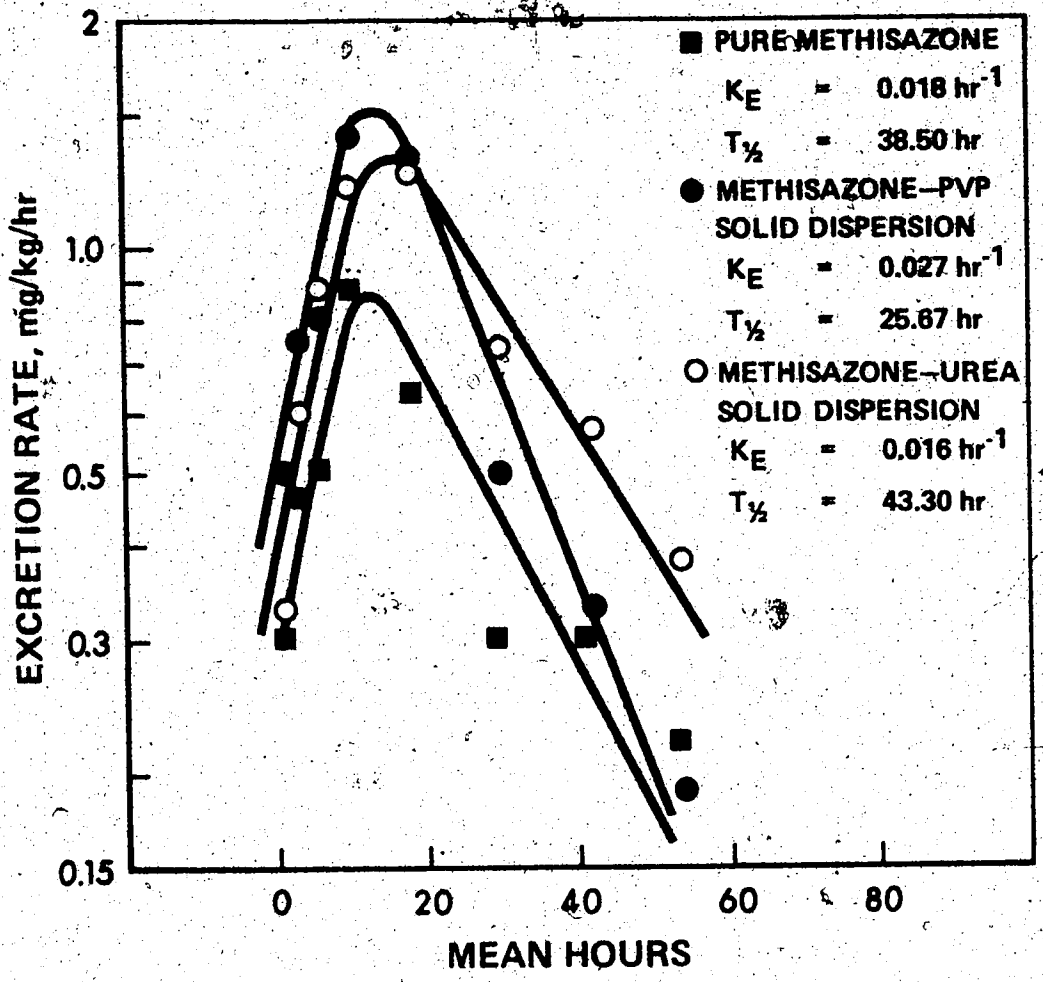

Figure 54 - Semilogarithmic Plots of Urinary Excretion Rate as a function of Time following Single-Dose Oral Administration to Three Rats. Dose used was Equivalent to 500 mg/kg of Methisazone.

the semilogarithmic plots. The terminal ends of the descending curves were fitted by least squares regression analysis using the PDP-8/L minicomputer. In-as-much as the urinary excretion studies were conducted under uncontrolled pH conditions, the fluctuations in the excretion rate could be attributed to changes in urinary pH.

DISCUSSION

Preliminary investigation conducted with 100-mg samples of evaporated binary mixtures revealed that sulfisoxazole-urea solid dispersions with compositions ranging from 30 to 80% of sulfisoxazole produced DTA thermograms which were difficult to interpret and correlate with phase diagrams. This anomalous behavior was partly attributed to concomitant thermal decomposition of sulfisoxazole on fusion. For this reason, additional thermal studies, using the capillary melting point method, were conducted to investigate the nature of phase diagrams. An examination of the phase diagram (Fig. 4) indicates that the sulfisoxazole-urea solid dispersion typifies a eutectic system with incongruent complex having a composition of 70% sulfisoxazole - 30% urea. Based on these visual thermal analysis findings, attempts were made to reproduce the phase diagram, showing the existence of complex formation with incongruent melting points, through differential thermal analysis, but without much success. However, by careful control of operational variables and by selecting a sample size of 8-mg, DTA thermograms could be obtained which were amenable to interpretation insofar as detection of incongruent melting points was concerned.

As is seen in Figure 6, the solid dispersion containing 20% sulfisoxazole and 80% urea yielded only one endotherm

as a major peak near 130°C, demonstrating the fact that the melting point of 100% urea, in presence of sulfisoxazole, is lowered by 4°C. In contrast with Figure 6, it can be seen from Figure 7, that the DTA thermograms of solid dispersions containing 2, 5, and 20% urea show first the appearance of extra endothermic peaks due to incongruent complex formation, and then the major endothermic peaks corresponding to fusion of sulfisoxazole in excess of the complex. A marked shift in peak temperatures of successive major endotherms towards lower peak temperature of the complex endotherm clearly indicates that presence of urea in the binary mixture lowers the melting point of sulfisoxazole as a result of the complex formation. On close inspection of the DTA thermograms, as shown in Figure 7, it becomes clear that with increasing amounts of urea in sulfisoxazole-urea binary mixtures, the complex endotherm becomes larger and better defined, and consequently the area under its peak grows at the expense of area under the 100% sulfisoxazole endotherm, indicating transition of energy accompanying complex formation. Finally, the energy transition associated with complex formation reaches a maximum at the composition of 70% sulfisoxazole and 30% urea. This estimate of complex composition available from DTA is consistent with that obtained from the phase diagram.

It is evident from DTA thermograms for 40 and 60% urea in the sulfisoxazole-urea binary mixture, as depicted in

Figures 6 and 7, that fusion peaks contributed by peritectic and eutectic reactions occur within such a narrow temperature range that it becomes difficult to differentiate between closely occuring thermal events. Because of superimposition of two adjacent peaks, the heat effects due to peritectic reaction are simply overshadowed by the eutectic endotherm. The overlapping of thermal effects is characterized by the indentation of DTA peaks. An examination of the phase diagram in Figure 4 reveals the existence of complex formation on the basis of incongruent melting points observed in evaporated mixtures, despite the fact that the jump in the solidus is rather small.

The phase diagram, as shown in Figure 5, indicates that sulfamethoxazole-urea binary mixture can be classified as a eutectic system with partial solid solution. The eutectic isotherm in Figure 5 occurs near 118°C, and extends from 10 to 95% sulfamethoxazole. The DTA thermograms of sulfamethoxazole-urea binary system (Figs. 8 and 9) reflect the tendency of the major endothermic peaks to shift towards a lower temperature of about 118°C where the formation of the eutectic endotherm is self-evident. As can be seen from Figures 5 and 9, the eutectic composition of the binary system corresponds to 60% sulfamethoxazole - 40% urea. The DTA thermograms of 5% sulfamethoxazole - 95% urea (Fig. 8) and 95% sulfamethoxazole - 5% urea (Fig. 9) binary systems indicate that the mutual solid solubility of sulfamethoxazole and urea is less than 5% and hence considered negligible.

The phase diagram of methisazone-urea binary system (Fig. 10) consists of two distinct isotherms, the eutectic and the peritectic. The eutectic and peritectic temperatures are 128°C and 187°C, respectively. It can be inferred from the phase diagram that a complex with a composition of 50% methisazone - 50% urea is formed between the components. The DTA thermograms of 40% methisazone - 60% urea (Fig. 11) and 49% methisazone - 51% urea (Fig. 12) binary systems exhibit three endothermic peaks as opposed to two endothermic peaks, indicating the existence of the peritectic reaction.

The DTA thermograms of binary mixtures, as depicted in Figures 13-15, indicate that systems containing PVP exhibit only major endotherms as fusion peaks of those drug components which are in excess of the complex composition. Since PVP, like glass, has no sharp or specific melting point, the endothermic peaks corresponding to the fusion of PVP are absent from the DTA thermograms. It is interesting to note that the major endotherms tend to shift towards lower temperatures as the concentration of PVP in the binary systems increases until it reaches a critical concentration beyond which the endotherms just disappear. The binary mixtures containing PVP in amounts greater than its critical concentration do not exhibit any characteristic melting points. On heating, they gradually soften before turning to liquid state. Since PVP can exist in a vitreous state (15), the solubilization of sulfisoxazole, sulfamethoxazole, and methisazone by PVP would result in the formation of glass

solutions. The characteristic quenching of the endothermic peaks explicitly reveals the existence of glass solution formation.

In the development of a solid dosage form, the proper use of a metastable polymorph should result in a more rapid and complete absorption of the drug. However, the polymorphic change of the drug from metastable to stable form can cause problems in the areas of aqueous solubility, dissolution rate, and bioavailability of the drug. For this reason, in the preparation of all solid dispersions, the stable polymorphic forms of the drugs were used throughout the present study. An examination of the DTA thermograms revealed no evidence of polymorphism in the sulfisoxazole, sulfamethoxazole, and methisazone used. The heats of fusion of these drugs, and of urea were determined by DTA calorimetry. The data obtained from the DTA thermograms are summarized in Table XXIV. It can be seen from the table that the heat of fusion of sulfamethoxazole determined in this study does not agree with published values. Sunwoo and Eisen (101) reported the presence of a major endothermic peak at 166.3°C whereas Yang and Guillory (38) have reported the presence of the major endothermic peak at 170°C in addition to an extra endothermic peak at 166°C. On the basis of information available there appears to be no satisfactory evidence to account for this lack of agreement.

TABLE XXIV

Heat of Fusion Measurements[a] for Sulfisoxazole, Sulfamethoxazole, Methisazone and Urea

Specimen	Peak Temp., °C	Calibration Coefficient, mcal/deg/min	Peak Area[b], sq.in.	Heat of Fusion, Kcal/mole	
				Observed	Reported
Sulfisoxazole	192.0	1.350	1.00±0.04	9.267±0.368	6.990±0.013[c]
					7.550±0.188[d]
Sulfamethoxazole	165.0	1.325	0.68±0.02	18.760±0.552	6.852±0.110[c]
					5.860±0.117[d]
Methisazone	250.0	1.460	0.28±0.02	7.873±0.562	
Urea[e]	134.0	1.290	2.00±0.08	3.976±0.160	

[a] Mean values from three thermograms with standard deviation

[b] Peak area normalized to a chart speed of 1 in min^{-1}

[c] Reported literature value (101)

[d] Reported literature value (38)

[e] Operating conditions were identical to those described for sulfisoxazole

The effects of urea and polyvinylpyrrolidone on the solubility of sulfisoxazole, sulfamethoxazole, and methisazone in distilled water are depicted in Figures 17-20. The results of these studies indicate the linear dependency of both sulfisoxazole and sulfamethoxazole solubility on the concentration of urea and polyvinylpyrrolidone. Similarly, the solubility of methisazone was found to increase linearly with the concentration of polyvinylpyrrolidone. On the other hand, urea seemed to have no effect on the solubility of methisazone. This solubilizing action of both the urea and polyvinylpyrrolidone may be attributed to the formation of soluble complexes. Because of the high solubility of these reaction products, the plateau formation due to saturation is not seen. The linear increase in aqueous solubility of the drugs as a function of urea or polyvinylpyrrolidone concentration suggests that the complexes formed have one mole of either urea or polyvinylpyrrolidone. The data presented in Tables IX and X indicate that the slopes of the linear plots are less than 1 for all except the sulfamethoxazole-polyvinylpyrrolidone system. The slopes for the sulfamethoxazole-polyvinylpyrrolidone system at 25 and 37°C are 1.68 and 2.54, respectively. As suggested by Connors and Mollica (102), these slopes would imply that stoichiometry of the systems having slopes less than 1 is probably one-to-one. The same reasoning would

suggest that the stoichiometric ratios for the sulfamethoxazole-polyvinylpyrrolidone system at 25 and 37°C are two-to-one and three-to-one, respectively. The interactions which have an association equilibrium constant, K_a, greater than 1 proceed spontaneously and those with less than 1 require energy for initiation of the reaction. Further, the negative sign of the free energy change, $\Delta F°$, signifies that the formation of the complexes is spontaneous and the positive sign signifies that the complex formation is non-spontaneous. Similarly, the positive sign of the heat of formation, $\Delta H_f°$, indicates that formation of the complexes is endothermic in nature. The positive entropy changes indicate that the water molecules have acquired a random configuration as a result of complexation. Hence, the formation of complexes is accompanied by an increase in entropy. As can be seen from Tables IX and X, the entropy changes correlate well with the corresponding heats of formation.

The complex formation may be attributed to hydrogen bonding. Since the hydrogen bonds are considered to be weak chemical bonds due to dipole-dipole interaction, the hydrogen-bonded complexes will exhibit reversibility of the association under normal conditions. Higuchi et al. (112) have discussed the importance of hydrogen-bonding interactions in the formation of various complexes. The mechanism of hydrogen bond formation may be better explained on the basis of the electron theory of dative-covalent linkages. Both urea and polyvinylpyrrolidone have an electron-donating

carbonyl group. This electron-rich carbonyl group will attract electrophilic groups. The imide groups of sulfisoxazole, sulfamethoxazole, and methisazone will accept electrons donated by the carbonyl groups of urea and polyvinylpyrrolidone molecules. DeLuca et al. (113) have reported that the solubility of glutethimide, a sparingly soluble drug, can be increased by solubilizing it with substituted amides which have two independent electron-donating groups.

Having obtained data on the thermodynamics of complex formation from the equilibrium solubility studies, kinetic studies were conducted to investigate the dissolution characteristics of the interacting systems. Higuchi et al. (114) have demonstrated the dependence of dissolution kinetics on both the diffusion coefficient of the complexing component in the solvent and the association equilibrium constant of the complex. Drug complexes are usually included in dosage forms to enhance the solubility and subsequently the dissolution characteristics of the drugs. The complexes that dissolve slowly in water will have dissolution rates less than those of the pure drugs. Higuchi and Pitman (115) synthesized 1:1 and 1:2 complexes of caffeine with gentisic acid, and compared their dissolution rates with that of caffeine. They found that caffeine from the complexes dissolved more slowly than caffeine itself.

The data for the calibration of sulfisoxazole, sulfamethoxazole, and methisazone in distilled water are presented in Table VIII. A linear relationship between absorbance

and drug concentration was found to exist in each case, indicating compliance with Beer's law. Typical Beer's law plots for these drugs are depicted in Figure 16. These standard curves were used in the analysis of samples obtained from dissolution studies.

During the preliminary dissolution studies conducted by the rotating-basket method, it was found that, since binary systems containing PVP released drugs faster than those containing urea, the surface area of the faster disintegrating pellets could not be controlled during the dissolution process. Since the purpose of the dissolution studies was to determine the intrinsic dissolution rate constant, it became necessary to use the rotating-disc method which allows only one surface of the pellet to be exposed to the dissolution medium. A study concerned with the comparative evaluation of the rotating-basket and rotating-disc methods was, therefore, undertaken. The results of this study are shown in Figure 21 which illustrates the usefulness of the rotating-disc method in controlling the dissolution of methisazone from fast-disintegrating pellets. The suitability of the method was checked by running dissolution tests on both the physical mixture and the solid dispersion samples. It can be seen that the rotating-disc method is applicable to the physical mixture as well as the solid dispersion samples. Based on this criterion, the subsequent pellets containing urea and polyvinylpyrrolidone were evaluated by the rotating-basket and rotating-disc methods, respectively.

As seen in Figure 22, the addition of 0.01% Tween 80 to the dissolution medium increased the dissolution rate of pure methisazone powder. This observation suggests that methisazone is hydrophobic in nature, and that the dissolution rate depends on the ability of the dissolution medium to wet the surface of the drug. Figures 25 and 26 show that the semilogarithmic plots are non-linear, indicating the absence of first-order kinetics. In order to test whether these data fit the diffusion-controlled model, the plots of the logarithm of the amount dissolved versus the logarithm of time were constructed and the slopes determined. It can be seen from Figure 32 that the slopes of the linear curves are very close to 0.5, indicating that the dissolution of methisazone is a diffusion-controlled process.

In order to determine whether there were significant differences in the dissolution rate constants of sulfisoxazole and sulfamethoxazole preparations containing urea, a t-test was performed on each possible combination of pairs. It was found that the difference between any pair was statistically significant at the 5% level. From an examination of Figures 23 and 24 it becomes apparent that the dissolution profiles of both sulfisoxazole and sulfamethoxazole for physical mixtures are better than those for the solid dispersions. This unusual effect could possibly be due to complex formation between the components during the dissolution process. Since the percent dissolved-time plots for the physical mixtures of sulfisoxazole and sulfamethoxazole containing PVP, as represented in upper halves of Figures 23

and 24, were non-linear, the percent undissolved-time data were plotted in Figure 27 to see if the dissolution rates obeyed first-order kinetics. These plots indicate that there are two first-order components to each dissolution profile. To test whether the dissolution data are fitted by the logarithmic normal distribution functions, the logarithmic normal probability plots were constructed. The data plotted on a logarithmic-probability graph paper are shown in Figures 30 and 31. The deviation from linearity of these plots suggest that the data do not adhere to the logarithmic-normal distribution functions. Based on these observations, it may be concluded that the mechanism of dissolution of sulfisoxazole and sulfamethoxazole from physical mixtures containing PVP is rather complex. It would appear that further studies would be necessary in order to elucidate the mechanism in full.

In the case of methisazone preparations, probability plots, as shown in Figures 28 and 29, yielded a straight-line relationship, indicating that the dissolution data can be described by logarithmic normal distribution functions. From these linear plots, percent dissolution times were determined for statistical evaluation. A summary of results presented in Table XIII indicates that the differences in the percent dissolution times are significant at the 5% level.

Since sulfisoxazole and sulfamethoxazole exhibit dose-independent kinetics as indicated in Figure 40, the bio-availability of these drugs can be estimated by comparing

areas under the blood concentration-time curves. Similarly dose-independent kinetics for methisazone has been reported in rats on the basis of urinary excretion data (39). Therefore, the estimation of bioavailability of methisazone can be based on the comparison of cumulative amounts excreted in urine. A summary of some pharmacokinetic parameters obtained by graphical analysis according to the feathering method is presented in Table XXV. It is evident that the extent of absorption, as reflected by AUC, increases with dose whereas the elimination half-life does not. This lends support to the hypothesis that both absorption and elimination follow first-order (dose-independent) kinetics.

In order to determine significant differences between treatments, the areas under the blood concentration-time curve and cumulative amounts excreted in urine were subjected to a one-way analysis of variance, using a completely random design. When the F values for the treatments were significant, the least significant difference test was applied to determine the source of the difference. The least significant difference (116) is basically a Student's t test, which uses a pooled error variance in the calculation of the standard error of the mean difference. The results of the statistical analyses for sulfisoxazole, sulfamethoxazole, and methisazone are presented in Tables XXVI-XXXIII. It is apparent from Figures 43 and 44 that urea significantly reduced the extent of absorption of sulfisoxazole from the solid dispersion. Urea also modified the absorption profiles

TABLE XXV

Summary of Pharmacokinetic Parameters of N^1-substituted Sulfonamides according to One Compartment Open Model following Oral Administration of Single Doses in Male Wistar Rats

Parameters[a]	Dose Levels		
	250 mg/kg	500 mg/kg	1000 mg/kg
Sulfisoxazole			
K_A (hr^{-1})	1.260	1.100	0.693
K_E (hr^{-1})	0.340	0.400	0.340
$T_{1/2}$ (hr)	2.000	1.700	2.000
F.D/V (mcg/ml)	366.000	630.900	1299.000
AUC[b] (mcg.hr/ml)	906.200	1656.200	3562.500
Sulfamethoxazole			
K_A (hr^{-1})	0.894	0.579	0.343
K_E (hr^{-1})	0.117	0.115	0.120
$T_{1/2}$ (hr)	5.900	6.000	5.800
F.D/V (mcg/ml)	651.800	1162.000	2535.600
AUC[c] (mcg.hr/ml)	5125.000	10000.000	20500.000

[a] Mean values from three rats
[b] Area calculated from 0 to 12 hr.
[c] Area calculated from 0 to 28 hr.

TABLE XXVI

Areas under the Blood Concentration-Time Curve (AUC) and Their Statistical Analysis following Single-Dose Oral Administration of pure Sulfisoxazole and its Preparations containing Urea

Preparations	AUC[a], mcg hr ml^{-1}
A. Pure Powder	1656.20±189.9
B. Physical Mixture	1661.67±138.5
C. Solid Dispersion	1420.33±120.8

Analysis of Variance

Source of Variation	DF	SS	MS	F	P
Between Preparations	2	113908	56954.0	2.447	P>0.05
Error	6	139668	23278.0		
Total	8	253576			

Least Significant Difference

SE = 124.57

DF = 6.0

A - B = not significant at P>0.05

A - C = not significant at P>0.05

B - C = not significant at P>0.05

[a]Mean values from three rats with standard deviation

TABLE XXVII

Areas under the Blood Concentration-Time Curve (AUC) and Their Statistical Analysis following Single-Dose Oral Administration of pure Sulfamethoxazole and its Preparations containing Urea

Preparations	AUC[a], mcg hr ml^{-1}
A. Pure Powder	10000.00±500.0
B. Physical Mixture	11875.00±625.0
C. Solid Dispersion	7937.50±634.3

Analysis of Variance

Source of Variation	DF	SS	MS	F	P
Between Preparations	2	23273500	11636700	33.477	P<0.01
Error	6	2085630	347605		
Total	8	25359100			

Least Significant Difference

SE = 481.39

DF = 6.0

A - B = significant at P<0.01

A - C = significant at P<0.01

B - C = significant at P<0.01

[a]Mean values from three rats with standard deviation

TABLE XXVIII

Areas under the Blood Concentration-Time Curve (AUC) and Their Statistical Analysis following Single-Dose Oral Administration of Sulfisoxazole-Urea Solid Dispersions

Type of Solid Dispersion	AUC[a], mcg hr ml^{-1}	t value	P
Incongruent[b]	1420.30±120.8	2.660	0.10>P>0.05
Eutectic[c]	1153.30±125.0		

[a]Mean values from three rats with standard deviation

[b]Incongruent composition: 70% sulfisoxazole, 30% urea

[c]Eutectic composition: 25% sulfisoxazole, 75% urea

TABLE XXIX

Areas under the Blood Concentration-Time Curve (AUC) and Their Statistical Analysis following Single-Dose Oral Administration of Sulfamethoxazole-Urea Solid Dispersions

Method of Preparation	AUC[a], mcg hr ml^{-1}	t value	P
Evaporation	7937.50±634.3	0.365	P>0.50
Fusion	8125.00±625.0		

[a]Mean values from three rats with standard deviation

TABLE XXX

Areas under the Blood Concentration-Time Curve (AUC) and Their Statistical Analysis following Single-Dose Oral Administration of pure Sulfisoxazole and its Preparations containing PVP.

Preparations	AUC[a], mcg hr ml^{-1}
A. Pure Powder	1656.20±189.9
B. Physical Mixture	2006.70±125.0
C. Solid Dispersion	1560.00±135.3

Analysis of Variance

Source of Variation	DF	SS	MS	F	P
Between Preparations	2	331592	165796.0	7.104	0.05>P>0.01
Error	6	140040	23340.0		
Total	8	471632			

Least Significant Difference

SE = 124.74

DF = 6.0

A - B = significant at 0.05>P>0.01

A - C = not significant at P>0.05

B - C = significant at 0.05>P>0.01

[a]Mean values from three rats with standard deviation

TABLE XXXI

Areas under the Blood Concentration-Time Curve (AUC) and Their Statistical Analysis following Single-Dose Oral Administration of pure Sulfamethoxazole and its Preparations containing PVP.

Preparations	AUC[a], mcg hr ml^{-1}
A. Pure Powder	10000.00±500.0
B. Physical Mixture	10479.00±580.7
C. Solid Dispersion	8312.50±845.5

Analysis of Variance

Source of Variation	DF	SS	MS	F	P
Between Preparations	2	7771780	3885890	8.954	0.05>P>0.01
Error	6	2604030	434005		
Total	8	10375800			

Least Significant Difference

SE = 537.90

DF = 6.0

A - B = not significant at P>0.40

A - C = significant at 0.05>P>0.01

B - C = significant at P<0.01

[a]Mean values from three rats with standard deviation

TABLE XXXII

Statistical Analysis of the Cumulative Amounts Excreted in 72 hr following Single-Dose Oral Administration of pure Methisazone and its Preparations containing Urea

Preparations	Cumulative Amount[a] Excreted, mg/kg
A. Pure Powder	26.30±1.9
B. Physical Mixture	35.40±4.7
C. Solid Dispersion	49.78±5.7

Analysis of Variance

Source of Variation	DF	SS	MS	F	P
Between Preparations	2	840.908	420.454	21.813	P<0.01
Error	6	115.652	19.275		
Total	8	956.561			

Least Significant Difference

SE = 3.585

DF = 6.0

A - B = significant at 0.05>P>0.01

A - C = significant at P<0.01

B - C = significant at P<0.01

[a]Mean values from three rats with standard deviation

TABLE XXXIII

Statistical Analysis of the Cumulative Amounts Excreted in 72 hr following Single-Dose Oral Administration of pure Methisazone and its Preparations containing PVP.

Preparations	Cumulative Amount[a] Excreted, mg/kg
A. Pure Powder	26.30±1.9
B. Physical Mixture	47.98±5.7
C. Solid Dispersion	42.59±4.6

Analysis of Variance

Source of Variation	DF	SS	MS	F	P
Between Preparations	2	764.399	382.199	19.767	P<0.01
Error	6	116.010	19.335		
Total	8	880.408			

Least Significant Difference

SE = 3.590

DF = 6.0

A - B = significant at P<0.01

A - C = significant at P<0.01

B - C = not significant at P>0.10

[a]Mean values from three rats with standard deviation

of sulfamethoxazole as is evident from Figure 46. Although the presence of urea in the sulfamethoxazole-urea solid dispersion results in the reduction of the AUC, its presence in the physical mixture increases the AUC. It is possible that the interaction between the uncomplexed urea and sulfamethoxazole in the physical mixture may contribute to the enhancement of bioavailability of sulfamethoxazole. As can be seen in Figure 47, the areas under the curve for sulfamethoxazole-urea solid dispersions prepared by the solvent and the fusion methods do not differ significantly. This indicates that the method of preparation has little effect on the total absorption of sulfamethoxazole. It is interesting to note that polyvinylpyrrolidone behaves in the same way as urea. On the basis of area analysis, the data presented in Figures 45 and 48 indicate that the presence of PVP in solid dispersions significantly reduces the systemic uptake of both sulfisoxazole and sulfamethoxazole. There would seem to be a tendency for solid dispersions to reduce the extent of absorption of these drugs.

The biological half-life of methisazone estimated from the blood level data by analog simulation was approximately 2 hr. However, the biological half-life obtained from the urinary excretion data varied from 25 to 49 hr as illustrated in Figures 53 and 54. This discrepancy in the estimation

of biological half-lives could be due to the presence of a peripheral compartment. Assuming such a possibility, it is not surprising to see methisazone concentration in blood fall below the sensitivity level of the assay procedure after 8 hours post-administration while the urinary excretion continues to be detectable for at least 72 hr beyond the 8 hr period. The time course of methisazone in blood may be adequately described by at least a two-compartment open model (Scheme II):

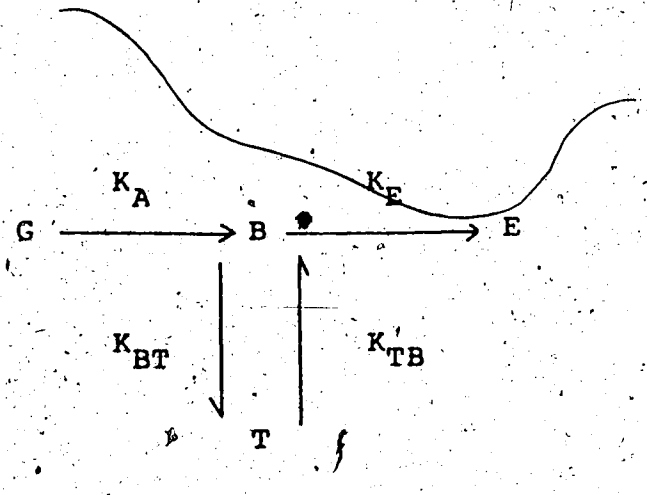

Scheme II

where T is the peripheral (tissue) compartment and K_{BT} and K_{TB} are the first-order rate constants for the distribution of the drug between the central and peripheral compartments. The integrated equation describing the model may be written as:

$$B_t = C\, e^{-\alpha t} + D\, e^{-\beta t} \qquad \text{(Eq. 36)}$$

where C and D are the ordinate axis intercepts, and α and β are hybrid first-order disposition rate constants. The

first exponential corresponds to the fast disposition rate and the second exponential corresponds to the slow disposition rate. The fast and slow disposition rates reflect the distribution phase of the drug from the central to peripheral compartment and the elimination phase of the drug from the body, respectively.

It is believed that the half-lives obtained from the blood level and urinary excretion data reflect the fast and slow disposition half-lives of methisazone, respectively. [redacted] the existence of the two-compartment open model could not be proven conclusively due to the lack of a pharmacokinetic profile following the intravenous administration of methisazone. In practice, it was not found feasible to administer methisazone intravenously to rats.

This concept of a peripheral compartment is presented on the assumption that the methisazone assay procedure was sufficiently specific for the unchanged drug. In bioavailability studies, the specificity of an assay procedure for unchanged drug in the presence of its metabolites plays a vital role. In those instances where colorimetric methods are non-specific, metabolites with cognate absorption characteristics will interfere with the determination of unchanged drug in biological samples. The lack of specificity of the assay will in such cases result in an overestimation of unchanged drug.

Information pertaining to metabolites of methisazone could not be located in the literature. For that reason, no attempt was made to demonstrate the specificity of the analytical procedure used in the present study. With this in mind, the relatively low recovery of methisazone from spiked blood as opposed to the high recovery from spiked urine could suggest that the half-life as determined from the blood data was underestimated. After such considerations, it becomes difficult to speculate on whether the differences obtained for the biological half-lives of methisazone are really due to the presence of a second compartment, or whether they are due to the overestimation of the half-lives as a result of the non-specificity of the assay procedure employed for the urine samples.

The statistical analysis of 72-hr urinary excretion data for methisazone, as presented in Tables XXXII and XXXIII, reveals that both urea and polyvinylpyrrolidone significantly increase the bioavailability of methisazone from solid dispersions.

In the present study, phase diagrams were constructed to ascertain the physical nature and the percent composition of solid dispersions formed. Thermodynamic and kinetic parameters for the binary systems were determined to help elucidate the operative mechanism by which solid dispersions could influence bioavailability of drugs. On the basis of thermodynamic analysis of the methisazone binary systems, interaction between the components could be considered as negligible. On the other hand, in the case of sulfisoxazole

and sulfamethoxazole, the magnitude of the thermodynamic parameters obtained indicated that interaction between the components could not be ruled out as one of the mechanisms affecting bioavailability of the drugs.

It was shown earlier that the dissolution rates for the two sulfonamides from the physical mixtures were faster than those from the solid dispersions. This fact seemed to indicate that the enhancement of dissolution rates from physical mixtures could be due to simultaneous release of both the uncomplexed and the complexed species of the drugs. In other words, the dissolution rates of the drugs from physical mixtures would be the sum of the dissolution rates of the uncomplexed and the complexed drugs. In contrast to this, the dissolution of drugs from solid dispersions would depend upon the dissolution rates of the complexed drugs alone.

Based on such concepts, it seems reasonable to assume that the differences in the dissolution rates of sulfisoxazole and sulfamethoxazole between the solid dispersions and the physical mixtures are again most likely due to interaction between the components. It should be noted, however, that insofar as the methisazone binary systems are concerned such differences can not be attributed to interaction between the components. The fact that dissolution rates of this drug from solid dispersions were faster than dissolution rates from physical mixtures would support such a conclusion. Thus, if the assumption is correct that absorption

of sparingly soluble drugs is rate-limited by the dissolution process, differences in dissolution rates will be related to differences in bioavailability of drugs. The findings of the present study seem to support this assumption in that the differences in the dissolution rates of sulfisoxazole, sulfamethoxazole, and methisazone between the solid dispersions and the physical mixtures are related to the differences in the observed bioavailability of these drugs.

SUMMARY

Solid dispersions of sulfisoxazole, sulfamethoxazole, and methisazone were prepared by the solvent evaporation technique using both urea and polyvinylpyrrolidone as water soluble carriers. Thermal analyses of the binary systems were carried out by the capillary melting point and differential thermal analysis methods. Phase diagrams were constructed from the thermal analysis data obtained on the evaporated mixtures. Equilibrium solubility studies were conducted to investigate the effects of urea and polyvinylpyrrolidone on the solubilities of sulfisoxazole, sulfamethoxazole, and methisazone in water. On the basis of the solubility data, thermodynamic parameters were determined for the interactions between drugs and carriers. Dissolution rate studies were undertaken to ascertain the rate constants and percent dissolution times for the pure drugs, physical mixtures, and solid dispersions. Finally, comparative bioavailabilities of pure drugs, physical mixtures, and solid dispersions were were evaluated in rats using a completely random design.

As a result of the present investigation, the following may be concluded:

1. Sulfisoxazole interacts with urea to form a complex with incongruent melting point.
2. Sulfamethoxazole and urea constitute a eutectic system.

3. The interaction between methisazone and urea is indicative of peritectic complex formation.
4. On the basis of the DTA studies, it is suggested that sulfisoxazole, sulfamethoxazole, and methisazone form glass solutions with PVP.
5. The stoichiometry of the binary hydrogen-bonded complexes is apparently 1:1 in all the cases except sulfamethoxazole-polyvinylpyrrolidone system. The stoichiometeric ratios for sulfamethoxazole-polyvinylpyrrolidone system at 25 and 37°C appear to be 2:1 and 3:1, respectively.
6. Significant differences were found in the dissolution profiles of sulfisoxazole, sulfamethoxazole, and methisazone.
7. In the case of sulfisoxazole and sulfamethoxazole, the dissolution rates from physical mixtures were significantly faster than those from solid dispersions. This is presumably due to the interaction between the intact drug and the carrier molecules during the dissolution process. However, these unexpected interactions were not observed during the dissolution of methisazone from physical mixtures.
8. Both urea and polyvinylpyrrolidone significantly reduced the extent of absorption of sulfisoxazole and sulfamethoxazole from solid dispersions. Con-

versely, urea and polyvinylpyrrolidone significantly increased the bioavailability of methisazone from solid dispersions.

9. The reduction in the bioavailability of sulfisoxazole and sulfamethoxazole from solid dispersions containing urea and polyvinylpyrrolidone may be accounted for, in part at least, by the fact that the drug and carrier molecules exist as complexes in the solid state.

10. The enhancement in the bioavailability of sulfisoxazole and sulfamethoxazole from physical mixtures containing urea and polyvinylpyrrolidone would appear to be related to the formation of soluble complexes between drug and carrier molecules in aqueous solution.

11. The absence of complexation between the components would suggest that the enhancement in the bioavailability of methisazone from solid dispersions containing urea and polyvinylpyrrolidone could possible be due to particle size reduction of the drug.

REFERENCES

1. G. Levy, Am. J. Pharm., 135: 78 (1963).
2. J.H. Fincher, J. Pharm. Sci., 57: 1825 (1968).
3. L.G. Miller and J.H. Fincher, ibid., 60: 1733 (1971).
4. K. Sekiguchi, K. Ito, E. Owada, and K. Ueno, Chem. Pharm. Bull., 12: 1192 (1964).
5. K. Sekiguchi and N. Obi, ibid., 9: 866 (1961).
6. K. Sekiguchi, N. Obi, and Y. Ueda, ibid., 12: 134 (1964).
7. A.H. Goldberg, M. Gibaldi, and J.L. Kanig, J. Pharm. Sci., 54: 1145 (1965).
8. ibid., 55: 482 (1966).
9. ibid., 55: 487 (1966).
10. A.H. Goldberg, M. Gibaldi, J.L. Kanig, and M. Mayersohn, ibid., 55: 581 (1966).
11. M. Mayersohn and M. Gibaldi, ibid., 55: 1323 (1966).
12. A. Simonelli, S.C. Mehta, and W.I. Higuchi, ibid., 58: 538 (1969).
13. W.L. Chiou and S. Riegelman, ibid., 58: 1505 (1969).
14. ibid., 59: 937 (1970).
15. ibid., 60: 1281 (1971).
16. ibid., 60: 1376 (1971).
17. W.L. Chiou, ibid., 60: 1406 (1971).
18. W.L. Chiou and L.D. Smith, ibid., 60: 125 (1971).
19. W.L. Chiou and S. Niazi, ibid., 60: 1333 (1971).
20. ibid., 62: 498 (1973).
21. T.R. Bates, J. Pharm. Pharmacol., 21: 710 (1969).
22. E.I. Stunak and T.R. Bates, J. Pharm. Sci., 61: 400 (1972).

23. R.G. Stoll, T.R. Bates, K.A. Nieforth, and J. Swarbrick, ibid., 58: 1457 (1969).

24. R.G. Stoll, T.R. Bates, and J. Swarbrick, ibid., 62: 65 (1973).

25. A. Noyes and W. Whitney, J. Am. Chem. Soc., 19: 930 (1897).

26. J.D. Mullins and T.J. Macek, J. Am. Pharm. Assoc., Sci. Ed., 49: 245 (1960).

27. J.W. Poole, G. Owen, J. Silverio, J.N. Freyhor, and S.B. Rosenman, Current Therap. Res., 10: 292 (1968).

28. J.W. Poole and C.K. Bahal, J. Pharm. Sci., 57: 1945 (1968).

29. W.I. Higuchi, P.K. Lau, T. Higuchi, and J.W. Shell, ibid., 52: 150 (1963).

30. A.J. Aguiar, J. Krc, Jr., A.W. Kinkel, and J.C. Samyn, ibid., 56: 847 (1967).

31. T. Higuchi and D.A. Zuck, J. Am. Pharm. Assoc., 41: 10 (1952).

32. ibid., 42: 132 (1953).

33. ibid., 42: 138 (1953).

34. T. Higuchi and J.L. Lach, ibid., 43: 349 (1954).

35. ibid., 43: 465 (1954).

36. T. Higuchi and Kuramoto, ibid., 43: 393 (1954).

37. ibid., 43: 398 (1954).

38. S.S. Yang and J.K. Guillory, J. Pharm. Sci., 61: 26 (1972).

39. A. Axon, J. Mond. Pharm., 15: 221 (1972).

40. S.A. Kaplan, R.E. Weinfeld, C.W. Abruzzo, and M. Lewis, J. Pharm. Sci., 61: 773 (1972).

41. D.E. Schwartz and J. Rieder, Chemotherapy, 15: 337 (1970).

42. J.H. Fincher, J.G. Adams, and H.M. Beal, J. Pharm. Sci. 54: 704 (1965).

43. K. Kakemi, H. Sezaki, S. Muranishi, and H. Matusi, Chem. Pharm. Bull., 15: 172 (1967).

44. J.A. Biles, J. Pharm. Sci., 51: 601 (1962).

45. A.J. Aguiar and J.E. Zelmer, ibid., 58: 983 (1969).

46. G. Milosovich, ibid., 53: 484 (1964).

47. J. Haleblian and W. McCrone, ibid., 58: 911 (1969).

48. R.K. Callow and O. Kennard, J. Pharm. Pharmacol., 13: 723 (1961).

49. S.H. Maron and C.F. Prutton, "Principles of Physical Chemistry", 4th Ed., The MacMillan Co., New York, 1965, p. 361.

50. ibid., p. 371.

51. A. Findlay, A.N. Campbell, and N.O. Smith, "Phase Rule", 9th Ed., Dover Publication, Inc., New York, 1951, p. 137.

52. ibid., p. 168.

53. R.F. Schwenker and P.D. Garn, "Thermal Analysis", Vol. 2, Academic Press, Inc., New York, 1969, pp. 829-850.

54. G.L. Clark and G.G. Hawley, "The Encyclopedia of Chemistry", 2nd Ed., Reinhold, New York, 1966, p. 981.

55. L. Bruner and S. Tolloczko, Z. Physik. Chem., 35: 283 (1900).

56. E. Brunner, ibid., 47: 56 (1904).

57. H. Nogami, T. Nagai, and A. Suzuki, Chem. Pharm. Bull., 14: 329 (1966).

58. A.W. Hixson and J.H. Crowell, Ind. Eng. Chem., 23: 923 (1931).

59. W.E. Hamlin, J.I. Northam, and J.G. Wagner, J. Pharm. Sci., 54: 1651 (1965).

60. R.J. Braun and E.L. Parrott, J. Pharm. Sci., 61: 175 (1972).

61. P. Finholt and S. Solvang, ibid., 57: 1322 (1968).

62. E. Nelson, Chem. Pharm. Bull., 10: 1099 (1962).

63. G. Levy and B.A. Sahli, J. Pharm. Sci., 51: 58 (1962).

64. A.R. Cooper and W.D. Kingery, J. Phys. Chem., 66: 665 (1962).

65. R.O. Searl and M. Pernarowski, Can. Med. Assoc. J., 96: 1513 (1967).

66. "National Formulary", 13th Ed., Mack Publishing Co., Easton, Pa., 1970, p. 802.

67. "The United States Pharmacopeia", XVIII, Mack Publishing Co., Easton, Pa., 1970, p. 934.

68. J. Tingstad, E. Gropper, L. Lachman, and E. Shami, J. Pharm. Sci., 62: 293 (1973).

69. T. Higuchi, ibid., 52: 1145 (1963).

70. S.J. Desai, A.P. Simonelli, and W.I. Higuchi, ibid., 54: 1459 (1965).

71. J.B. Schwartz, A.P. Simonelli, and W.I. Higuchi, ibid., 57: 274 (1968).

72. M. Gibaldi and S. Feldman, ibid., 56: 1238 (1967).

73. J.G. Wagner, ibid., 58: 1253 (1969).

74. H. Macdonald, V.A. Place, H. Falk, and M.A. Darken, Chemotherapia, 12: 282 (1967).

75. M. Kraml, J. Dubuc, and D. Beall, Can. J. Biochem. Physiol., 40: 1449 (1962).

76. J.T. Doluisio, G.H. Tan, N.F. Billups, and L. Diamond, J. Pharm. Sci., 58: 1200 (1969).

77. M. Mayersohn, Can. Pharm. J., 104: 164 (1971).

78. P. Borondy, W.A. Dill, T. Chang, R.A. Buchanan, and A.J. Glazko, Ann. N. Y. Acad. Sci., 226: 82 (1973).

79. J.R. Gillette, ibid., 226: 6 (1973).

80. M. Gibaldi and H. Weintraub, J. Pharm. Sci., 60: 624 (1971).

81. M. Rowland, ibid., 61: 70 (1972).

82. L.W. Dittert and A.R. DiSanto, J. Am. Pharm. Assoc., 13: 421 (1973).

83. D. Lalka and H. Feldman, J. Pharm. Sci., 63: 1812 (1974).

84. M. Gibaldi and S. Feldman, Eur. J. Pharmacol., 19: 323 (1972).

85. J.G. Wagner and E. Nelson, J. Pharm. Sci., 52: 610 (1963).

86. J.C.K. Loo and S. Riegelman, ibid., 57: 918 (1968).

87. J.G. Wagner and E. Nelson, ibid., 53: 1392 (1964).

88. R.E. Notari, J.L. DeYoung, and R.H. Reuning, ibid., 61: 135 (1972).

89. D. Perrier and M. Gibaldi, ibid., 62: 225 (1973).

90. L.J. Leeson and H. Weintraub, ibid., 62: 1936 (1973).

91. H.J. Borchardt and F. Daniels, J. Am. Chem. Soc., 79: 41 (1957).

92. J.K. Guillory, J. Pharm. Sci., 56: 72 (1967).

93. "Hand Book of Chemistry and Physics", 53rd Ed., The Chemical Rubber Co., Cleveland, Ohio, U.S.A., 1972, pp. B-240, C-717.

94. D.E. Wurster and P.W. Taylor, J. Pharm. Sci., 54: 670 (1965).

95. W. Turner, D.J. Bauer, and R.H. Nimm-Smith, Brit. Med. J., 1; 1317 (1962).

96. C.H. Kempe, D. Rodgerson, and O.F. Sieber, Jr., Lancet, 1: 824 (1965).

97. D.J. Bauer and P.W. Sadler, Brit. J. Pharmacol., 15: 101 (1960).

98. A.C. Bratton and E.K. Marshall, Jr., J. Biol. Chem., 128: 537 (1939).

99. K. Sekiguchi, Y. Ueda, and Y. Nakamori, Chem. Pharm. Bull., 11: 1108 (1963).

100. K. Sekiguchi, K. Ito, and Y. Nakamori, ibid., 11: 1123 (1963).

101. C. Sunwoo and H. Eisen, J. Pharm. Sci., 60: 238 (1971).

102. K.A. Connors and J.A. Mollica, Jr., ibid., 55: 772 (1966).

103. A. Ringbom, Z. Anal. Chem., 115: 332 (1939).

104. E. Nelson, J. Pharm. Sci., 50: 181 (1961).

105. J.G. Wagner, Can. J. Pharm. Sci., 1: 55 (1966).

106. ibid., Clin. Pharm. and Therap., 8: 201 (1967).

107. W.J. Westlake, J. Pharm. Sci., 62: 1579 (1973).

108. P.J. Niebergall, E.T. Sugita, and R.L. Schnaare, ibid., 63: 100 (1974).

109. S.A. Kaplan, K. Alexander, M.L. Jack, C.V. Puglisi, J.A.F. de Silva, T.L. Lee, and R.E. Weinfeld, ibid., 63: 527 (1974).

110. W.H. Barr, Am. J. Pharm. Educ., 32: 958 (1968).

111. N. Khalafallah, S.A. Khalil, and M.A. Moustafa, J. Pharm. Sci., 63: 861 (1974).

112. T. Higuchi, J.H. Richards, S.S. Davis, A. Kamada, J.P. Hou, M. Nakano, N.I. Nakano, and I.H. Pitman, ibid., 58: 661 (1969).

113. P.P. DeLuca, L. Lachman, and H.G. Schroeder, ibid., 62: 1320 (1973).

114. T. Higuchi, S. Dayal, and I.H. Pitman, ibid., 61: 695 (1972).

115. T. Higuchi and I.H. Pitman, ibid., 62: 55 (1973).

116. R.G.D. Steel and J.H. Torrie, "Principles and Procedures of Statistics", McGraw-Hill Book Co. Inc., New York, N.Y., 1960, p. 106.

APPENDIX

TABLE A-1

Effect of Urea Concentrations on Aqueous Solubility of Various Drugs at 25°C

Urea, % W/V	Solubility[a], mg/100 ml		
	Sulfisoxazole	Sulfamethoxazole	Methisazone
0.00	15.353±0.706[b]	39.475±0.877[b]	1.301±0.070[b]
0.50	16.765±0.294	42.105±0.526	1.301±0.041
1.00	18.824±0.294	43.859±0.526	1.233±0.041
1.50	20.088±0.176	46.491±0.526	1.370±0.041
2.00	21.765±0.294	48.246±0.526	1.301±0.070
2.50	23.824±0.294	50.000±0.526	1.301±0.041
3.00	25.500±0.353	52.632±0.526	1.301±0.041
3.50	27.353±0.294	54.386±0.530	1.301±0.070
4.00	28.618±0.353	57.018±0.530	1.370±0.070
4.50	30.794±0.353	58.772±0.530	1.370±0.070
5.00	32.558±0.353	61.404±0.530	1.438±0.070

[a]Average of three determinations with standard deviation

[b]Solubility of pure drug in distilled water at 25°C

TABLE A-2

Effect of Urea Concentrations on Aqueous Solubility of Various Drugs at 37°C

Urea,	Solubility[a], mg/100 ml		
% W/V	Sulfisoxazole	Sulfamethoxazole	Methisazone
0.00	26.485±1.610[b]	77.193±1.579[b]	1.712±0.041[b]
0.50	33.382±0.882	85.438±1.053	1.753±0.041
1.00	43.088±3.676	92.983±1.754	1.918±0.041
1.50	50.000±1.470	105.263±1.754	1.918±0.041
2.00	58.382±3.676	110.526±1.754	1.890±0.041
2.50	65.735±0.882	120.526±1.053	1.959±0.041
3.00	73.529±2.941	129.825±1.754	2.164±0.040
3.50	82.353±1.470	138.070±1.053	2.123±0.070
4.00	91.176±1.470	146.842±1.053	2.123±0.070
4.50	98.529±1.470	156.140±1.754	2.192±0.070
5.00	104.853±0.882	166.140±1.053	2.370±0.040

[a]Average of three determinations with standard deviation

[b]Solubility of pure drug in distilled water at 37°C

TABLE A-3

Effect of PVP. Concentrations on Aqueous Solubility of Various Drugs at 25°C

PVP., %W/V	Solubility[a], mg/100 ml		
	Sulfisoxazole	Sulfamethoxazole	Methisazone
0.00	15.353±0.706[b]	39.475±0.877[b]	1.301±0.070[b]
0.50	17.941±0.294	45.614±0.000	1.781±0.040
1.00	20.294±0.294	49.123±0.877	2.055±0.000
1.50	21.471±0.290	55.263±0.000	2.329±0.000
2.00	24.029±0.176	60.526±0.877	2.603±0.000
2.50	26.176±0.290	66.667±0.800	2.945±0.070
3.00	28.235±0.290	71.053±1.490	3.288±0.070
3.50	30.382±0.353	76.316±0.877	3.630±0.070
4.00	32.147±0.882	81.579±1.490	3.973±0.070
4.50	34.912±0.353	87.719±0.877	4.452±0.070
5.00	36.853±0.353	92.982±1.754	4.863±0.040

[a]Average of three determinations with standard deviation
[b]Solubility of pure drug in distilled water at 25°C

TABLE A-4

Effect of PVP. Concentrations on Aqueous Solubility of Various Drugs at 37°C

PVP., %W/V	Solubility[a], mg/100 ml		
	Sulfisoxazole	Sulfamethoxazole	Methisazone
0.00	26.485±1.610[b]	77.193±1.579[b]	1.712±0.040[b]
0.50	29.603±0.485	84.737±1.053	2.123±0.070
1.00	32.029±0.971	94.211±1.053	2.534±0.070
1.50	35.766±0.291	101.754±1.754	3.151±0.000
2.00	39.163±0.291	107.018±1.750	3.493±0.070
2.50	42.706±0.485	119.298±1.750	4.178±0.070
3.00	45.957±0.290	122.807±1.800	4.520±0.137
3.50	49.160±0.582	132.807±1.053	5.137±0.070
4.00	52.752±0.582	140.351±1.750	5.658±0.103
4.50	55.663±0.680	150.877±1.800	6.233±0.070
5.00	59.206±0.970	157.895±1.750	6.849±0.070

[a]Average of three determinations with standard deviation

[b]Solubility of pure drug in distilled water at 37°C

TABLE A-5

Data[a] for Dissolution of Pure Sulfisoxazole[b] in Distilled Water at 37°C

Hours	Amount Dissolved[c]	Percent Dissolved	Percent Undissolved
0.25	2.27±0.210	0.56	99.44
0.50	3.74±0.221	0.92	99.08
0.75	5.32±0.300	1.31	98.69
1.00	6.63±0.290	1.63	98.37
1.50	9.30±0.446	2.28	97.72
2.00	11.57±0.432	2.84	97.16
3.00	15.98±1.537	3.92	96.08
4.00	21.66±1.815	5.32	94.68
5.00	28.05±1.931	6.88	93.12
6.00	32.23±2.150	7.91	92.09

[a]Rotating-Basket Method used

[b]Weight of pellets = 407.63±0.503 mg.

[c]Average of three determinations with standard deviation

TABLE A-6

Data[a] for Dissolution of Sulfisoxazole-Urea Physical Mixture[b] in Distilled Water at 37°C

Hours	Amount Dissolved[c]	Percent Dissolved	Percent Undissolved
0.25	2.63±0.275	0.90	99.10
0.50	4.32±0.224	1.50	98.50
0.75	5.66±0.081	1.95	98.05
1.00	7.17±0.180	2.50	97.50
1.50	9.59±0.145	3.30	96.70
2.00	12.00±0.223	4.12	95.88
3.00	18.70±1.125	6.42	93.58
4.00	26.56±0.735	9.12	90.88
5.00	33.46±1.103	11.50	88.50
6.00	37.89±1.147	13.00	87.00

[a]Rotating-Basket Method used

[b]Weight of pellets = 408±0.570 mg. (Sulfisoxazole = 70%)

[c]Average of three determinations with standard deviation

TABLE A-7

Data[a] for Dissolution of Sulfisoxazole-Urea Solid Dispersion[b] in Distilled Water at 37°C

Hours	Amount Dissolved[c]	Percent Dissolved	Percent Undissolved
0.25	2.45±0.173	0.85	99.15
0.50	4.57±0.140	1.60	98.40
0.75	6.24±0.100	2.20	97.80
1.00	7.63±0.180	2.65	97.35
1.50	9.74±0.390	3.38	96.62
2.00	11.83±0.192	4.10	95.90
3.00	17.95±0.440	6.23	93.77
4.00	24.10±0.900	8.36	91.64
5.00	27.30±1.440	9.47	90.53
6.00	32.20±0.800	11.20	88.80

[a]Rotating-Basket Method used

[b]Weight of pellets = 408.43±0.900 mg. (Sulfisoxazole = 70%)

[c]Average of three determinations with standard deviation

TABLE A-8

Data[a] for Dissolution of Sulfisoxazole-PVP Physical Mixture[b] in Distilled Water at 37°C

Hours	Amount Dissolved[c]	Percent Dissolved	Percent Undissolved
0.25	12.45±0.615	12.45	87.55
0.50	25.81±3.660	25.81	74.19
0.75	39.08±3.685	39.08	60.92
1.00	51.64±1.480	51.64	48.36
1.50	66.88±3.066	66.88	33.12
2.00	81.64±6.963	81.64	18.36
2.50	92.98±3.905	92.98	7.02
3.00	98.00±4.507	98.00	2.00
4.00	103.80±3.075	103.80	0.00

[a] Rotating-Disc Method used

[b] 400 mg. quantitatively transferred and compressed (PVP = 75%)

[c] Average of three determinations with standard deviation

TABLE A-9

Data[a] for Dissolution of Sulfisoxazole-PVP Solid Dispersion[b] in Distilled Water at 37°C

Hours	Amount Dissolved[c]	Percent Dissolved	Percent Undissolved
0.25	6.62±0.440	6.50	93.50
0.50	12.60±0.750	12.40	87.60
0.75	19.66±2.245	19.27	80.73
1.00	26.06±2.593	25.54	74.46
1.50	39.33±2.104	38.55	61.45
2.00	50.15±3.210	49.16	50.84
3.00	73.74±3.910	72.29	27.71
4.00	102.26±3.406	100.25	00.00

[a]Rotating-Disc Method used

[b]400 mg. quantitatively transferred and compressed (PVP = 75%)

[c]Average of three determinations wtih standard deviation

TABLE A-10

Data[a] for Dissolution of Pure Sulfamethoxazole[b] in Distilled Water at 37°C

Hours	Amount Dissolved[c]	Percent Dissolved	Percent Undissolved
0.25	4.21±0.351	1.05	98.95
0.50	8.77±1.228	2.18	97.82
0.75	11.99±0.365	2.98	97.02
1.00	15.15±0.664	3.80	96.20
1.50	23.68±0.877	5.90	94.10
2.00	29.90±0.000	7.43	92.57
3.00	43.98±0.800	10.90	89.10
4.00	56.32±0.885	13.99	86.01
5.00	69.23±1.843	17.20	82.80
6.00	83.04±1.336	20.60	79.40

[a]Rotating-Basket Method

[b]Weight of pellets = 405±2 mg.

[c]Average of three determinations with standard deviation

TABLE A-11

Data[a] for Dissolution of Sulfamethoxazole-Urea Physical Mixture[b] in Distilled Water at 37°C

Hours	Amount Dissolved[c]	Percent Dissolved	Percent Undissolved
0.25	4.62±0.564	1.90	98.10
0.50	8.38±0.708	3.45	96.55
0.75	11.61±0.767	4.77	95.23
1.00	14.84±0.871	6.10	93.90
1.50	21.98±1.520	9.04	90.96
2.00	29.91±0.885	12.30	87.70
3.00	43.40±1.350	17.85	82.15
4.00	57.50±2.800	23.64	76.36
5.00	69.25±3.366	28.50	71.50
6.00	83.02±2.83	34.15	65.85

[a]Rotating-Basket Method used

[b]Weight of pellets = 407.80±3.340 mg. (Sulfamethoxazole = 60%)

[c]Average of three determinations with standard deviation

TABLE A-12

Data[a] for Dissolution of Sulfamethoxazole-Urea Solid Dispersion[b] in Distilled Water at 37°C

Hours	Amount Dissolved[c]	Percent Dissolved	Percent Undissolved
0.25	4.45±0.520	1.80	98.20
0.50	8.05±0.115	3.30	96.70
0.75	11.44±0.185	4.66	95.34
1.00	14.80±0.365	6.03	93.97
1.50	21.16±0.900	8.61	91.39
2.00	28.20±0.880	11.50	88.50
3.00	40.50±1.750	16.50	83.50
4.00	51.90±0.870	21.10	78.90
5.00	63.40±1.500	25.80	74.20
6.00	73.88±3.405	30.00	70.00

[a] Rotating-Basket Method used

[b] Weight of pellets = 406±1.30 mg. (Sulfamethoxazole = 60%)

[c] Average of three determinations with standard deviation

TABLE A-13

Data[a] for the Dissolution of Sulfamethoxazole-PVP Physical Mixture[b] in Distilled Water at 37°C

Hours	Amount Dissolved[c]	Percent Dissolved	Percent Undissolved
0.25	14.02±0.870	13.50	86.50
0.50	26.35±0.875	25.50	74.50
0.75	39.60±1.750	38.24	61.76
1.00	48.42±1.775	46.75	53.25
1.50	70.53±2.380	68.10	31.90
2.00	98.60±1.750	95.20	4.80
3.00	105.10±1.040	101.50	

[a]Rotating-Disc Method used

[b]400 mg. quantitatively transferred and compressed (PVP = 75%)

[c]Average of three determinations with standard deviation

TABLE A-14

Data[a] for Dissolution of Sulfamethoxazole-PVP Solid Dispersion[b] in Distilled Water at 37°C

Hours	Amount Dissolved[c]	Percent Dissolved	Percent Undissolved
0.25	8.10±0.171	7.60	92.40
0.50	15.41±0.251	14.50	85.50
0.75	22.90±0.850	21.50	78.50
1.00	30.22±1.315	28.40	71.60
1.50	43.70±0.490	41.10	58.90
2.00	58.10±0.910	54.60	45.40
3.00	85.60±0.468	80.50	19.50
4.00	106.77±0.981	100.00	00.00

[a]Rotating-Disc Method used

[b]400 mg. quantitatively transferred and compressed (PVP = 75%)

[c]Average of three determinations with standard deviation

TABLE A-15

Data[a] for Dissolution of Pure Methisazone[b] in Distilled Water at 37°C

Hours	Amount Dissolved[c]	Percent Dissolved	Percent Undissolved
24	1.50±0.182	0.37	99.63
48	2.24±0.180	0.55	99.45
72	2.82±0.100	0.70	99.30
96	3.28±0.160	0.81	99.19
120	3.97±0.180	1.00	99.00

[a]Rotating-Basket Method Used

[b]Weight of pellets = 404.90±0.550 mg.

[c]Average of three determinations with standard deviation

TABLE A-16

Data[a] for Dissolution of Pure Methisazone[b] in Distilled Water containing 0.01% Tween 80 at 37°C

Hours	Amount Dissolved[c]	Percent Dissolved	Percent Undissolved
6	1.38±0.020	0.34	99.66
12	2.14±0.250	0.53	99.47
24	3.50±0.265	0.86	99.14
48	5.12±0.355	1.26	98.74
72	5.94±0.300	1.46	98.54
96	6.22±0.340	1.53	98.47
120	6.22±0.290	1.53	98.47

[a]Rotating-Basket Method used

[b]Weight of pellets = 406.70±1.74 mg.

[c]Average of three determinations with standard deviation

TABLE A-17

Data[a] for Dissolution of Methisazone-Urea Physical Mixture[b] in Distilled Water at 37°C

Hours	Amount Dissolved[c]	Percent Dissolved	Percent Undissolved
3	2.80±0.095	1.38	98.62
6	4.30±0.340	2.12	97.88
18	5.12±0.101	2.52	97.48
24	5.34±0.005	2.63	97.37
30	5.63±0.098	2.77	97.23
42	5.98±0.107	2.94	97.06
54	5.99±0.101	2.95	97.05
78	6.17±0.104	3.04	96.96
96	6.23±0.170	3.07	96.93
120	6.23±0.170	3.07	96.93

[a]Rotating-Basket Method used

[b]Weight of pellets = 406.33±1.27 mg. (Methisazone = 50%)

[c]Average of three determinations with standard deviation

TABLE A-18

Data[a] for Dissolution of Methisazone-Urea Solid Dispersion[b] in Distilled Water at 37°C

Hours	Amount Dissolved[c]	Percent Dissolved	Percent Undissolved
9	1.27±0.210	0.62	99.38
24	2.24±0.520	1.10	98.90
42	3.21±0.260	1.57	98.43
54	3.73±0.440	1.83	98.17
78	4.49±0.700	2.20	97.80
96	4.84±0.500	2.40	97.60
120	5.30±0.430	2.60	97.40

[a]Rotating-Basket Method Used

[b]Weight of pellets = 404.40±0.930 mg. (Methisazone = 50%)

[c]Average of three determinations with standard deviation

TABLE A-19

Data[a] for Dissolution of Methisazone-PVP Physical Mixture[b] in Distilled Water at 37°C

Hours	Amount Dissolved[c]	Percent Dissolved	Percent Undissolved
0.25	1.44±0.091	1.42	98.58
0.50	2.65±0.091	2.62	97.38
0.75	3.10±0.053	3.06	96.94
1.00	3.40±0.101	3.36	96.64
1.50	3.77±0.050	3.73	96.27
2.00	3.91±0.100	3.87	96.13
3.00	3.91±0.100	3.87	96.13
6.00	3.91±0.100	3.87	96.13

[a]Rotating-Basket Method used

[b]Weight of pellets = 408.80±0.854 mg. (PVP = 75%)

[c]Average of three determinations with standard deviation

TABLE A-20

Data[a] for Dissolution of Methisazone-PVP Solid Dispersion[b] in Distilled Water at 37°C

Hours	Amount Dissolved[c]	Percent Dissolved	Percent Undissolved
0.25	1.57±0.132	1.53	98.47
0.50	3.27±0.160	3.20	96.80
0.75	4.76±0.107	4.63	95.37
1.00	6.43±0.101	6.25	93.75
1.25	6.75±0.050	6.57	93.43
1.50	7.07±0.175	6.90	93.10
2.00	7.32±0.113	7.12	92.88
3.00	7.32±0.210	7.12	92.88
6.00	7.42±0.175	7.22	92.78

[a]Rotating-Basket Method used

[b]Weight of pellets = 405.60±1.50 mg. (P[illegible] = 75%)

[c]Average of three determinations with standard deviation

TABLE A-21

Data[a] for Dissolution of Methisazone-PVP Physical Mixture[b] in Distilled Water at 37°C

Hours	Amount Dissolved[c]	Percent Dissolved	Percent Undissolved
0.25	0.89±0.050	0.90	99.10
0.50	1.55±0.170	1.56	98.44
0.75	2.00±0.212	2.02	97.98
1.00	2.24±0.090	2.26	97.74
1.50	2.63±0.050	2.65	97.35
2.00	2.96±0.052	3.00	97.00
2.50	3.14±0.050	3.17	96.83
3.50	3.30±0.052	3.33	96.67
4.50	3.40±0.101	3.44	96.56
5.50	3.51±0.046	3.55	96.45

[a]Rotating-Disc Method used

[b]400 mg. quantitatively transferred and compressed (PVP = 75%)

[c]Average of three determinations with standard deviation

TABLE A-22

Data[a] for Dissolution of Methisazone-PVP Solid Dispersion[b] in Distilled Water at 37°C

Hours	Amount Dissolved[c]	Percent Dissolved	Percent Undissolved
0.25	0.48±0.050	0.47	99.53
0.50	0.97±0.098	0.96	99.04
0.75	1.72±0.170	1.70	98.30
1.00	2.27±0.140	2.24	97.76
1.25	2.80±0.215	2.76	97.24
1.50	3.50±0.108	3.45	96.55
2.00	4.35±0.050	4.29	95.71
2.50	5.10±0.072	5.03	94.97
3.00	5.55±0.050	5.50	94.50
4.00	5.83±0.050	5.75	94.25
5.00	6.02±0.050	5.94	94.06
6.00	6.25±0.050	6.20	93.80

[a] Rotating-Disc Method used

[b] 400 mg. quantitatively transferred and compressed (PVP = 75%)

[c] Average of three determinations with standard deviation

TABLE A-23

Blood Level Data for Sulfisoxazole-Urea[a] Physical Mixture following Single-Dose Oral Administration in Male Wistar Rats[b]

Hours	Blood Concentration[c], mcg/ml
0.25	97.24±11.80
0.50	124.85±10.00
1.00	172.87±24.00
2.00	262.90±10.00
3.00	316.93±24.00
4.00	298.92±15.88
6.00	134.85±24.26
8.00	46.00±18.00
12.00	18.40± 1.38

[a]Dose level: 500 mg/kg sulfisoxazole equivalent

[b]The rats weighed 445±9 g

[c]Mean values from three rats with standard deviation

TABLE A-24

Blood Level Data for Sulfisoxazole-Urea Solid Dispersions following Oral Administration of Single Doses in Male Wistar Rats

Hours	Blood Concentration[a], mcg/ml		
	500-mg/kg Dose Equivalent		250-mg/kg Dose Equivalent
	Eutectic[b]	Incongruent[c]	Incongruent[c]
0.25	72.83± 9.20	140.85±15.10	90.84±12.50
0.50	122.85±12.50	178.87±18.00	120.85± 9.20
1.00	164.86± 6.93	250.90± 6.00	162.86± 7.00
2.00	230.89±15.10	304.92±12.00	186.90± 9.20
3.00	208.88±12.00	262.90±36.50	158.86± 9.20
4.00	158.86±15.10	180.87±38.12	106.84±15.80
6.00	104.84± 9.20	80.83±30.00	52.82±12.00
8.00	27.61± 9.06	40.82±10.00	17.60± 1.00
12.00	12.80± 3.60	15.20± 2.70	12.00± 4.00
Rats weighed:	436±6 g	403±6 g	448±12 g

[a]Mean values from three rats with standard deviation

[b]Eutectic composition: 25% sulfisoxazole, 75% urea

[c]Incongruent composition: 70% sulfisoxazole, 30% urea

TABLE A-25

Blood Level Data for Sulfisoxazole-PVP[a] Physical Mixture following Single-Dose Oral Administration in Male Wistar Rats[b]

Hours	Blood Concentration[c], mcg/ml
0.25	142.85±12.00
0.50	234.89±19.30
1.00	328.93±10.40
2.00	368.95±18.33
3.00	336.93±18.00
4.00	296.92±18.30
6.00	138.85±22.72
8.00	44.82±13.86
12.00	16.00± 3.66

[a]Dose level: 500 mg/kg sulfisoxazole equivalent

[b]The rats weighed 463±20 g

[c]Mean values from three rats with standard deviation

TABLE A-26

Blood Level Data for Sulfisoxazole-PVP[a] Solid Dispersion following Single-Dose Oral Administration in Male Wistar Rats[b]

Hours	Blood Concentration[c], mcg/ml
0.25	162.86±35.20
0.50	284.91±36.67
1.00	432.97±34.65
2.00	336.93±12.50
3.00	234.89±22.70
4.00	156.86±24.99
6.00	68.82± 3.50
8.00	31.61± 3.85
12.00	12.80± 3.60

[a]Dose level: 500 mg/kg sulfisoxazole equivalent

[b]The rats weighed 407±12 g

[c]Mean values from three rats with standard deviation

TABLE A-27

Blood Level Data for Sulfisoxazole-PVP[a] Solid Dispersion following Single-Dose Oral Administration in Male Wistar Rats[b]

Hours	Blood Concentration[c], mcg/ml
0.25	118.85±27.50
0.50	156.86±36.67
1.00	222.89±29.60
2.00	192.88±24.98
3.00	142.86±15.88
4.00	90.84± 9.20
6.00	60.82±18.34
8.00	20.00± 3.46
12.00	11.20± 1.40

[a]Dose level: 250 mg/kg sulfisoxazole equivalent

[b]The rats weighed 465±22 g

[c]Mean values from three rats with standard deviation

TABLE A-28

Blood Level Data for Sulfamethoxazole-Urea[a] Physical Mixture following Single-Dose Oral Administration in Male Wistar Rats[b]

Hours	Blood Concentration[c], mcg/ml
0.25	190.50±34.60
0.50	320.10±27.87
1.00	531.75±42.00
2.00	727.50±27.87
3.00	756.60±18.33
4.00	762.00±27.50
6.00	719.57±18.33
8.00	661.40± 9.20
12.00	603.20±15.87
20.00	198.40±15.90
28.00	82.00± 9.16

[a]Dose level: 500 mg/kg sulfamethoxazole equivalent

[b]The rats weighed 427±8 g

[c]Mean values from three rats with standard deviation

TABLE A-29

Blood Level Data for Sulfamethoxazole-Urea[a] Solid Dispersions following Single-Dose Oral Administration in Male Wistar Rats

	Blood Concentration[b], mcg/ml	
Hours	Solvent Method	Fusion Method
0.25	214.28±28.60	195.80±27.87
0.50	349.20±49.60	328.00±47.84
1.00	555.50±79.40	455.00±56.30
2.00	761.90±63.49	616.40±69.34
3.00	693.12±40.00	711.64±52.80
4.00	677.25±18.33	706.35±49.60
6.00	619.05± 7.94	653.44±16.50
8.00	558.20± 4.60	605.82±40.73
12.00	275.13±33.00	283.10±32.10
20.00	82.00±12.12	100.53±16.52
28.00	37.04± 9.98	35.70±10.50
Rats weighed:	440±5 g	440±5 g

[a]Dose level: 500 mg/kg sulfamethoxazole equivalent

[b]Mean values from three rats with standard deviation

TABLE A-30

Blood Level Data for Sulfamethoxazole-PVP[a] Physical Mixture following Single-Dose Oral Administration in Male Wistar Rats[b]

Hours	Blood Concentration[c], mcg/ml
0.25	222.00±36.40
0.50	412.70±47.00
1.00	666.70±48.00
2.00	804.20±51.00
3.00	825.40±42.00
4.00	777.80±41.90
6.00	751.30±33.00
8.00	677.25±40.00
12.00	510.60±32.10
20.00	108.50±12.00
28.00	47.62± 7.90

[a]Dose level: 500 mg/kg sulfamethoxazole equivalent

[b]The rats weighed 436±16 g

[c]Mean values from three rats with standard deviation

TABLE A-31

Blood Level Data for Sulfamethoxazole-PVP[a] Solid Dispersion following Single-Dose Oral Administration in Male Wistar Rats[b]

Hours	Blood Concentration[c], mcg/ml
0.25	349.20±28.62
0.50	513.23±24.25
1.00	653.44±69.34
2.00	767.20±40.00
3.00	809.52±31.75
4.00	746.00±27.50
6.00	640.21±24.25
8.00	571.43±15.87
12.00	299.00±32.10
20.00	92.60±16.50
28.00	34.40± 6.10

[a]Dose level: 500 mg/kg sulfamethoxazole equivalent

[b]The rats weighed 453±12 g

[c]Mean values from three rats with standard deviation

TABLE A-32

Blood Level Data for Pure Methisazone[a] following Single-Dose Oral Administration in Male Wistar Rats.

Hours	Blood Concentration[b], mcg/ml
0.50	7.60±0.44
1.00	8.82±0.73
2.00	10.30±0.74
3.00	11.26±0.300
4.00	9.56±0.74
5.00	7.35±0.73
6.00	6.32±0.85

[a]Dose level: 500 mg/kg methisazone

[b]Mean values from three rats with standard deviation

TABLE A-33

Blood Level Data for Methisazone-Urea[a] Physical Mixture following Single-Dose Oral Administration in Male Wistar Rats.

Hours	Blood Concentration[b], mcg/ml
0.50	7.40±0.73
1.00	9.11±0.85
2.00	10.00±1.53
3.00	10.80±0.42
4.00	8.82±0.74
5.00	7.10±0.88
6.00	6.25±0.97

[a]Dose level: 500 mg/kg methisazone equivalent

[b]Mean values from three rats with standard deviation

TABLE A-34

Blood Level Data for Methisazone-Urea[a] Solid Dispersion following Single-Dose Oral Administration in Male Wistar Rats.

Hours	Blood Concentration[b], mcg/ml
0.50	8.38±0.88
1.00	9.56±0.74
2.00	12.00±0.90
3.00	13.20±1.50
4.00	12.25±0.88
5.00	9.80±0.90
6.00	7.80±0.50

[a]Dose level: 500 mg/kg equivalent

[b]Mean values from three rats with standard deviation

TABLE A-35

Blood Level Data for Methisazone-PVP[a] Physical Mixture following Single-Dose Oral Administration in Male Wistar Rats.

Hours	Blood Concentration[b], mcg/ml
0.50	9.00±0.78
1.00	10.30±0.73
2.00	11.52±1.53
3.00	14.00±1.95
4.00	12.25±1.70
5.00	11.00±0.85
6.00	8.10±0.74

[a]Dose level: 500 mg/kg methisazone equivalent.

[b]Mean values from three rats with standard deviation

TABLE A-36

Blood Level Data for Methisazone-PVP[a] Solid Dispersion following Single-Dose Oral Administration in Male Wistar Rats.

Hours	Blood Concentration[b] mcg/ml
0.25	10.40±0.43
0.50	14.70±0.70
1.00	17.65±0.75
2.00	20.00±0.45
3.00	22.80±0.80
4.00	20.50±1.50
5.00	17.35±1.20
6.00	11.80±1.50
7.00	9.80±0.90
8.00	8.20±0.74

[a]Dose level: 500 mg/kg methisazone equivalent

[b]Mean values from three rats with standard deviation

TABLE A-37

Urinary Excretion Data for Pure Methisazone[a] in Male Wistar Rats[b] under uncontrolled urinary pH conditions.

Hours	Amount[c] Excreted, mg/kg	Mean Cumulative Amount Excreted, mg/kg	Excretion Rate, mg/kg/hr
1	--		0.312
2	0.625±0.050	0.625	--
3	--	--	0.465
4	0.930±0.120	1.555	--
6	--	--	0.500
8	1.970±0.250	3.525	--
10	--	--	0.862
12	3.450±0.040	6.975	--
18	--	--	0.640
24	7.600±0.160	14.575	--
30	--	--	0.295
36	3.540±0.500	18.119	--
42	--	--	0.317
48	3.800±0.500	21.920	--
54	--	--	0.228
60	2.740±0.500	24.659	--
66	--	--	0.136
72	1.640±0.050	26.300	--

[a] Dose level: 500 mg/kg methisazone

[b] The rats weighed 380±10 g.

[c] Mean values from three rats with standard deviation

TABLE A-38

Urinary Excretion Data for Methisazone-Urea[a] Physical Mixture in Male Wistar Rats[b] under uncontrolled urinary pH conditions.

Hours	Amount[c] Excreted, mg/kg	Mean Cumulative Amount Excreted, mg/kg	Excretion Rate, mg/kg/hr
1	--	--	0.400
2	0.720±0.08	0.720	--
3	--	--	0.680
4	1.360±0.08	2.080	--
6	--	--	1.000
8	4.000±0.800	6.080	--
10	--	--	1.100
12	4.400±0.400	10.480	--
18	--	--	0.800
24	9.490±2.200	19.980	--
30	--	--	0.500
36	6.000±2.000	25.980	--
42	--	--	0.300
48	3.680±0.560	29.600	--
54	--	--	0.320
60	3.900±0.800	33.500	--
66	--	--	0.155
72	1.860±0.120	35.400	--

[a]Dose level: 500 mg/kg methisazone equivalent

[b]The rats weighed 390±10 g.

[c]Mean values from three rats with standard deviation

TABLE A-39

Urinary Excretion Data for Methisazone-Urea[a] Solid Dispersion in Male Wistar Rats[b] under uncontrolled urinary pH conditions.

Hours	Amount[c] Excreted, mg/kg	Mean Cumulative Amount Excreted, mg/kg	Excretion Rate, mg/kg/hr
1	--	--	0.330
2	0.660±0.100	0.660	--
3	--	--	0.600
4	1.200±0.080	1.860	--
6	--	--	0.880
8	3.520±0.140	5.380	--
10	--	--	1.200
12	4.800±0.400	10.180	--
18	--	--	1.270
24	15.200±1.000	25.380	--
30	--	--	0.733
36	8.800±1.600	34.180	--
42	--	--	0.570
48	6.800±1.600	40.980	--
54	--	--	0.380
60	4.600±1.000	45.58	--
66	--	--	0.350
72	4.200±1.600	49.780	--

[a]Dose level: 500 mg/kg methisazone equivalent

[b]The rats weighed 390±10 g.

[c]Mean values from three rats with standard deviation

TABLE A-40

Urinary Excretion Data for Methisazone-PVP[a] Physical Mixture in Male Wistar Rats[b] under uncontrolled urinary pH conditions.

Hours	Amount[c] Excreted, mg/kg	Mean Cumulative Amount Excreted, mg/kg	Excretion Rate, mg/kg/hr
1	--	--	0.360
2	0.720±0.150	0.720	--
3	--	--	0.550
4	1.100±0.200	1.820	--
6	--	--	1.120
8	4.500±0.600	6.320	--
10	--	--	1.050
12	4.200±2.000	10.520	--
18	--	--	1.300
24	15.600±0.150	26.120	--
30	--	--	0.500
36	6.000±2.000	32.120	--
42	--	--	0.600
48	7.200±3.600	39.320	--
54	--	--	0.400
60	5.300±3.500	44.620	--
66	--	--	0.280
72	3.360±0.390	47.980	--
84	--	--	0.190
96	4.700±0.080	52.68	--

[a]Dose level: 500 mg/kg methisazone equivalent

[b]The rats weighed 400±10 g.

[c]Mean values from three rats with standard deviation

TABLE A-41

Urinary Excretion Data for Methisazone-PVP[a] Solid Dispersion in Male Wistar Rats[b] under uncontrolled urinary pH conditions.

Hours	Amount[c] Excreted, mg/kg	Mean Cumulative Amount Excreted, mg/kg	Excretion Rate, mg/kg/hr
1	--	--	0.500
2	0.988±0.150	0.988	--
3	--	--	0.750
4	1.500±0.360	2.488	--
6	--	--	0.800
8	3.200±0.600	5.688	--
10	--	--	1.400
12	5.500±0.650	11.188	--
18	--	--	1.300
24	15.500±2.900	26.688	--
30	--	--	0.500
36	6.000±2.910	32.688	--
42	--	--	0.333
48	4.000±1.800	36.688	--
54	--	--	0.191
60	2.300±0.300	38.988	--
66	--	--	0.300
72	3.600±0.360	42.588	--

[a]Dose level: 500 mg/kg methisazone equivalent

[b]The rats weighed 430±10 g.

[c]Mean values from three rats with standard deviation

GLOSSARY OF SYMBOLS

A = area under the DTA peak, sq. in.

AUC = area under the blood concentration-time curve, mcg hr ml^{-1}

α = fast disposition rate constant

B = blood concentration, mcg/ml

β = slow disposition rate constant

C_o = original concentration of carrier added to the system, moles/liter

D = dose administered, mg/kg

D_c = total concentration of drug in presence of carrier, moles/liter

D_s = saturation solubility of drug in absence of carrier, moles/liter

DF = degrees of freedom

E = quantity of drug eliminated

F = fraction of dose absorbed

FD/V = concentration of drug absorbed per unit volume of distribution

ΔF^o = free energy change, cal $mole^{-1}$

G = quantity of drug in the gut

ΔH = heat of fusion, Kcal $mole^{-1}$

ΔH_f^o = enthalpy of formation for the interaction, cal $mole^{-1}$

J = calibration coefficient for the DTA instrument, mcal $deg^{-1} min^{-1}$

k = apparent dissolution rate constant, 1/time

K = intrinsic dissolution rate constant, cm/time

K_a = association equilibrium constant

K_A = first order absorption rate constant, hr^{-1}

K_E = first order elimination rate constant, hr^{-1}

K_{BT} = first order rate constant for the transfer of drug from the central to the peripheral compartment

K_{TB} = first order rate constant for the return of drug from the peripheral to the central compartment

m = number of moles of drug

M = mass of sample, mg

MS = mean square

P = program rate, deg min^{-1}

Q = amount of drug dissolved, mg

R = correlation coefficient

S = surface area, cm^2

ΔS^o = entropy change, cal deg^{-1} $mole^{-1}$

SS = sum of squares

SD = standard deviation

SE = standard error of the mean

T = tissue concentration

$T_{1/2}$ = elimination half-life

T_s = reference temperature sensitivity (5 millivolt full-scale)

ΔT_s = differential temperature sensitivity (100 microvolts full-scale)

U_s = size of the sample removed from the dissolution flask

V = volume of the dissolution medium

X_n = uncorrected amount dissolved in the nth sample

X_t = uncorrected amount dissolved at time t

Y = corrected amount dissolved in the nth sample

VITA

NAME:	Ram Nanikram Gidwani
DATE OF BIRTH:	March 11, 1936
BACCALAUREATE DEGREE:	B.S. in Pharmacy
	L.M. College of Pharmacy
	Gujarat University, India
OTHER DEGREES:	M.S. in Pharmaceutical Chemistry
	College of Pharmacy
	St. John's University, New York
PUBLICATIONS:	J.J. Sciarra and R.N. Gidwani, J. Soc. Cosmet. Chem., 21: 667 (1970).
	J.J. Sciarra and R.N. Gidwani, J. Pharm. Sci., 61: 754 (1972).
	R. Gidwani, Aerosol Age, 16: 22 (1971).
MEMBERSHIP:	American Pharmaceutical Association
	Academy of Pharmaceutical Sciences
	Society of Cosmetic Chemists
PATENTS:	United States Patent No. 3,833,518